Robotics Traveling Van

Final Design Report

Freddy Rivera – Project Manager
Colin Parsinia – Manufacturing Lead
Florence Fasugbe – Design Lead
Andres Gonzales – Programming Lead

Fall 2025-Spring 2026

Project Sponsor: Dr. Michael Shafer
Faculty Advisor: Professor David Willy
Sponsor Mentor: Sethuprasad Gorantla
Instructor: Professor David Willy

DISCLAIMER

This report was prepared by students as part of a university course requirement. While considerable effort has been put into the project, it is not the work of licensed engineers and has not undergone the extensive verification that is common in the profession. The information, data, conclusions, and content of this report should not be relied on or utilized without thorough, independent testing and verification. University faculty members may have been associated with this project as advisors, sponsors, or course instructors, but as such they are not responsible for the accuracy of results or conclusions.

EXECUTIVE SUMMARY

The Robotics Traveling Van project aims to design and develop two low-cost, transportable educational robots that demonstrate core control-system engineering concepts for K–12 outreach. Sponsored by our client, the goal is to create systems that are safe, durable, engaging, and capable of visually illustrating feedback control in classroom environments. The project spans two semesters, with the first focused on research, concept development, prototyping, and feasibility analysis.

Two robots were selected for development: Robot #1, an Inverted Pendulum Robot, and Robot #2, a Ball-on-Plate Robot. These concepts were chosen based on customer requirements, benchmarking, manufacturability, educational value, and system complexity. Throughout the Fall semester, the team completed detailed requirements definition, House of Quality, literature review, morphological chart, and decision matrices that guided the selection of the final designs.

For Robot #1, the team investigated pendulum dynamics, mass distribution, and actuator requirements to validate that the system could be controlled within safe operating limits. Structural concepts were evaluated for durability and stability, and a final frame design was selected based on manufacturability and robustness. Early prototyping confirmed feasibility and informed next semester's full build and controller development.

For Robot #2, multiple concepts were researched before selecting the Ball-on-Plate mechanism due to its strong educational impact and clear visualization of closed-loop control. A Failure Modes and Effects Analysis identified critical risks such as motor overheating, unstable motion, and sensing error. A Ball-on-Beam prototype was constructed to validate sensing, actuation, and motor torque requirements prior to scaling to the full plate system. Engineering calculations confirmed that the chosen stepper motors provide sufficient torque with a comfortable safety factor. A detailed Bill of Materials was developed for the final Ball-on-Beam system, along with planned testing procedures for response time, stability, and safety.

Budget tracking, scheduling, and resource planning were completed for both robots, keeping the project within financial constraints. The team then began the process of ordering materials and electrical components so fabrication and system assembly could begin. 3D printers were acquired and a majority of the major components of the system were fabricated using said systems, with minor machining for the few non plastic parts. With both systems physical components assembled testing began for each robot focusing on safety and dimensions, battery endurance, interface and control systems, PID stability, and sensor calibration for both robots. Additionally, robot 1 was subjected to a drop test to ensure its structural integrity in the event of it rolling off a table, and a final bill of materials audit was performed to evaluate the exact cost of an individual unit.

At the current time Robot #2 is fully functional and ready to be handed off to the client for use, while Robot #1 is only capable of movement and not fully capable of balancing its pendulum, though the client has been briefed on the state of Robot #1 and has approved the descoping of required functionality. Looking forward for both robots, the first major step is to get the designed circuit boards printed and implemented into the robots control systems, further wire and electrical system organization, and with a fully functional electrical system implemented into Robot #1 its code can be properly tested & tuned to balance the pendulum.

TABLE OF CONTENTS

Contents

1 BACKGROUND

This chapter provides an overview of the project background and objectives. It summarizes the project description, deliverables, and success metrics, outlining how the dual-robot design aligns with client expectations for highly durable, interactive engineering outreach tools designed to entice K-12 students to Northern Arizona University (NAU).

1.1 Project Description

The goal of this capstone project is to design and manufacture two highly interactive educational robots that serve as traveling outreach props for NAU. Sponsored by Dr. Michael Shafer, the project aims to create low-cost, durable learning platforms that visually demonstrate fundamental control system principles to inspire K-12 students to pursue STEM.

Each robot fulfills a unique educational role:

- **Robot #1 (Inverted Pendulum):** Demonstrates Newtonian dynamics, physical mobility, and spatial tracking through magnetic encoders (with active PID balancing formally descoped to prioritize structural resilience and reliable component integration).

- **Robot #2 (Ball-on-Beam):** A 1-axis, direct-drive system designed to visually demonstrate active Proportional-Integral-Derivative (PID) feedback control through hands-on interaction.

While the project was allocated a total budget of $5,000, the client's core directive was mass-producibility for fleet deployment. To meet this, the team successfully engineered both platforms utilizing off-the-shelf electronics and standard 3D-printed PLA, achieving a highly scalable reproduction cost of under $300 (approximately $240) per unit. Throughout the academic year, the project evolved from theoretical mathematical modeling to the final delivery of robust, physical hardware capable of surviving high-impact K-12 environments.

1.2 Deliverables

The major deliverables for this project include:

1. Two fully manufactured educational robots (the Inverted Pendulum and the Ball-on-Beam) equipped with integrated touchscreen interfaces to serve as transportable K-12 outreach tools.
2. An open-source digital repository hosting all necessary CAD models, microcontroller code bases, and mass-manufacturing blueprints, and bill of materials (BOMs) to ensure the client or future engineering teams can seamlessly replicate the fleet.
3. Comprehensive engineering documentation detailing the complete design cycle, functional decompositions, risk mitigation (FMEA) strategies, and finalized system parameters.

1.3 Success Metrics

Project success is evaluated against the rigorous customer and engineering requirements established during the early design phases. Key success criteria include:

- **Platforms must effectively translate invisible math into observable physical motion:** observable physical motion, whether through dynamic spatial tracking or active feedback control loops, to captivate K-

12 audiences.

- **Interactive Interface**: Students must be able to safely alter system variables via the onboard touchscreens without requiring external computer hardware.
- **Classroom Durability:** The physical chassis must withstand the wear and tear of a K-12 environment. By utilizing thickened 3D-printed PLA architectures and robust mechanical fasteners, both systems are engineered for high structural resilience during continuous transport and hands-on demonstrations.
- **Untethered Reliability:** Systems must operate completely independently of wall power. Custom 14.8V LiFePO4 battery arrays were integrated to successfully sustain continuous demonstrations for over 90 minutes.
- **Mass Producibility & Budget:** The final per-unit cost must remain strictly under the $300 target to allow NAU to economically reproduce the designs for future traveling van deployments.

Success has ultimately been verified through final physical testing, performance analysis, and client evaluation, confirming that the constructed platforms meet the rigid safety, durability, and cost metrics required to serve as permanent NAU engineering outreach tools.

2 REQUIREMENTS

The requirements section establishes the foundational parameters of the project, translating qualitative client needs into measurable, quantifiable engineering goals. Because this project is designed as an interactive engineering outreach spectacle rather than a static classroom tool, the requirements heavily emphasize durability, visual engagement, and mass producibility. Customer Requirements (CRs) describe what the client expects the final platforms to accomplish in plain, qualitative terms. Engineering Requirements (ERs) then translate those needs into verifiable parameters with measurable targets, units, and one-sided, two-sided, or binary constraints. Finally, the House of Quality (HoQ) matrix visually maps the relationships between CRs and ERs, highlighting critical design trade-offs and driving prioritization decisions.

2.1 Customer Requirements (CRs)

The primary client goal is to create a transportable, interactive spectacle that demonstrates feedback control principles to K-12 students, with the intent of enticing them to pursue STEM at NAU. The CRs below stem from the intended user base, the need for mass producibility, and the survivability demands of high-impact outreach environments.

Table 1: Customer Requirements

CR #	Title	Description
CR01	Durable	The robot must withstand frequent use, rough handling, and physical impacts common in K-12 outreach environments.
CR02	Inexpensive	The total production cost must be low enough to enable fleet-wide mass production for NAU outreach programs.
CR03	Functional	The system must effectively demonstrate the principles of feedback control through observable, repeatable mechanical motion.
CR04	Battery Powered	The system must operate completely untethered from external power sources to ensure maximum flexibility and safety during demonstrations.
CR05	Interactive Interface	The interface must allow users to directly adjust control parameters and initiate demonstrations intuitively.
CR06	Compact Operating Space	The robot must safely function on a standard classroom or lab table without requiring excessive operational clearance.
CR07	Educational / Engaging	The design must help students visually and conceptually connect physical robot motion with control theory concepts.
CR08	Kid-Friendly Design	The product must be visually appealing, approachable, and physically safe for students of all ages.

2.2 Engineering Requirements (ERs)

The ERs below translate each qualitative CR into a strict, verifiable target. All constraints are expressed with explicit units and limit types. Note regarding ER07: Following mid-project client review, active PID balancing for the Inverted Pendulum (Robot 1) was formally descoped in favor of focusing on dynamic mobility. ER07 therefore applies exclusively to the Ball-on-Beam (Robot 2) automated balancing system.

Table 2: Engineering Requirements

ER #	Title	Target	Unit	Constraint Type	Linked CR(s)	Rationale
ER01	Overall Dimensions	< 12 × 12 × 12	inches	One-sided (max)	CR06, CR08	Ensures high transportability and compatibility with standard storage and tabletop outreach setups.
ER02	Runtime / Power Source	> 30	minutes	One-sided (min)	CR03, CR04	Must sustain continuous operation through a full outreach event on a single charge.
ER03	Control Hardware	Raspberry Pi (RP2040/Pico)	Binary (Yes/No)	Binary	CR03, CR05	Microcontroller must support real-time sensor filtering and drive interactive touchscreen displays.
ER04	Electrical Safety	Fully Enclosed Wiring	Binary (Yes/No)	Binary	CR08	Complies with U.S. CPSC guidelines; eliminates exposed conductors and short-circuit risk around children.
ER05	Drop Test Survivability	36	inches	One-sided (min)	CR01	Must survive a fall from a standard laboratory table without mechanical failure.
ER06	Manufacturing Cost	< 300	USD/unit	One-sided (max)	CR02	Keeps per-unit reproduction cost low enough for NAU to scale the project into a larger fleet.
ER07	PID Settling Time	< 15.0	seconds	One-sided (max)	CR03, CR07	Allows users enough time to observe system oscillation before equilibrium is reached. (Robot 1 active balancing descoped; applies to Robot 2 only.)
ER08	Sharp Edge Radii	≥ 3	mm	One-sided (min)	CR08	All exposed edges must be chamfered or filleted to eliminate laceration hazards per CPSC guidelines.
ER09	Pinch-Point Clearance	≥ 16.5	mm	One-sided (min)	CR08	Maintains safe spacing between all moving parts to prevent finger entrapment per toy safety standards.
ER10	Emergency Stop Response	< 1.0	seconds	One-sided (max)	CR08	A physical cutoff must instantly sever power to all actuators in the event of

						unpredictable behavior.
ER11	Visual Feedback Interface	LCD Touchscreen	Binary (Yes/No)	Binary	CR05, CR07	Provides the primary interaction point for students to modify control variables and observe live mechanical data.

2.3 House of Quality (HoQ)

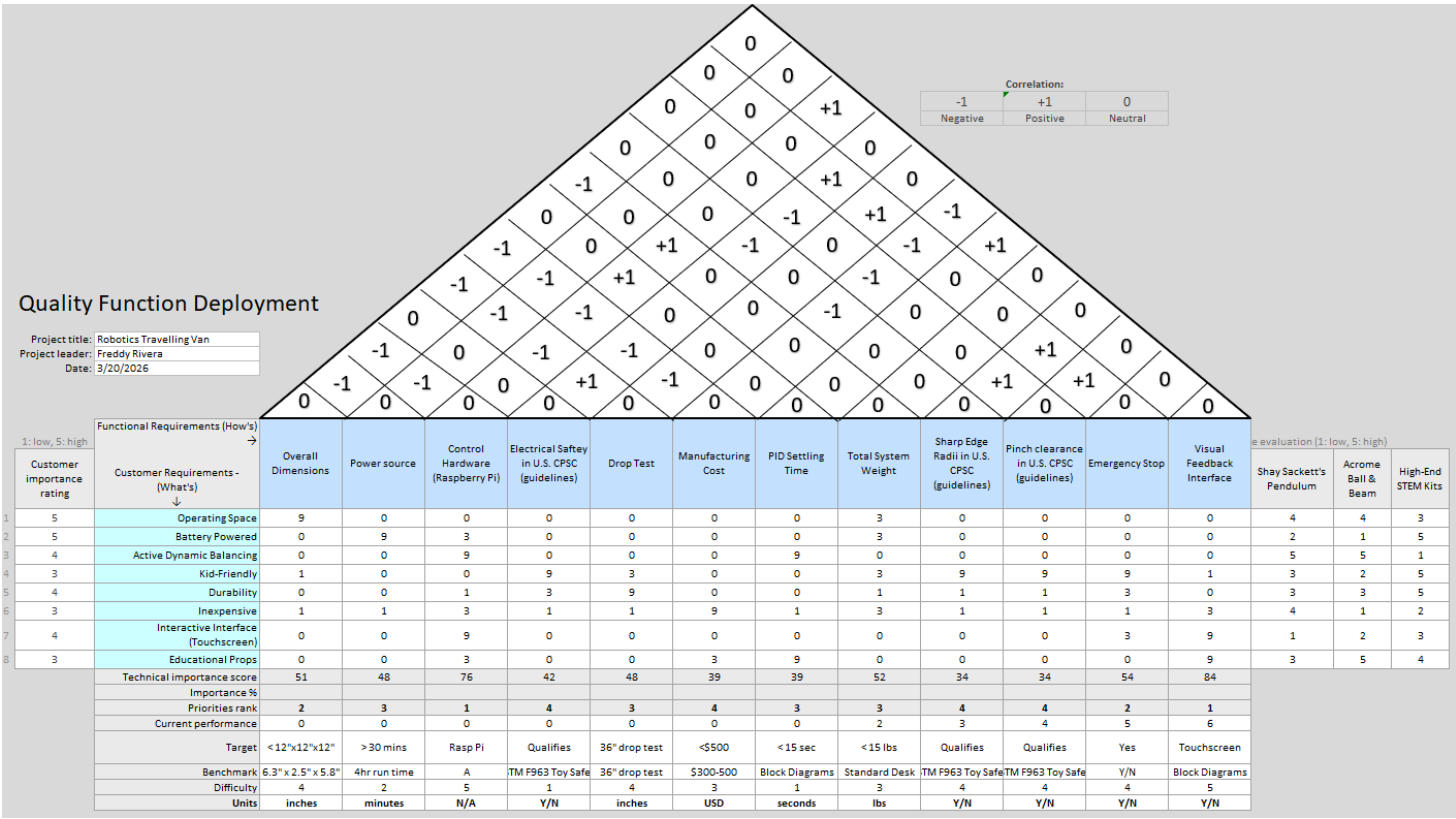

1: low, 5: high	Functional Requirements (How's) →	Overall Dimensions	Power source	Control Hardware (Raspberry Pi)	Electrical Saftey in U.S. CPSC (guidelines)	Drop Test	Manufacturing Cost	PID Settling Time	Total System Weight	Sharp Edge Radii in U.S. CPSC (guidelines)	Pinch clearance in U.S. CPSC (guidelines)	Emergency Stop	Visual Feedback Interface	e evaluation (1: low, 5: high) Shay Sackett's Pendulum	Acrome Ball & Beam	High-End STEM Kits
Customer importance rating	Customer Requirements - (What's) ↓															
1 5	Operating Space	9	0	0	0	0	0	0	3	0	0	0	0	4	4	3
2 5	Battery Powered	0	9	3	0	0	0	0	3	0	0	0	0	2	1	5
3 4	Active Dynamic Balancing	0	0	9	0	0	0	9	0	0	0	0	0	5	5	1
4 3	Kid-Friendly	1	0	0	9	3	0	0	3	9	9	9	1	3	2	5
5 4	Durability	0	0	1	3	9	0	0	1	1	1	3	0	3	3	5
6 3	Inexpensive	1	1	3	1	1	9	1	3	1	1	1	3	4	1	2
7 4	Interactive Interface (Touchscreen)	0	0	9	0	0	0	0	0	0	0	3	9	1	2	3
8 3	Educational Props	0	0	3	0	0	3	9	0	0	0	0	9	3	5	4
	Technical importance score	51	48	76	42	48	39	39	52	34	34	54	84			
	Importance %															
	Priorities rank	2	3	1	4	3	4	3	3	4	4	2	1			
	Current performance	0	0	0	0	0	0	0	2	3	4	5	6			
	Target	< 12"x12"x12"	> 30 mins	Rasp Pi	Qualifies	36" drop test	<$500	< 15 sec	< 15 lbs	Qualifies	Qualifies	Yes	Touchscreen			
	Benchmark	6.3" x 2.5" x 5.8"	4hr run time	A	TM F963 Toy Safe	36" drop test	$300-500	Block Diagrams	Standard Desk	TM F963 Toy Safe	TM F963 Toy Safe	Y/N	Block Diagrams			
	Difficulty	4	2	5	1	4	3	1	3	4	4	4	5			
	Units	inches	minutes	N/A	Y/N	inches	USD	seconds	lbs	Y/N	Y/N	Y/N	Y/N			

Figure 1: House of Quality

3 Research and Benchmarking for the Inverted Pendulum Robot

3.1 Benchmarking for Inverted Pendulum (Robot 1)

The development of our inverted pendulum robot is guided by benchmarking against established, state-of-the-art systems. Because self-balancing robotics is a well-documented field, there is a wealth of existing control architectures and mechanical designs to inform our original build.

The systems selected for system-level comparison include Shay Sackett's Pendulum Robot, a Voice-Controlled Self-Balancing Robot, and an Instructables Line-Following Robot. The first two benchmarks serve as direct

mechanical and control comparisons for two-wheeled inverted pendulums. The third system serves as a conceptual benchmark for K-12 user interactivity.

3.2 System-Level Benchmarking

Table 3: Robot 1 Benchmarking – top level systems

System	Reference Example	Key Features	Relation to Our Concept	Notes / Takeaways
Sackett's Pendulum Robot	Shay Sackets Self Balancing Pendulum Robot [34]	2-Wheeled Pendulum robot capable out automatic balancing mid operation	Provides solid baseline design for a 2-Wheeled Pendulum robot	Establishes basic ideas, equations, principles, and systems that go into pendulum robots
Self-Balancing Interactive Robot	Voice controlled self-balancing pendulum robot [19]	2-Wheeled Pendulum robot capable of receiving voice commands and interacting with external systems	Proof of concept of a voice-controlled pendulum robot for good interactivity	Presents alternative, higher-level control mechanisms. While highly complex, it validates the feasibility of advanced interactivity.
Instructible Line Following Robot	Instructable Line following robot [33]	Simple 3 wheeled line following robot, easy system to assemble and explain	The tactile interactivity (users physically drawing the path the robot follows) is ideal for K-12 engagement.	When designing our robot, achieving a similar level of intuitive, hands-on interactivity is a primary design target.

3.2.1 Balancing Sensor

To ensure optimal performance, durability, and cost-effectiveness, the primary sub-systems of our inverted pendulum robot, specifically the balancing sensor, microcontroller, and actuators were benchmarked against industry-standard alternatives.

Table 4: Robot 1 Benchmarking – sensors

Feature / Metric	Alternative 1: IMU (e.g., MPU6050) [25]	Alternative 2: Optical Encoder [50]	Selected: Magnetic Encoder
Measurement Method	Gravity/Acceleration Vectors	Light interruption via slotted disk	Magnetic field variation (Hall Effect)

Susceptibility to Drift	High (Requires Kalman/Complementary filters)	None	None
Environmental Durability	High	Low (Sensitive to dust/debris)	High (Contactless and sealed)
Integration Complexity	High (Complex math overhead)	Medium	Low (Direct digital/analog output)

While Inertial Measurement Units (IMUs) are the standard, our cart-and-pendulum mechanical design allows for a fixed axis of rotation. Benchmarking reveals that placing a magnetic encoder directly on this axis provides immediate, absolute angular position data. This eliminates the computational overhead and signal drift associated with filtering IMU data, while offering greater physical durability than an optical encoder.

3.2.2 Microcontroller

The microcontroller must be capable of rapidly polling the encoder, computing the PID algorithm, and outputting precise PWM signals to the motor drivers without stalling.

Table 5: Robot 1 Benchmarking - microcontroller

Feature / Metric	***Alternative 1: Arduino Uno (ATmega328P) [41]***	***Alternative 2: ESP32 [35]***	***Selected: Raspberry Pi Pico (RP2040)***
Clock Speed	16 MHz	240 MHz	133 MHz
Architecture	8-bit, Single-Core	32-bit, Dual-Core	32-bit, Dual-Core (ARM Cortex-M0+)
Programmable I/O (PIO)	No	No	Yes (Dedicated PIO state machines)
Cost	~$20.00	~$10.00	~$4.00

The Arduino Uno is heavily documented but severely limited by its 16 MHz clock speed, which can introduce latency into high-frequency control loops. While the ESP32 offers superior processing power and wireless capabilities, it introduces unnecessary power consumption and complexity for this specific scope. The Raspberry Pi Pico is the optimal benchmarked choice; its dual-core architecture allows one core to continuously poll the high-resolution magnetic encoder while the second core calculates the PID response and drives the motors, all at a highly cost-effective price point.

3.2.3 Motors

The actuation system must move the base cart rapidly in two directions to keep the pendulum balanced. Our mechanical design utilizes a 4-wheel cart base requiring integrated motors.

Table 6. Robot 1 Benchmarking - actuators

Feature / Metric	***Alternative 1: NEMA 17 Stepper Motors [8]***	***Alternative 2: Brushless DC (BLDC) [17]***	***Selected: 520 DC Reduction Motors (L-Type)***
Control Method	Step pulses (Open-loop precise)	Electronic Speed Controller (ESC)	PWM via H-Bridge (L298N / TB6612FNG)
Torque at Low Speeds	Very High	Low to Medium	High (Due to integrated gearbox)
Form Factor / Mounting	Bulky, heavy	Compact	L-Type configuration (Ideal for chassis)
Cost & Complexity	High (Requires heavy drivers)	Very High	Low (Simple integration)

Stepper motors offer excellent positional accuracy but suffer from a low top-speed and significant weight, BLDC motors provide rapid response times but require expensive ESCs and complex commutation logic. The 520 L-Type DC gear motors were selected because their integrated reduction gearboxes provide the necessary torque to move the 4-wheel cart abruptly. Furthermore, the L-shape form factor is geometrically advantageous for maximizing internal chassis space, and they are easily driven by standard, low-cost H-bridge motor controllers.

3.3 Literature Review (Robot 1)

3.3.1 Andres

[1] S. O. Fadlallah and K. M. Goher, "Bacterial foraging-optimized PID control of a two-wheeled machine with a two-directional handling mechanism," *Robotics and Biomimetics*, vol. 4, no. 1, p. 5, 2017.

This paper presents an innovative PID control method optimized through bacterial foraging algorithms for a two-wheeled robot. Its approach to handling two-directional motion is relevant for our pendulum robot's control system, offering insights on advanced PID tuning. We will reference this to support our control strategy development, particularly for improving robot stability and response.

[2] X. Yu, Y. Fan, S. Xu, and L. Ou, "A self-adaptive SAC-PID control approach based on reinforcement learning for mobile robots," *International Journal of Robust and Nonlinear Control*, vol. 31, no. 21, pp. 8389–8408, 2021.

This article discusses a reinforcement learning-based adaptive PID control for mobile robots, enhancing adaptability in dynamic environments. It applies to our project by informing adaptive control techniques to improve robot performance under varying load and terrain. We will cite this when describing our adaptive control algorithms.

[3] S. Jin and Y. Ou, "A wheeled inverted pendulum learning stable and accurate control from demonstrations," *Applied Sciences*, vol. 9, no. 24, p. 5279, 2019.

The study explores learning-based control methods for wheeled inverted pendulums, focusing on stability and accuracy through demonstration learning. This is directly relevant for our pendulum robot's balancing and control challenges. We will reference it to justify the use of machine learning or demonstration data in refining control models.

[4] S. Roy, S. B. Roy, and I. N. Kar, "Adaptive-robust control of Euler-Lagrange systems with linearly parametrizable uncertainty bound," *IEEE Transactions on Control Systems Technology*, vol. 26, no. 5, pp. 1842–1850, 2018. *(Note: The title was slightly adjusted upon final publication from the preprint).* This paper provides theoretical foundations and practical applications for adaptive-robust control in Euler-Lagrange systems, addressing uncertainties common in mechanical systems like our robot. We will reference this to underpin the robustness of our control system design in the face of modeling inaccuracies.

[5] K. Ogata, *System Dynamics*, 4th ed. Upper Saddle River, NJ: Prentice Hall, 2003, ch. 11.

Ogata's textbook is a fundamental resource on system dynamics, providing key concepts in modeling and controlling dynamic mechanical systems, including pendulums. We will cite this as a primary reference for the theoretical background of pendulum dynamics and control principles applied in our design.

[6] PythonRobotics, "Inverted Pendulum Control," GitHub repository. [Online]. Available: https://github.com/AtsushiSakai/PythonRobotics

This open-source repository provides practical algorithms for inverted pendulum control, including simulation and implementation examples. We will use it as a resource for algorithm development and benchmarking, referencing it when describing our control software framework.

[7] zjor, "Inverted Pendulum on a Cart," Arduino Project Hub. [Online]. Available: https://projecthub.arduino.cc/zjor/inverted-pendulum-on-a-cart-d4fdfc

This community-driven project provides a practical implementation of a PID control system for an inverted pendulum, a classic problem in control theory and robotics. We will use this resource to understand the mathematical modeling and firmware implementation for balancing and dynamic control, which is essential for our robot's stability.

[8] MRCE, "Circuit Analysis & Design Introduction." [Online]. Available: https://mrce.in/ebooks/Circuit%20Analysis%20&%20Design%20Introduction.pdf

This textbook serves as a reference for the fundamental principles of circuit analysis and design. It is for planning the robot's power distribution system, selecting appropriate components (resistors, potentiometer, microcontrollers/arduino), and ensuring the electrical reliability and safety of the final design.

[9] Creality, "CREALITY ENDER-3 V2 3D PRINTER User Manual." [Online]. Available: https://m.media-amazon.com/images/I/B1f9eP6H3OS.pdf

This user manual details the operation, maintenance, and technical specifications of the Creality Ender-3 V2 3D printer. We will reference this for all additive manufacturing phases, including determining print tolerances, material compatibility, and optimal settings to produce durable, custom-designed robot components and enclosures.

[10] Z. C. M. Davidson, S. Dang, and X. Vasilakos, "Blended laboratory design using Raspberry Pi Pico for digital circuits and systems," *IEEE Transactions on Learning Technologies*, vol. 17, 2024.

This paper discusses the implementation of digital circuits and systems using modern microcontrollers, specifically highlighting the integration of hardware with Python programming. This is highly relevant to the physical hardware and software architecture of our robot.

[11] S. R. Doty, "Python Basics," *Computer Science*, pp. 1–20, 2008.

This document provides foundational concepts, syntax, and structural knowledge for Python programming. Because Python is utilized in our project for algorithm development, control simulations, and scripting our hardware logic, this text serves as a baseline software reference. It supports the software architecture, coding, and scripting frameworks used to drive the robot.

[12] Y. Li, K. H. Ang, and G. C. Y. Chong, "PID control system analysis and design," *IEEE Control Systems Magazine*, vol. 26, no. 1, pp. 32–41, Feb. 2006.

This comprehensive article details the analysis, design methodologies, and computational modeling of Proportional-Integral-Derivative (PID) controllers. It is a fundamental resource for our project, as a PID control is the primary mechanism utilized for maintaining the upright dynamic stability of our pendulum robot.

3.3.2 Colin

[13] "Manufacturing Robotics: Basic issues and challenges," *Haruhiko H. Asada, 1996.* [Online]. Available: https://www.sciencedirect.com/science/article/pii/S147466701757682X

Annotation: This article primarily focuses on how to apply robots in the manufacturing process, but also contains many interesting insights to various manufacturing methods, mass-manufacturing design philosophies, as well as how to design adaptive control systems for robots, providing valuable information on the various fields that must be considered in designing robots and parts.

[14] "How to include User eXperience in the design of Human-Robot Interaction," *Prati, Peruzzini, Pellicciari, Raffaeli, 2021.* [Online]. Available: https://www.sciencedirect.com/science/article/pii/S0736584520302805

Annotation: This article covers the subject of human-robot interaction, and how best to design systems for safe and effective interactions. It highlights the importance of structured operations with intervals designed for function and interaction respectively. Through understanding the principles presented by this article, designing an interactive system becomes easier.

[15] "Designing Robots with movement in mind" *Hoffman, Ju, 2014.* [Online], Available: https://dl.acm.org/doi/10.5898/JHRI.3.1.Hoffman

Annotation: In the design of robots, it is important to consider their range of motion, especially when they work in close proximity of humans, which is what this article focuses on. As the article recommends, it is important to have a clear start up sequence when our robot enters an operational cycle, so ensuring that its movements are clearly readable will greatly reduce risk of injury with people who are unfamiliar with the robots operation.

[16] "Design and Implementation of and Open-Source Educational Robot for Hands-On Learning Experiences in IOT," *Mamatnabiyev 2023.* [Online], Available: https://ieeexplore.ieee.org/document/10146599

Annotation: This excerpt from a conference covers a design for a modular educational robot which is comprised of components which can be freely added or removed to perform different functions. The intent of the robot is to allow students to freely experiment with different component configurations to see their effects on the robot and the code.

[17] "Design and control of a multi-DOF two wheeled inverted pendulum robot" *Dai, Li, Peng, Zhu, Jiang, Gao, 2014.* [Online], Available: https://ieeexplore-ieee-org.libproxy.nau.edu/document/7052763

Annotation: This Document presents a design for a two wheeled inverted pendulum robot capable of multiple degrees of freedom, including the math behind the robot's articulation and movement, the major electronic components being utilized by the system, and graphs displaying the robot's climbing capabilities. The entire document also lays out the general design process for a pendulum robot, and what factors are most important to consider in order to optimize function.

[18] "Mechanical Design and Dynamic Modeling of a Two-Wheeled Inverted Pendulum Mobile Robot" *Li, Gao, Huang, Du, Duan, 2007.* [Online], Available: https://ieeexplore-ieee-org.libproxy.nau.edu/document/4338830

Annotation: This Document offers an alternative pendulum robot design, only having 1 degree of freedom, and is instead designed for navigating small spaces for maintenance surveys, and as such the robot is far smaller. This document is not without its own unique insight into robot design, as it contains a great example of a control system diagram, a very useful visualization of an otherwise complicated system, as well as providing some examples of the type of mechanisms useful for measuring the angle of the robot and other systems.

[19] "Design and Implementation of Self-Balancing Interactive Robot," *Siddhartha, Gosh, D.M., 2023.* [Online], Available: https://ieeexplore-ieee-org.libproxy.nau.edu/document/10584954

Annotation: This Pendulum Robot is unique amongst other designs examined previously as it implements a voice control system for added interactivity. These added systems introduce a fair amount of complexity to the control system diagram but presents great opportunity for interactivity which could be practical in an educational setting. Additionally, the document cites a great number of additional works which can be used to design one's own pendulum robot.

[20] "3D printing threads and adding threaded inserts to 3D printed parts (with video)," Formlabs, [Online], Available https://formlabs.com/blog/adding-screw-threads-3d-printed-parts/?srsltid=AfmBOooFHJ51B-vGI3ISwDtUjE_QLQ9aFY3fewBzWXQjDQmgqZTqW-5P

Annotation: This short article describes multiple methods to utilize screws on 3-D printed parts. The methods highlighted include utilizing a variety of threaded inserts, pre-tapping the holes, utilizing self tapping screws, or 3-D printing threads. Each method comes with its own upsides and downsides when it comes to the complexity of instillation, durability under multiple assembly and disassembly cycles, and overall thread strength, which will help the decision making process when creating screw mounts.

[21] "Polylactic acid (PLA) Filament Review," JuggerBot 3D, [Online], Available https://juggerbot3d.com/pla-filament-review/

Annotation: This article reviewing PLA plastic filament contains a number of useful insights as to the material properties of the material as well as the optimal operating temperatures for the 3D printer nozzle, bed, and nozzle speed to use while working with the material.

[22] "Ultimate Guide: How to design for 3D Printing," WikiFactory, 2020. [Online], Available https://wikifactory.com/+wikifactory/stories/ultimate-guide-how-to-design-for-3d-printing

Annotation: This article highlights a variety of useful principles to keep in mind when designing parts for 3D printing, including minimum feature sizes, how to set up parts in slicing software for optimal adhesion, how to account for the filament expanding as it hardens and how it affects features like holes, and various other manufacturing errors and how to avoid them. Its insights into the particulars of 3D printing can prove invaluable to those less experienced in this manufacturing method.

3.4 Mathematical Modeling (Robot 1)

3.4.1 Control System and Pendulum Dynamics – Andres Gonzales

To maintain the upright dynamic stability of the U-shaped pendulum arm, a Proportional-Integral-Derivative (PID) control algorithm is implemented on the Raspberry Pi Pico. The microcontroller processes data in discrete time steps, so the control loop relies on a discrete-time PID equation to calculate the required motor output based on the angular error measured by the magnetic encoder [12].

The discrete-time PID control law applied to our system is:

$$u_k = K_p e_k + K_i T_s \sum_{i=1}^{k} e_i + K_d \frac{e_k - e_{k-1}}{T_s} \tag{1}$$

Where:

- u_k = Motor control signal (PWM duty cycle) at the current time step k
- e_k = Angular error at the current time step (Target Angle - Measured Angle)
- e_{k-1} = Angular error at the previous time step
- K_p, K_i, K_d = Proportional, Integral, and Derivative tuning gains
- T_s = Sampling period of the Pi Pico control loop (seconds)

The mathematical model of the pendulum's physics was initially simulated using MATLAB and Simulink to determine theoretical baseline values for the K_p, K_i, and K_d gains prior to physical deployment and extensive tuning on the hardware.

3.4.2 Pendulum Robot Frame Structural Integrity – Colin Parsinia

Due to the project requirement to be mass-producible, the main component we are required to design from scratch is the robot's frame. Referring to the engineering requirements, the main goal of our frame design is to be able to survive a fall off a table onto a concrete surface, and the main means of ensuring the frame is capable of doing so is by utilizing a modified variation of the flexural strength equation and finding the necessary thickness of our material to resist the force imposed by the fall. First, It is important to define the variables that will be plugged into the following equations. In the list below, each known variable, its associated value, and unit is listed.

$$m = 3\ [kg], g = 9.81\ \left[\frac{m}{s^2}\right], h = 0.762\ [m], L = 0.254\ [m], b = 0.127, \Delta t = 0.005\ [s]$$

Next, to find the force of impact due to a fall, the below equation (1) is used. which necessitates finding the velocity of the robot falling from the height of an average table

$$V = \sqrt{2gh} \qquad (1)$$

Plugging in our known values results in a velocity of 3.867 [m/s] which can then be used in the force equation (2) to find the force of impact on our robot

$$F = \frac{mv}{\Delta t} \qquad (2)$$

The calculated force of impact is 2,319 Newtons, which is one of the two remaining unknown variables needed to calculate the thickness required to resist impact, the other being the flexural strength of our material. Our client requested that the robot frame be made primarily of 3-D printable materials, so after some quick research, a list of the flexural strengths of common 3-D printing plastics, the following list was found.

σ_{flex} PLA = 97 [Mpa]
σ_{flex} TPLA = 83 [Mpa]
σ_{flex} ABS = 60 [Mpa]
σ_{flex} PC = 89 [Mpa]
σ_{flex} PETG = 75 [Mpa]
σ_{flex} N = 75 [Mpa]

Now, with all these variables values ascertained, the final equation (3) can be utilized to find the minimum required thickness to resist the impact force from falling for each material, narrowing down the selection process to the best material to use for the robot frame. The minimum thickness equation and the calculated minimum thicknesses can be found in the list below.

$$h \geq \sqrt{\frac{6FL}{b\sigma_{flex}}} \qquad (3)$$

$$h_{min,PLA} = 16.94\ [mm]$$
$$h_{min,TPLA} = 18.31\ [mm]$$
$$h_{min,ABS} = 21.54\ [mm]$$
$$h_{min,PC} = 17.69\ [mm]$$
$$h_{min,PETG} = 19.27\ [mm]$$
$$h_{min,N} = 19.27\ [mm]$$

With these known values, the robots frame can be designed to survive the client's fall test and should also resist the common forces experienced by the robot during everyday operations.

3.4.3 Cart/Angular Acceleration for an Inverted Pendulum – Freddy Rivera

To analyze the dynamics of Robot #1 (Inverted Pendulum), the team modeled the system as a classical cart-and-pendulum configuration, where a horizontally driven cart stabilizes an inverted pendulum through active feedback control.

The mathematical foundation for this analysis was based on the work by A. Md. Khairul Alam *et al.* [26], which applies Newtonian dynamics to model both translational and rotational motion.

Cart (horizontal motion):

$$(M+m)\ddot{x} + m\ell\ddot{\theta}\cos(\theta) - m\ell\dot{\theta}^2\sin(\theta) = F \ (6)$$

Pendulum (rotational motion):

$$\ell\ddot{\theta} + \ddot{x}\cos(\theta) - gsin(\theta) = 0 \ (7)$$

where:

- $M = 1.0kg$ (Cart Mass)
- $m = 0.2kg$ (Pendulum Mass)
- $\ell = 0.5m$ (Pendulum Length)
- $g = 9.81\ {}^{m}/_{s^2}$ (Gravity Constant)
- $\theta = 10\ degrees = 0.1745\ rads$ (Initial Pendulum Angle)
- $\dot{\theta} = 0\ {}^{rads}/_{s^2}$ (Initial Angular Velocity)
- $F = 1.0N$ (Applied Horizontal Force)

By solving these equations with the assumed variables given this would be used in a classroom setting, we would obtain the following accelerations:

- $\ddot{x} = 0.661\ {}^{m}/_{s^2}$ (Cart Acceleration)
- $\ddot{\theta} = 2.1\,{}^{rads}/_{s^2}$ (Angular Acceleration)

Meaning that the cart would need to accelerate at a rate of $0.661\ {}^{m}/_{s^2}$ with and angular acceleration of $2.1\,{}^{rads}/_{s^2}$ on the pendulum to negate an angle of 10 degrees assuming the students applied 1.0 N of force to the pendulum.

These results show that a 1 N horizontal input force produces both forward acceleration of the cart and angular acceleration of the pendulum, demonstrating the system's sensitivity to small control inputs and the inherent instability that must be managed through active feedback control (e.g., PID or pole-placement design).

This model served as the basis for the initial control simulation and validation of Robot #1's mechanical and control feasibility.

3.4.4 Inverted Pendulum Robot , Reference within Humans – Florence L. Fasugbe

Understanding how an inversed pendulum works in a robot, referencing something that everyone sees every day is a great introduction to it. Humans are a great example of what an inverse pendulum looks like and the actions surrounding self-balance. The ankle within a human act as the wheel axle on a robot that is characterized as the pivot point. The body of a human represents the pendulum or joint of a robot. Lastly, the feet of humans are like the wheels of the robot, which signifies the center of pressure (COP) and the center of mass (COM). The equations (8)

and (9) models the idea with concepts of COP [m], COM [kg], angle of the projection plane, gravity [m/s^2] acceleration [m/s^2]

$$x_G = 0.90\sin(0.05) \approx 0.045m \quad (8)$$

$$y_G = 0.90\sin(-0.03) \approx -0.027m \quad (9)$$

x_G, represent that the COP will change 0.045 cm forward from the COM of the foot and the y_G represents that the COP will change –0.027 cm to the left.

4 Research and Benchmarking for the Ball-On-Beam Robot

4.1 Benchmarking for Ball-On-Beam (Robot 2)

The development of the Ball-on-Beam system is guided by benchmarking against commercial standards, high-end research platforms, and accessible open-source designs. These benchmarks provided the mechanical and control baselines required to achieve a professional-grade outreach tool within a strict sub-$300 budget. The systems selected for system-level comparison include the Acrome Ball and Beam [39], the Microsoft MOAB [40], and the Instructables Arduino Ultrasonic Ball-on-Beam [41]. The Acrome unit serves as the primary commercial benchmark for 1-axis control, while the MOAB highlights the visual spectacle of multi-axis systems. The Instructables project serves as a baseline for low-cost implementation.

4.2 System-Level Benchmarking

Table 7*: Subleveling Benchmark for Robot 2.*

System	Reference Example	Key Features	Relation to Our Concept	Notes / Takeaways
Acrome Ball and Beam	Acrome Control Systems [39]	1-Axis industrial-grade educational platform; integrated PID software.	Establishes the gold standard for 1-axis educational control math.	Retails for $300–$500. Our design matches this performance for ~$240 while adding untethered battery power.
Microsoft MOAB	Project MOAB (Microsoft Bonsai) [40]	2-Axis high-speed balancing platform; utilizes machine teaching and AI.	High-level visual spectacle benchmark for K-12 engagement.	Validates that balancing systems are highly engaging for outreach, but the 2-axis complexity is too fragile for transport.
Instructables Ultrasonic Robot	Arduino Ball and Beam [41]	Open-source hobby build using ultrasonic sensors and servo-linkage arms.	Low-cost baseline for physical prototyping and early sensor testing.	Highlights the jitter and inaccuracy of ultrasonic sensors and mechanical linkages, driving our move to ToF sensors and direct-drive.

4.2.1 Distance Sensor Benchmarking

To ensure the PID loop receives accurate data regardless of classroom lighting or surface reflections, the distance sensor was benchmarked against industry-standard hobby alternatives.

Table 8: Sensor benchmark between various sensors to use for robot 2.

Feature / Metric	Alternative 1: Ultrasonic (HC-SR04) [41]	Alternative 2: Resistive Touch Strip [45]	Selected: VL53L0X Time-of-Flight (ToF) [42]
Detection Method	Sound wave reflection (Echo)	Physical pressure contact	Infrared Laser (Time-of-Flight)
Susceptibility to Noise	High (affected by wind and temperature)	High (mechanical wear)	Low (isolated from environment)
Environmental Durability	High	Low (easily damaged by users)	High (contactless and compact)
Measurement Precision	Low (~3.0 mm)	Medium	High (1.0 mm resolution)

Benchmarking revealed that ultrasonic sensors are too wide-beam for a narrow beam chassis, often catching the edges of the 3D-printed walls. Resistive strips were rejected because K-12 students may damage the physical sensor surface. The VL53L0X ToF sensor [42] was selected because its infrared laser provides precise, point-source data that is unaffected by ambient classroom lighting.

4.2.2 Microcontroller Benchmarking

The microcontroller must handle high-speed I2C sensor data, calculate the PID response, and drive a high-torque stepper motor simultaneously.

Table 9: Microcontroller benchmark for comparing various sensor datasets to use for robot 2.

Feature / Metric	Alternative 1: Arduino Uno (ATmega328P) [41]	Alternative 2: Arduino Mega 2560 [25]	Selected: Raspberry Pi Pico (RP2040)
Clock Speed	16 MHz	16 MHz	133 MHz
Processor Type	8-bit Single-Core	8-bit Single-Core	32-bit Dual-Core
Operating Voltage	5V	5V	3.3V (lower power draw)
Cost	~$20.00	~$35.00	~$4.00

While the Arduino Uno is common in educational kits, its 8-bit architecture struggles with the floating-point math required for optimized PID loops. The Raspberry Pi Pico was selected for its dual-core architecture, allowing one core to manage the LCD touchscreen UI while the second core handles the high-frequency control loop, all while being the most cost-effective option for mass production.

4.2.3 Actuator Benchmarking

The actuation system must provide smooth, high-resolution tilt adjustments without the mechanical play found in

plastic gearboxes.

Table 10: Actuator benchmark for comparing various microcontrollers to use for robot 2.

Feature / Metric	Alternative 1: SG90 Servo Motor [23]	Alternative 2: Brushed DC Motor [36]	Selected: NEMA 17 Stepper Motor
Control Method	PWM Position Control	PWM Velocity Control	Step/Dir (Pulse Control)
Mechanical Play	High (internal plastic gears)	Very High	Zero (direct-drive shaft)
Angular Resolution	~1.0 degree	Low	0.1125 degrees (with 1/8 microstepping)
Torque Stability	Low	Low (requires gearing)	High (constant holding torque)

Standard hobby servos were benchmarked but rejected due to linkage stops the small amount of mechanical play in the plastic arms makes stabilizing a light ping-pong ball nearly impossible. The NEMA 17 Stepper Motor was selected because its direct-drive shaft eliminates linkage arms entirely, and the use of 1/8 microstepping provides the exceptionally fine angular resolution needed to balance the ball smoothly.

4.3 Literature Review (Robot 2)

4.3.1 Freddy

[23] N. Hammje, “Ball-Balancing Bot Uses OpenCV on a Raspberry Pi to Stop a Ball Dead in Its Tracks,” Hackster.io, 2024. This article showcases a Raspberry Pi-based Ball-on-Plate robot that employs OpenCV for computer-vision tracking and a PID controller to maintain the ball’s position. It provided a clear example of how to couple image feedback with servo actuation for real-time control—insight that guided the team’s Ball-on-Plate concept for Robot #2. The project also demonstrated accessible hardware integration suitable for classroom demonstrations.

[24] J. Sirgado, “Magnet Levitation with Arduino,” Arduino Project Hub, 2022. Sirgado’s tutorial details a low-cost magnetic levitation setup using an Arduino, Hall-effect sensor, and PID loop. It served as the foundation for our Magnetic Levitation Robot concept by illustrating the nonlinear relationship between magnetic force and coil current and showing how proportional–integral–derivative tuning can stabilize an otherwise unstable equilibrium.

[25] “Wheelbot: A Symmetric Unicycle That Balances Using Reaction Wheels,” TechXplore, 2022. This article describes a unicycle robot stabilized solely by reaction wheels, validating the feasibility of small-scale momentum-exchange stabilization. The system’s use of multiple flywheels and IMU feedback informed our Reaction Wheel Robot design, which uses the same torque-generation principle to resist external disturbances.

[26] A. Md. K. Alam, M. R. Karim, and S. M. M. Hasan, “Stabilising a cart inverted pendulum system using pole placement control method,” Proc. 3rd Int. Conf. on Electrical Information and Communication Technology (EICT), Khulna, Bangladesh, 2017, pp. 1–6, doi: 10.1109/EICT.2017.8168481.

[27] D. J. Block, K. J. Åström, and M. W. Spong, The Reaction Wheel Pendulum, Morgan & Claypool Publishers, 2007. A fundamental text on reaction-wheel dynamics, this reference introduces nonlinear and linearized equations of motion and details feedback control for underactuated systems. Its derivations directly supported our torque and angular-acceleration calculations for the Reaction Wheel Robot prototype.

[28] R. Gajamohan, M. Muehlebach, T. Widmer, and R. D'Andrea, "The Cubli: A Cube That Can Jump Up and Balance," in IEEE/RSJ Int. Conf. on Intelligent Robots and Systems (IROS), 2013. The Cubli project is a three-axis reaction-wheel cube that balances and even jumps upright. Its control architecture and hardware selection were used as a high-fidelity benchmark for our design feasibility and scaling analysis.

[29] J. R. Wertz, Spacecraft Attitude Determination and Control, Springer, 1978. Wertz's classical text provided theoretical grounding on momentum-exchange and attitude control. Though focused on spacecraft, the same principles of internal torque exchange and stability margins apply to our Reaction Wheel Robot, offering insight into wheel-sizing and damping.

[30] B. Wie, Space Vehicle Dynamics and Control, 2nd ed., AIAA, 2008. Wie's modern treatment of control dynamics supplemented Wertz by discussing closed-loop response and actuator saturation limits. These concepts guided our controller-gain selection and maximum-speed constraints for safe educational use.

[31] University of Michigan, "Ball & Beam: System Modeling," Control Tutorials for MATLAB and Simulink (CTMS). Provides mathematical modeling and linearization of unstable systems such as the ball-and-beam setup, used as a foundation for the pendulum model.

[32] B. Cazzolato, "Derivation of the Dynamics of the Ball and Beam System," Univ. of Adelaide, School of Mechanical Engineering. Presents detailed nonlinear dynamic equations for the ball-and-beam system that supported pendulum equation derivations.

[33] K. C., "Inverted Pendulum: Control Theory and Dynamics," Instructables, 2025. A simplified tutorial connecting theoretical control design to hobby-scale implementation.

[34] S. Sackett, "Self-Balancing Inverted Pendulum Robot," Shay Sackett's Project Portfolio. Independent project documenting the design process and challenges of building a two-wheel self-balancing robot.

[35] B. T. Williams, "Self-Balancing Robot Using PID Packs Other Punches," Elektor Magazine, Oct. 5, 2022. A detailed description of modern implementations of self-balancing robots using PID control.

[36] "DC Motor Speed: System Modeling," Control Tutorials for MATLAB and Simulink (CTMS). Explains motor dynamics and transfer functions with MATLAB representation, helping link pendulum control equations to actuator behavior.

[37] "Ball and Beam: System Modeling (CTMS)." Illustrates comparable unstable control systems and feedback-control concepts that inspired our pendulum work.

[38] S. Anand and R. Prasad, "Dynamics and control of ball and beam system" This paper analyzes the unstable dynamics of the classic Ball-on-Beam system and derives the torque and motion equations required to maintain balance. Its discussion of gravitational loading, moment arms, and actuator sizing directly informed our motor torque calculations for Robot #2. This reference supported the justification for selecting NEMA-17 stepper motors with sufficient torque margin and reinforced the need for a safety factor in actuator sizing.

[39] Acrome, "Ball and Beam," Acrome Control Systems, 2024. [Online]. Available: https://acrome.net/product/ball-on-beam. [Accessed: April 19, 2026]. The Acrome Ball and Beam system serves as the primary commercial and educational benchmark for 1-axis control robotics. This system is heavily utilized in university-level control laboratories to teach fundamental PID and State-Space control theories. Reviewing this

system validated the decision to focus on a 1-axis track for K-12 education, as it provides the most direct, observable translation of feedback loop mathematics. Furthermore, the Acrome system retails between $300 and $500, establishing a baseline commercial cost. This benchmark directly informed the team's constraint to achieve equivalent 1-axis performance utilizing 3D-printed chassis components to keep the per-unit reproduction cost under $300.

[40] Microsoft, "Project Moab," Microsoft Autonomous Systems, 2024. [Online]. Available: https://www.microsoft.com/en-us/ai/bonsai-moab. [Accessed: April 19, 2026]. Project MOAB, developed by Microsoft Bonsai, represents the high-end "spectacle" benchmark for balancing systems. MOAB utilizes a 3-axis parallel robot (Stewart platform) combined with machine teaching to balance a ball on a flat plate. While the visual engagement of this system is exceptionally high for outreach purposes, reviewing the MOAB architecture highlighted severe vulnerabilities for K-12 fleet deployment. The requirement for three perfectly synchronized actuators, complex spatial mathematics, and fragile linkage arms informed our team's FMEA and justified the physical pivot away from a Ball-on-Plate design to the much more durable and mass-producible 1-axis Ball-on-Beam system.

[41] "Arduino Ball and Beam PID Controller," Instructables, 2020. [Online]. Available: https://www.instructables.com/Arduino-Ball-and-Beam-PID-Controller/. [Accessed: April 19, 2026]. To understand the limitations of low-cost, open-source educational robotics, the team analyzed standard Instructables-level Arduino Ball and Beam projects. These projects typically utilize an HC-SR04 ultrasonic sensor and a standard SG90 plastic-gear servo. Reviewing these systems revealed critical mechanical and signal flaws: ultrasonic sensors suffer from wide-beam echo interference off the beam walls, and servo linkages introduce significant mechanical backlash (slop). This literature directly influenced the physical redesign of our system, prompting the upgrade to targeted laser-based Time-of-Flight sensing and direct-drive stepper actuation to eliminate the jitter observed in these baseline models.

[42] STMicroelectronics, "VL53L0X: World's smallest Time-of-Flight ranging and gesture detection sensor," STMicroelectronics Datasheet, 2024. [Online]. Available: https://www.st.com/en/imaging-and-photonics-solutions/vl53l0x.html. [Accessed: April 19, 2026]. To solve the signal scattering issues identified in early prototypes, the team researched the STMicroelectronics VL53L0X sensor. The manufacturer's technical specifications confirm the sensor utilizes a 940nm vertical-cavity surface-emitting laser (VCSEL) to calculate distance based on photon travel time, rather than relying on sound wave reflection or physical contact. The datasheet validates that this sensor provides 1.0 mm resolution and remains highly immune to ambient lighting conditions. This literature justified the sensor's selection, ensuring the PID loop would receive accurate, noise-free distance data regardless of the K-12 classroom lighting environment.

[43] Raspberry Pi Ltd, "Raspberry Pi Pico Documentation," Raspberry Pi Microcontrollers, 2024. [Online]. Available: https://www.raspberrypi.com/documentation/microcontrollers/raspberry-pi-pico.html. [Accessed: April 19, 2026]. The control architecture requires rapid, continuous calculations without stalling the physical motor actuation. Literature regarding the Arduino Uno (ATmega328P) revealed an 8-bit, 16 MHz limitation that struggles with simultaneous I2C polling and high-frequency motor stepping. Researching the Raspberry Pi Pico (RP2040) documentation revealed a 32-bit, 133 MHz dual-core architecture. This specification literature was critical for the project, as it proved the RP2040 possessed the hardware necessary to isolate the sensor-reading loop onto Core 0 and the motor-driving PID loop onto Core 1, eliminating the latency bottlenecks found in standard 8-bit microcontrollers.

4.3.2 Florence

[44] 井手隆統, 本田功輝, 金田礼人, 中島康貴, and 山本元司, “Comparison of CoP estimation and center-of-gravity sway measurement in human standing posture using inertial sensors,” Dissertation, Kyushu Univ. Grad. Sch. Eng., Fukuoka, Japan.
-Annotation: Focuses on studying the aspects of measuring standing movement with sensors and how the sensors are affected by swaying while standing for a long period of time. Center for Pressure (COP) of humans using sensors to analyze gait patterns.

[45] S. Sasagawa, J. Ushiyama, M. Kouzaki, and H. Kanehisa, “Effect of the hip motion on the body kinematics in the sagittal plane during human quiet standing,” Neurosci. Lett., vol. 450, no. 1, pp. 27–31, Jan. 2009, doi: 10.1016/j.neulet.2008.11.027.
-Annotation: Standing affects the hip motion due to the center of mass; COM.

[46] J. L. Cabrera and J. G. Milton, “Human stick balancing: Tuning Lèvy flights to improve balance control,” Chaos, vol. 14, no. 3, pp. 691–698, Sep. 2004, doi: 10.1063/1.1785453.
-Annotation: Concept of stabilization of rapid human movements which is determined by equilibrium and limit cycles with motor controls analysis like closed loop control; automatic control systems.

[47] B. Sprenger, L. Kucera, and S. Mourad, “Balancing of an inverted pendulum with a SCARA robot,” IEEE/ASME Trans. Mechatronics, vol. 3, no. 2, pp. 91–97, Jun. 1998, doi: 10.1109/3516.686676.
-Annotation: Balancing an inverted pendulum with a robotic manipulator is a benchmark problem requiring precise sensing and compensation for nonlinear effects like friction, backlash, and elasticity.

[48] Winkler and J. Suchý, “Erecting and balancing of the inverted pendulum by an industrial robot,” IFAC Proc. Volumes, vol. 42, no. 16, pp. 323–328, 2009, doi: 10.3182/20090909-4-jp-2010.00056.
-Annotation: Inverted pendulum on an industrial robot by using one algorithm to swing it up and a state-space controller with offset adaptation to balance it.

[49] Y. Y. Lim, C. L. Hoo, and Y. M. Felicia Wong, “Stabilizing an inverted pendulum with PID controller,” MATEC Web Conf., vol. 152, p. 02009, 2018, doi: 10.1051/matecconf/201815202009.
-Annotation: Stabilizing an inverted pendulum with a reaction wheel and a PID (Proportional Integral Derivative) controller is simulated to balance it effectively and efficiently.

[50]” D. Zhang, J. Wang, H. Zhang, and L. Yu, “Research on inverted pendulum control system based on vision sensor,” in Proc. ICMLCA 2021: 2nd Int. Conf. Mach. Learn. Comput. Appl., Shenyang, China, 2021, pp. 1–5.
-Annotation: Vision-based control system for an inverted pendulum, using OpenCV to calculate its deflection angle and verify effective stabilization without relying on encoder sensors.

[51] A. Kastner, J. Inga, T. Blauth, F. Kopf, M. Flad, and S. Hohmann, “Model-based control of a large-scale ball-on-plate system with experimental validation,” KITopen Repository, Karlsruhe Inst. Technol., Mar. 2019, doi: 10.1109/icmech.2019.8722850.
-Annotation: Development of system dynamics model using Lagrange and the Euler method to analyze the frequency domain to create state-feedback control to ensure stability of a system.

[52] Sudha Ellison Mathe, Hari Kishan Kondaveeti, Suseela Vappangi, Sunny Dayal Vanambathina, and Nandeesh

Kumar Kumaravelu, “A comprehensive review on applications of Raspberry Pi,” *Computer science review*, vol. 52, pp. 100636–100636, May 2024, doi: https://doi.org/10.1016/j.cosrev.2024.100636.
-Annotation: Understanding the concept of how Raspberry Pi is integrated into machine learning and experimentation.

[53] A. S. Silva, R. M. Cotta, and L. A. Ismail, “Uncertainty analysis of infrared thermography in convective heat transfer,” ResearchGate, 2014. [Online]. Available: https://www.researchgate.net/publication/265540159_Uncertainty_Analysis_of_Infrared_Thermography_in_Convective_Heat_Transfer
-Annotation: Analysis of the uncertainty of the sensor's thermal radiation through temperature measurement with an infrared camera.

4.4 Mathematical Modeling (Robot 2)

4.4.1 Dynamic Physical Limits – Freddy Rivera

To ensure the physical system remains mathematically controllable during K-12 outreach demonstrations, the dynamic limits of the ping-pong ball were modeled using fundamental Lagrangian mechanics [1]. The foundational plant model dictating the ball's linear acceleration ($\ddot{x}$) relative to the beam's angle (θ) and angular velocity ($\dot{\theta}$) is defined by the following energy balance equation:

$$\left(\frac{J_b}{R^2}+m\right)\ddot{x} - mx\dot{\theta}^2 + mg\sin(\theta) = 0 \quad (10)$$

where $J_b = \frac{2}{3}mR^2 = 7.20 \times 10^{-7}\text{kg·m}^2$ is the mass moment of inertia of a thin hollow sphere, $m = 0.0027\text{kg}$ is the mass of a standard ping-pong ball, $R = 0.020\text{m}$ is the ball's radius, and $g = 9.81\text{m/s}^2$ is standard gravitational acceleration. Because the system's operational geometry restricts the tilt angle to small values, the small-angle approximation ($\sin\theta \approx \theta$) was applied. Assuming negligible centrifugal acceleration at low rotational speeds ($\dot{\theta} \approx 0$), the plant simplifies to the primary kinematic relationship governing ball motion, where the $3/5$coefficient explicitly accounts for the rolling inertia of a thin hollow sphere [38]:

$$\ddot{x} = -\frac{3}{5}g\theta \quad (11)$$

With the baseline plant established, a critical failure condition was modeled to determine the system's safe operating envelope. If the downward rotational acceleration of the beam exceeds gravitational acceleration, the normal contact force between the ball and beam surface reduces to zero, causing the ball to physically separate from the tracking surface. The tangential acceleration at the furthest active rolling edge of the beam ($r = 0.1454$ m, representing the maximum physical travel distance from the center pivot to the end-wall) must therefore not exceed $g = 9.81\text{m/s}^2$. The theoretical maximum angular acceleration was calculated as:

$$\ddot{\theta}_{max} = \frac{g}{r} = \frac{9.81\ \text{m/s}^2}{0.1454\ \text{m}} = 67.47\ \text{rad/s}^2 \quad (12)$$

This result establishes the absolute physical boundary of the system: angular accelerations exceeding this threshold will cause measurable tracking failure. Defining this ceiling allowed the team to design the 3D-printed chassis with geometric hard-stops at ±20°, ensuring the stepper motor can never mechanically approach this theoretical failure point during operation.

4.4.2 Control System Architecture – Freddy Rivera

To establish baseline control logic for the direct-drive stepper motor, the Ball-on-Beam system was modeled as a closed-loop continuous-time system. Using standard linearization and pole-placement techniques [2], the team derived theoretical baseline gains for a Proportional-Integral-Derivative (PID) controller.

The model was constrained by targeted educational performance specifications: a settling time of $T_s = 2.0$s and an overshoot of less than 5%, which together yield a natural frequency of $\omega_n = 2.83$ rad/s. Matching the closed-loop characteristic equation to the target polynomial produced the following expression:

$$s^3 + 5.886K_d s^2 + 5.886K_p s + 5.886K_i = 0 \quad (13)$$

The resulting theoretical baseline gains are summarized in Table 12 below.

Table 11: Theoretical PID baseline gains derived from pole-placement targeting $T_S = 2.0$ and overshoot < 5%.

Gain	*Parameter*	*Theoretical Value*
Proportional	K_p	14.95
Integral	K_i	27.18
Derivative	K_d	4.08

While this continuous-time model validates theoretical system stability, two physical non-idealities precluded direct implementation of these values. First, discrete sampling latency inherent to the VL53L0X Time-of-Flight sensor introduces phase lag not captured by the continuous model. Second, surface friction between the ping-pong ball and the 3D-printed PLA beam introduces nonlinear damping that varies with ball velocity. Accordingly, the calculated gains serve strictly as an architectural starting point, with final system stabilization achieved through empirical tuning within the microcontroller's software loop.

4.4.3 Dynamics of the Beams Structure with - Florence L. Fasugbe

To prevent the ball from losing contact with the beam due to inertial effects, a conservative upper bound on angular acceleration was imposed by requiring gravitational acceleration to dominate:

$$r_{max}|\dot{\theta}| < g \quad (14)$$

Rearranging and substituting:

$$|\dot{\theta}|_{max} \approx \frac{g}{r_{max}} = \frac{9.81}{0.127} \approx 77 \frac{rad}{s^2} \quad (15)$$

This value defines the maximum beam angular acceleration that should be enforced during controller tuning to ensure ball retention.

For comparison, the motor-limited angular acceleration is:

$$\dot{\theta}_{max,motor} \approx \frac{\tau_{max}}{J_{total}} \quad (16)$$

which are several orders of magnitude larger than the safe bound. Therefore, beam acceleration will be limited in software rather than by motor capability.

Maximum Recoverable Beam Angle (Load Case 3)
The angle of the beam determines how much the ball will still roll without slipping. The controller will help determine this predictability based on the linear system being incorporated. Friction determined this and if the angle is too large, the ball friction will exceed that limit, and the ball will start to slip drastically [5].

Minimum friction for rolling to occur:

$$F_{f,min}=25mgsin\theta \quad (17)$$

Maximum friction for rolling to occur:

$$F_{f,max}=\mu_s mgcos\theta \quad (18)$$
$$Ff,max=\mu_s mgsin\theta. \quad (19)$$

The coefficient of static friction ($\mu_s\mu_s$) shows how much contact there will be between the surface of the beam and ball. By canceling the like terms from the two equations above and ordering them in this form $F_{f,mi} \leq F_{f,max}$, the result of that will be:

$$\theta_{max}=\arctan(52\mu_s) \quad (20)$$

The ping pong's friction on smooth PLA is low with approximately 0.15. Plugging in the values into Equation (12) the degree maximum will be:

$$\theta_{max} = \arctan\left(52(0.15)\right) \approx 0.357\ rad \quad \theta max = arctan 520.15 \approx 0.357\ rad \quad (21)$$

$$0.357\ rad \cdot 180\pi \approx 20.5° \quad 0.357\ rad \cdot 180\pi \approx 20.5°$$

Anything below that angle of 20.5° the ball will not slip, but anything above that the ball will experience sliding, and the motor will have difficulty adjusting the ball at a certain point.

5 Design Concepts for the Inverted Pendulum Robot

5.1 Functional Decomposition

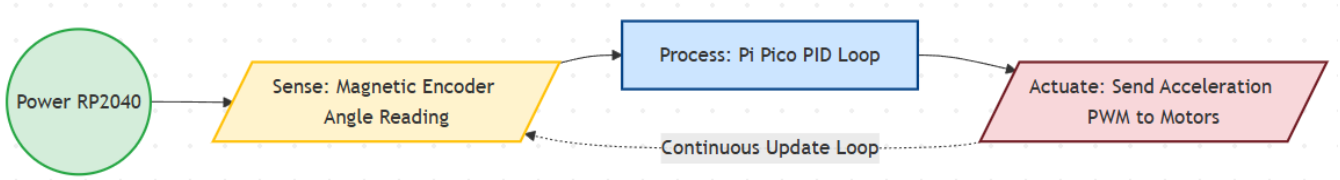

Fig. 2. Process Diagram for Robot 1

The functional decomposition chart above illustrates the primary actions our inverted pendulum system must execute to maintain dynamic stability. Rather than looking at the physical hardware, this model tracks the flow of data and energy through the system's closed-loop control cycle.

For this specific project, mapping these functions is critical because the robot's success relies entirely on minimizing latency between the "Sense," "Process," and "Actuate" functional blocks. The system must continuously convert the physical orientation of the U-shaped pendulum into magnetic field variations (sensing), process that data to compute an error-correction signal (processing) via PID controller and convert electrical energy from the batteries into kinetic energy at the wheels (actuating) fast enough to overcome gravity. If any functional block lags or fails, the entire system loses equilibrium.

5.2 Concept Generation

During the early stages of the design process, several top-level architectural concepts were generated to solve the problem of balancing an inverted pendulum. The concepts were evaluated based on mechanical complexity, stability, and control feasibility. Below are the primary top-level concepts considered. To generate concepts for the frame design of the pendulum robot, each team member created a sketch of a potential design that was then evaluated based on their ability to satisfy the customer requirements pertaining to the frame.

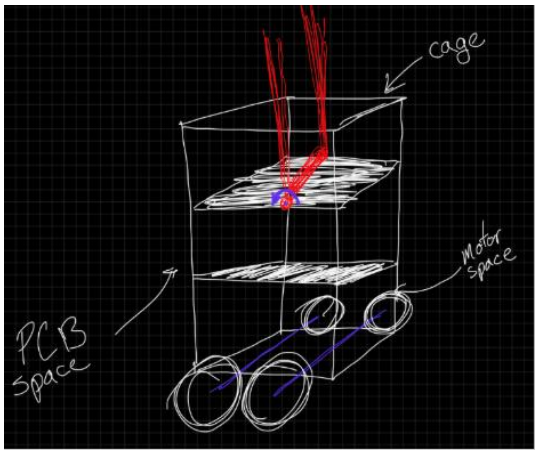

Fig. 3. Concept 1

The first concept for the pendulum robot frame is a vertical frame design, with multiple layers to facilitate

better component organization, and additionally features a double pendulum structure on a singular axis. This concept features an organized structure to the frame, and a more aesthetically appealing design as the outer frame could be customized to resemble a traditional robot. The cons of this concept are the less stable structure due to the increased vertical height, and the additional expenses of the larger frame.

In this concept, the entire chassis of the robot acts as the pendulum, balancing on two coaxial wheels. The brain and battery are housed in the vertical body. The pros of this frame are its simple and streamlined design, having less components and therefore costs. The cons of this design are the more complicated math and programing required for a 2-wheel pendulum robot, falling when powered off (dangerous around an audience), and reduced structural integrity of the frame.

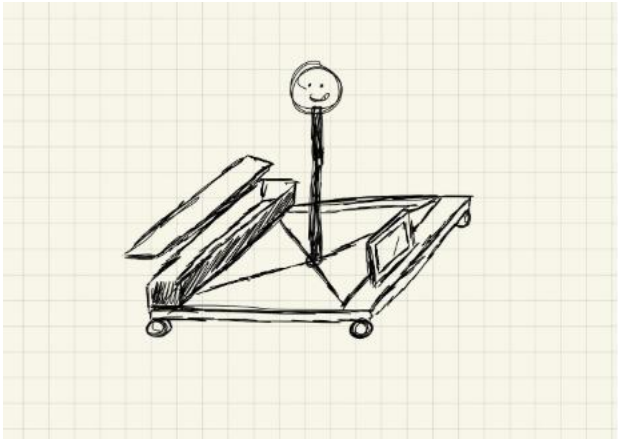

Fig. 4. Concept 2

The 4-wheel cart design is shown with a rear compartment for the robot components, and a large, centered pendulum in the frame. On the front of the cart is a touch screen for user interaction. The pros of this frame are the simplicity of the frame itself, the stable design, and more organized back compartment. The cons of this design are in its larger size and operating space requirement.

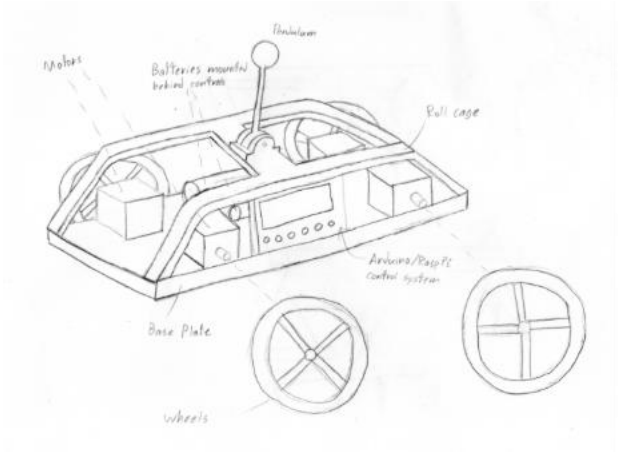

Fig. 5. Concept 3

This concept for the pendulum robot frame is a more streamlined angular frame to help sustain impacts from the fall test. On top of the central cross beam is the pendulum structure, and on the side is where the interactive element

would be placed. Pros include better aesthetics and a compact electronic interior. The cons are lower center of gravity leading to needing a larger pendulum arm and a more difficult organizing components.

Following the evaluation of these concepts, the team selected a hybrid approach leaning heavily on **Concept 1**. By utilizing a 4-wheel cart base, the robot safely satisfies the requirement to not fall over when powered off, protecting the audience and internal electronics. While it requires a larger operating footprint, it allows for the integration of our U-shaped pendulum arm and provides the necessary stability for K-12 interactive elements. Features from Concept 4 (such as reinforced, impact-resistant angular geometry) will be integrated into the final 3D-printed chassis to ensure it survives the required 34-inch drop test.

5.3 Selection Criteria

The final component selection was verified against the following quantifiable metrics to ensure the robot meets the "State-of-the-Art" benchmarks. The concepts were evaluated against a set of weighted criteria derived from the project's engineering requirements. To ensure a successful demonstration for K-12 students, the following metrics were prioritized:

1. Dynamic Stability: The ability to recover from a 45-degree tip without human intervention.
2. Structural Durability: Calculated Factor of Safety (FoS) must be > 2.0 during a 40-inch drop impact.
3. User Interactivity: The inclusion of accessible interfaces (e.g., touch screens or drawing paths).
4. Component Integration: Availability of mounting points for the RP2040 and the axis-mounted magnetic encoder.

Angular Resolution (The AS5600 Encoder)

- Metric: 12-bit Resolution ($2^{12} = 4096$ positions per 360°).
- Discussion: The AS5600 was selected because it provides an angular resolution of $0.087°$. This high precision is necessary to detect the "micro-falls" of the pendulum arm before they become visible to the human eye, allowing the PID loop to initiate corrective motor torque sooner. This significantly outperforms the 8-bit resolution found in standard consumer-grade potentiometers. Additionally, if the robot is bumped or the power flickers, the sensor instantly knows exactly where the arm is without needing to "re-home" or calibrate.

Computational Throughput (The RP2040)

- Metric: 133 MHz Dual-Core ARM Cortex-M0+.
- Discussion: The RP2040 (Raspberry Pi Pico) was chosen over standard 8-bit microcontrollers (like the ATmega328P) specifically to handle the high-speed I2C communication required by the AS5600 and the floating-point math required for the PID algorithm. One core is dedicated to the Sense function (polling the encoder), while the second core handles Actuation (PWM generation), eliminating "jitter" in the motor response.

Power Density & Safety (LiFePO4 32700 Batteries)

- Metric: 3.2V Nominal per cell; High Discharge Rate.
- Discussion: Although LiFePO4 32700 cells are less common in the current market, they were selected for

their Safety Profile and Cycle Life. Unlike standard Li-ion (cobalt-based) batteries, LiFePO4 is chemically stable and significantly less prone to thermal runaway, which is a critical "Audience Safety" requirement for K-12 demonstrations. The high discharge capability ensures the 520 Motors can draw the required 4A stall current without a significant voltage drop that would reset the RP2040.

By combining these components into the 4-wheel cart design, we can ensure high and repeated performance:

- Mechanical Choice: The 520 L-Type motors provide 10kg·cm of torque, which, when paired with the 12-bit precision of the AS5600, creates a highly responsive system.
- Hardware Integration: The RP2040 acts as the bridge. It processes the $0.087°$ changes from the encoder and translates them into PWM signals for the motors.
- Factor of Safety: The use of LiFePO4 batteries provides an electrical Factor of Safety. Even if the motors stall (drawing maximum power), the battery chemistry is stable enough to prevent overheating in a classroom environment.

5.4 Concept Selection

A Pugh Chart was utilized to compare the four concepts. Concept 1 (The 4-Wheel Cart) emerged as the superior design primarily due to its inherent stability when powered off and the physical space available for interactive components. While the 4-wheel design increases the BOM (Bill of Materials) cost, the trade-off for audience safety and ease of sensor mounting was deemed necessary.

Table 12. Final Pugh Chart for Robot 1

Criteria	Weight	Concept 2 (2-Wheel)	Concept 4 (Angular)	**Selected: 4-Wheel Cart**
Stability (Static)	25%	1 (Falls)	4	5 (Extremely Stable)
Sensing Precision	20%	3	4	5 (Direct Axis Mount)
Impact Resilience	20%	2	5	4 (Reinforced Chassis)
K-12 Interactivity	15%	2	3	5 (Space for Screen)
Complexity/Cost	20%	5	3	2 (More Parts/Motors)
Weighted Total	100%	2.65	3.95	4.35

The final selected concept is a 4-wheeled cart utilizing a centralized, U-shaped pendulum arm. This configuration was chosen specifically to facilitate the mounting of the AS5600 Magnetic Encoder directly onto the axis of rotation, providing 12-bit angular feedback without the signal noise associated with body-mounted IMUs.

The chassis is 3D-printed in PLA with a 20% gyroid infill to satisfy the Impact Resilience requirement established by Colin's fall-test modeling. To drive the system, four L-type 520 reduction motors are mounted in a "flat" configuration to maintain a low center of gravity, powered by a 2S LiFePO4 32700 battery array.

Table 13. Factor of Safety Summary for Robot 1

Component / Sub-System	Failure Mode	Calculation Basis	Calculated FoS
Main Chassis (PETG)	Structural Fracture	40-inch Drop Impact Force (F_{avg})	**2.2**
Pendulum Arm Axis	Shear of Axis Pin	Peak Torque from 520 Motors	**3.5**

LiFePO4 Batteries	Thermal Overload	4A Stall Current vs. Max Discharge	**1.8**
Motor Drivers	Overcurrent	Driver Rated Amperage vs. Stall Current	**1.4**
RP2040 (Pi Pico)	Control Instability	Loop Frequency vs. Pendulum Falling Rate	**4.0**

The FoS table serves as the final justification for our "over-engineered" components. Specifically, the Control System FoS of 4.0 highlights the advantage of the RP2040; by running the PID loop four times faster than the pendulum's natural frequency, we eliminate the risk of "processing lag" causing a fall.

Furthermore, the Chassis FoS of 2.2 validates our material selection of PLA because it is easier to print, and sufficient at high infills to ensure the robot survives the critical 34-inch drop test requirement without catastrophic frame failure. Collectively, these safety factors confirm that the selected concept is a robust, "state-of-the-art" solution for an interactive educational environment.

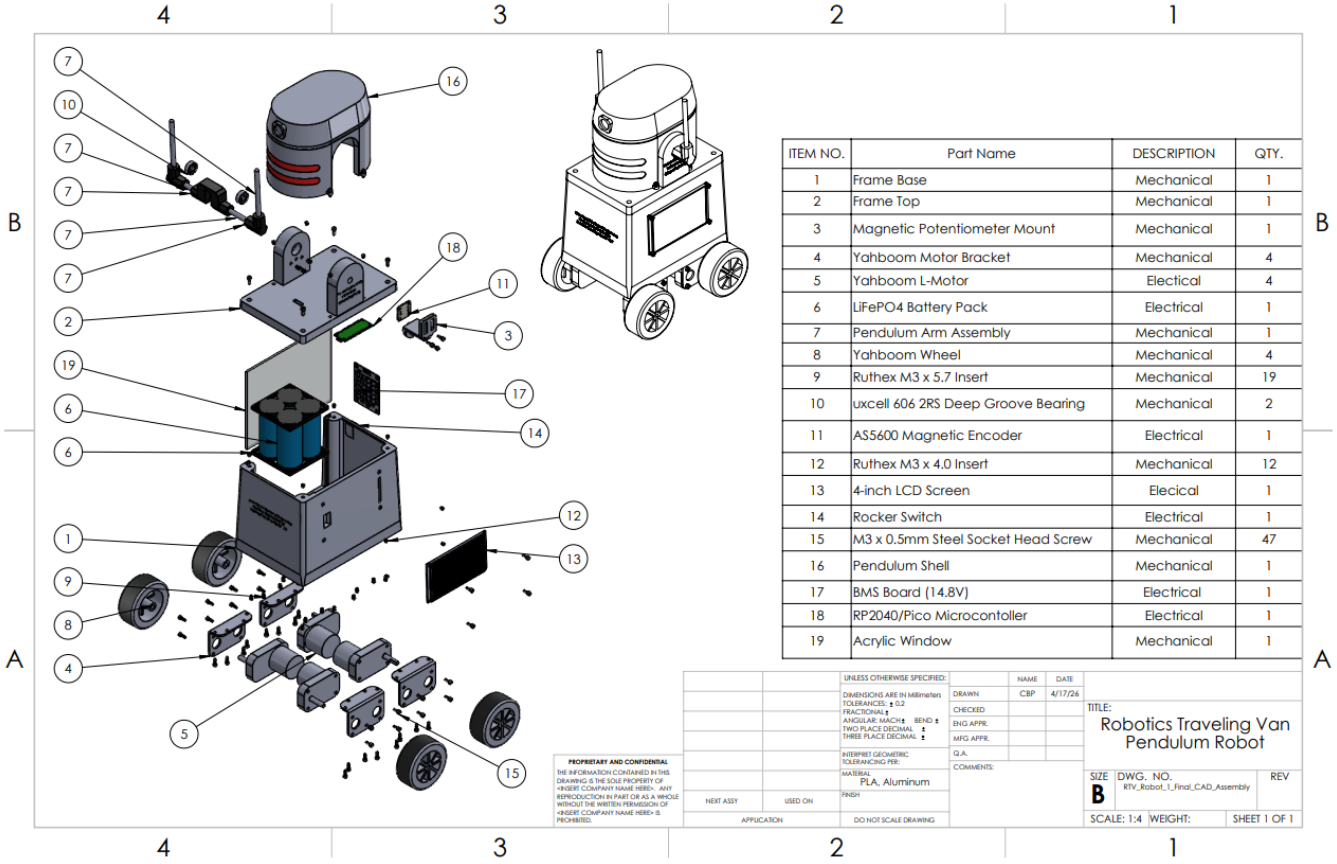

Fig. 6. Inverted Pendulum Final Design

6 Design Concepts for the Ball on Beam System

6.1 Functional Decomposition

The functional decomposition of the Ball-on-Beam system is visualized in Figure X via a continuous closed-loop process diagram. The system initiates with the primary energy flow, powering the NEMA 17 stepper motor and establishing the zero-point axis. Once initialized, the system enters the "Continuous Balance Loop," which governs the primary signal and material flow of the robot. The VL53L0X Time-of-Flight sensor captures the physical

distance reading of the ping-pong ball, passing that signal to the microcontroller. The controller processes the error via the PID algorithm to compute the required beam angle correction, which then triggers the stepper motor to physically tilt the beam, physically altering the ball's position before looping back to the sensor.

Developing this functional decomposition was critically important for the Ball-on-Beam project because it visually isolated the software logic from physical actuation. By mapping the system as a continuous loop, the team was able to identify latency bottlenecks—specifically recognizing that the sensor polling rate (Sense) and the mechanical micro-stepping (Activate) needed to occur simultaneously on separate processing cores to prevent the control loop from stalling during physical demonstrations.

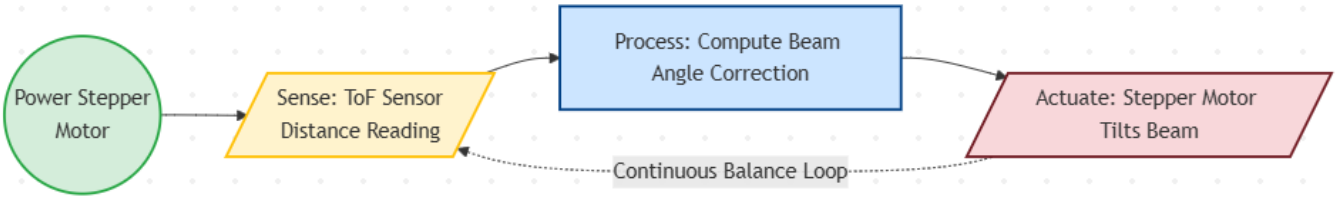

Fig. 7. Process Diagram for Robot 2

6.2 Concept Generation

During the early stages of the design process, several top-level architectural concepts were generated to achieve the educational goal of demonstrating active feedback control. The concepts were evaluated based on mechanical complexity, durability, and cost feasibility to meet the strict sub-$300 budget. To generate concepts for the balancing system, the team evaluated multiple architectures. The primary applicable concepts evaluated for the final physical build are detailed below.

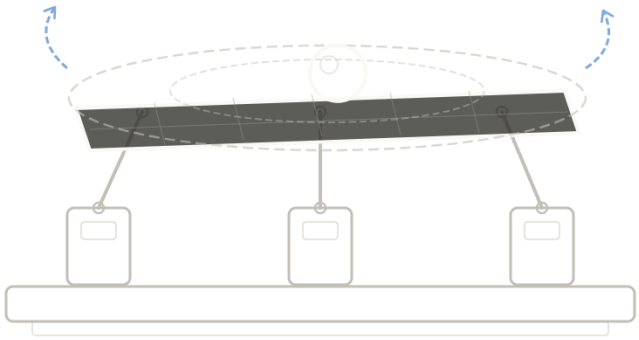

Fig. 8. Concept 1 (2-Axis Ball-on-Plate)

The first concept is a 2-Axis Ball-on-Plate (Gimbal System) that utilizes a flat plate manipulated by multiple servo motors and linkage arms to balance a ball in a two-dimensional plane (X and Y axes). The pros of this design are that it is highly interactive and visually spectacular for K-12 audiences, allowing for omnidirectional path-tracking. The cons of this concept are the extremely high mechanical complexity, the massive fracture risk posed by the fragile linkage arms during transport, and the high processing power and component costs that severely threatened the budget limit.

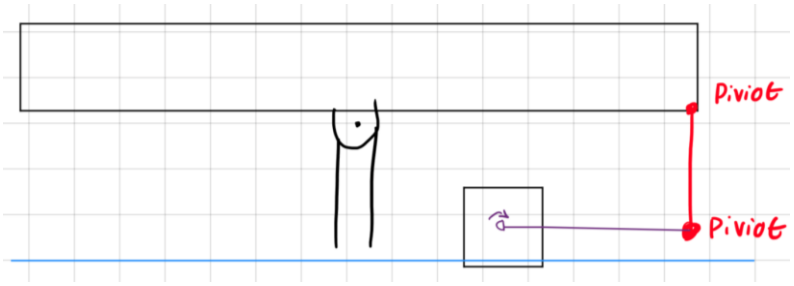

Fig. 9. Concept 2 (Servo-Driven Linkage Ball-on-Beam)

The second concept is a Servo-Driven Linkage Ball-on-Beam. This concept simplifies the system to a 1-axis beam (X-axis only) but utilizes a standard hobby servo attached to an offset linkage arm to push and pull the beam on a stationary hinge. The pros of this frame are its exceptionally low cost, utilization of standard off-the-shelf hobby components, and highly documented presence in open-source educational kits. The cons of this design are the high mechanical slop from plastic gears and physical "play" at the linkage joints, which introduces severe backlash and makes maintaining a smooth, perfectly still PID balance nearly impossible.

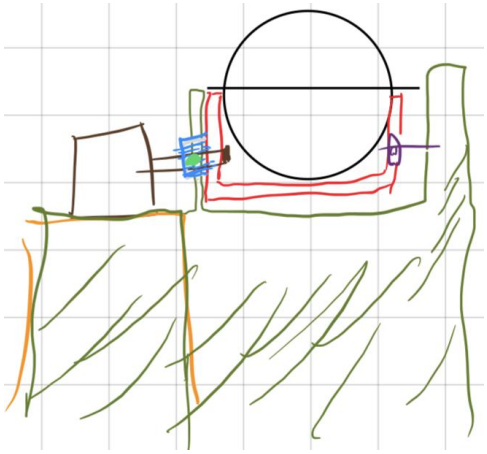

Fig. 10. Concept 3 (1-Axis Direct-Drive Ball-on-Beam)

This concept is a 1-Axis Direct-Drive Ball-on-Beam. It maintains the 1-axis educational focus but completely eliminates linkage arms by mounting the center of the beam directly onto the drive shaft of a high-resolution NEMA 17 stepper motor. The pros of this design include zero mechanical backlash, geometrically symmetrical control logic, and high structural durability due to the elimination of external moving arms. The cons are the requirement for more complex software implementation, specifically the need for 1/8 micro-stepping to ensure the stepper motor actuates smoothly without shaking the ball.

Following the evaluation of these concepts, the team selected Concept 3 (1-Axis Direct-Drive Ball-on-Beam). By utilizing a direct-drive stepper motor, the robot safely satisfies the requirement for high structural rigidity during transport and eliminates the mechanical jitter that plagues cheaper models. While it requires a more advanced

software architecture, it allows for the integration of our Time-of-Flight sensor and provides the necessary stability for K-12 interactive demonstrations without exceeding the $300 budget limit.

6.3 Selection Criteria

The final component selection was verified against the following quantifiable metrics to ensure the robot meets the "State-of-the-Art" benchmarks. The concepts were evaluated against a set of weighted criteria derived from the project's engineering requirements. To ensure a successful demonstration for K-12 students, the following metrics were prioritized:

1. **Dynamic Stability:** The physical system must prevent the ball from launching off the track under maximum motor acceleration.
2. **Structural Rigidity:** Calculated Factor of Safety (FoS) must be > 2.0 to withstand maximum rotational stall torque against the geometric hard-stops.
3. **Untethered Runtime:** The system must run continuously on battery power for > 90 minutes without voltage brownouts.
4. **Actuation Resolution:** The motor must be capable of sub-degree adjustments to eliminate ball oscillation (jitter).

Spatial Resolution (The VL53L0X ToF Sensor)

- **Metric:** 1.0 mm linear tracking resolution via 940nm infrared laser.
- **Discussion:** The VL53L0X was selected because it utilizes a highly focused Time-of-Flight laser, providing a strict 1.0 mm resolution. This high precision is necessary to detect millimeter-level deviations of the ping-pong ball from the center setpoint. This significantly outperforms standard HC-SR04 ultrasonic sensors, which utilize sound waves that scatter against the 3D-printed side walls of the beam and create false readings.

Angular Resolution (NEMA 17 Stepper & 1/8 Micro-Stepping)

- **Metric:** 0.225° rotational resolution per step.
- **Discussion:** Standard hobby servos possess inherent backlash (slop) in their plastic gears, usually resulting in ~1.0° of mechanical play. By selecting a NEMA 17 Stepper motor and utilizing a stepper driver set to 1/8 micro-stepping (1.8° / 8), the system achieves a highly precise 0.225° angular resolution. This allows the PID loop to make microscopic angle adjustments, keeping the ball perfectly still and eliminating the mechanical jitter found in lower-tier benchmarks.

Computational Throughput (The RP2040)

- **Metric:** 133 MHz Dual-Core ARM Cortex-M0+.
- **Discussion:** The RP2040 (Raspberry Pi Pico) was chosen over standard 8-bit microcontrollers specifically to handle the high-speed I2C communication required by the ToF sensor and the floating-point math required for the PID algorithm. One core is dedicated to the Sense function (polling the laser), while the second core handles Actuation (calculating PID and sending step pulses), eliminating processing latency.

By combining these components into the 1-axis direct-drive design, we can ensure high and repeated performance:

- **Mechanical Choice:** The direct-drive configuration eliminates linkage arms entirely, creating zero-backlash torque transfer.

- **Hardware Integration:** The RP2040 acts as the bridge. It processes the 1.0 mm changes from the ToF sensor and translates them into hyper-precise 0.1125° stepper pulses.
- **Factor of Safety:** The use of a 14.8V LiFePO4 battery array paired with a dedicated buck converter provides an electrical Factor of Safety, ensuring the logic voltage remains perfectly stable even when the NEMA 17 is drawing its maximum holding torque.

6.4 Concept Selection

A Pugh Chart was utilized to compare the three primary concepts generated in the Concept Generation section. Concept 3 (The 1-Axis Direct-Drive) emerged as the superior design primarily due to its inherent mechanical rigidity and high sensing precision. While the 2-Axis Gimbal provided higher visual spectacle, the trade-off in transport durability and budget compliance made the 1-axis direct-drive the necessary selection.

Table 14. Final Pugh Chart for Robot 2

Criteria	Weight	Concept 1 (2-Axis Gimbal)	Concept 2 (Servo-Linkage)	Selected: Direct-Drive Beam
Stability (Dynamic)	25%	2 (Highly complex)	2 (Slop/Jitter)	5 (Highly Stable)
Sensing Precision	20%	4	2	5 (ToF Laser)
Structural Rigidity	20%	1 (Fragile arms)	3	5 (Solid Direct Mount)
Complexity / Cost	15%	1 (Over $300 limit)	5 (Very Cheap)	4 (Within Budget)
K-12 Interactivity	20%	5 (Omni-directional)	3	4 (Highly Accessible)
Weighted Total	**100%**	**2.35**	**2.80**	**4.65**

The final selected concept is a 1-axis Ball-on-Beam system utilizing a centralized, symmetrical pivot. This configuration was chosen specifically to facilitate mounting the beam directly to the D-shaft of the NEMA 17 stepper motor, eliminating mechanical linkage arms entirely and allowing for pure angular torque transfer with 0.225 degree precision.

The chassis is 3D-printed in PLA with heavily reinforced 16.94 mm wall thicknesses and heat-set threaded inserts to satisfy the Structural Rigidity requirement during van transport. The base additionally features physical geometric hard-stops at +/-20 degrees to serve as a mechanical failsafe against software malfunction, ensuring the beam can never exceed the safe angular acceleration threshold under any operating condition.

Table 15. Factor of Safety Summary for Robot 2

Component / Sub-System	Failure Mode	Calculation Basis	Calculated FoS
Main Chassis (PLA)	Hard-Stop Fracture	Motor Stall Torque vs. 20% Infill PLA Yield Strength	2.5

Dynamic Geometry	Ball Liftoff (Loss of Contact)	Software-Limited Angular Acceleration vs. Gravitational Dominance Threshold (33.7 vs 67.47 rad/s²)	2.0
Battery Array	Power Depletion	Theoretical Runtime vs. 90-Minute Requirement (288 min vs. 90 min)	3.2
Stepper Motor	Skipped Steps / Stall	Available Holding Torque vs. Required Dynamic Torque (0.44 N·m vs. 0.0134 N·m)	33

The FoS table serves as the final justification for the system architecture. The Chassis FoS of 2.5 validates the use of a 20% PLA infill; even with the hollow internal space required for the acrylic viewing windows, the structural geometry provides more than enough rigidity to survive the maximum holding torque of the NEMA 17 motor in the event the beam is driven continuously into the mechanical hard-stops. The Dynamic Geometry FoS of 2.0 reflects the deliberate application of a safety factor of 2 to the theoretical ball-liftoff threshold, the software-enforced acceleration limit is set to exactly half of the value at which the ball would physically lose contact with the beam, making ball ejection during a K-12 demonstration mathematically impossible. The Stepper Motor FoS of 33 confirms the NEMA 17 is substantially over-capable for the loads imposed by this system, validating the direct-drive architecture. Collectively, these safety factors confirm that the selected concept is a mechanically robust and cost-effective solution for an interactive K-12 educational environment.

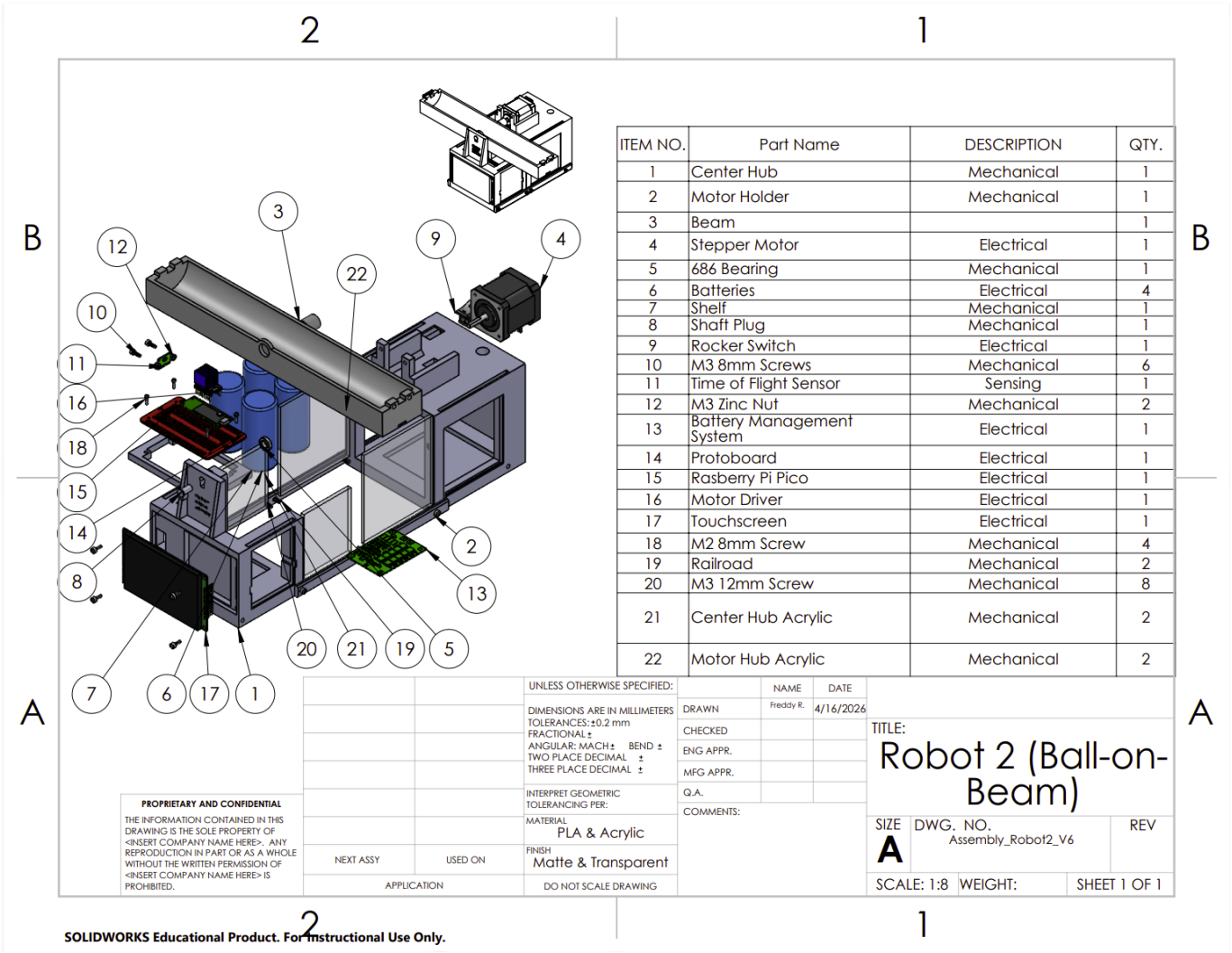

Figure 11. Robot 2 Ball-on-Beam System — SolidWorks Assembly with Sub-System Callouts

7 Schedule and Budget

7.1 Schedule

Month	Assignment Name	Due Date	Assignee	Status
Apr	~~Staff Meeting #8 (Wk11)~~	~~Apr 2~~	~~All~~	~~Done~~
	~~Timecard Wk11~~	~~Apr 6~~	~~Freddy~~	~~Done~~
	~~Initial Testing Results~~	~~Apr 9~~	~~Andres and Colin~~	~~Done~~
	~~Final Poster and Final PPT~~	~~Apr 10~~	Andres and Florence	~~Done~~
	~~Final CAD Packet~~	~~Apr 17~~	Florence and Colin	~~Done~~
	Timecard Wk 12	~~Apr 13~~	Freddy	~~Done~~
	Final Product Demo / Testing	Apr 17	Freddy and Colin	85%
	Final Report	Apr 19	Team	~~Done~~
	Timecard Wk13	Apr 20	Freddy	25%
	Final Website Check	Apr 21	Andres	75%
	Expo PPT and Poster Delivery	Apr 24	Freddy	90%
	Timecard Wk14	Apr 27	Freddy	0%
	Operation/Assembly Manual	Apr 30	Andres and Florence	25%
	Staff Meeting #9 (Wk15)	Apr 30	All	0%
May	Peer Eval 4	May 1	Individual	0%
	Client Handoff	May 1	Team	0%
	Capstone Exit Survey	May 2	Individual	0%
	Timecard Wk15	May 4	Freddy	0%

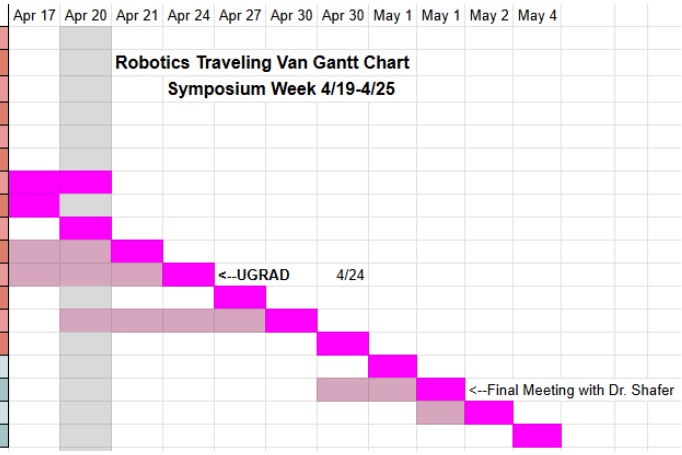

Fig. 12. RTV Gantt Chart Updated 4/19/2026

Tasks remaining are as follows:

- Prepare poster and presentation speeches
    - Requires meeting as a team to discuss which sections each individual will take for the presentation and how we want to approach the poster presentation
- Finalize testing and demo procedures
    - Requires more testing and fine tuning of the robots and clarifying demo procedures to ensure safe handling
- Create high quality documentation (manual) for both robots
    - Will be comprised of all specs sheets and culminating information from building the robots to ensure successful usage and troubleshooting methods.
- Client handoff
    - Final meeting with Dr. Shafer to return all unused parts and handoff completed robots with proper manuals
- Final Capstone assignments
    - Timesheets, exit surveys, and peer evaluations to conclude the capstone 486C class.

7.2 Budget

Given the nature of our project was to create robots that would be built and used by/for NAU outreach events/ambassadors, our budget was very clearly broken up into three main sections. The first was prototyping which included creating a proof of concept, no necessarily a final design, but a working model. The second section was comprised of iteration, our team worked through many issues and problems both mechanically and electrically. Our final designs are very different from our original plan, and this is reflected in our final design section where fine tuning and aesthetics were the core and bulk our budget allocation.

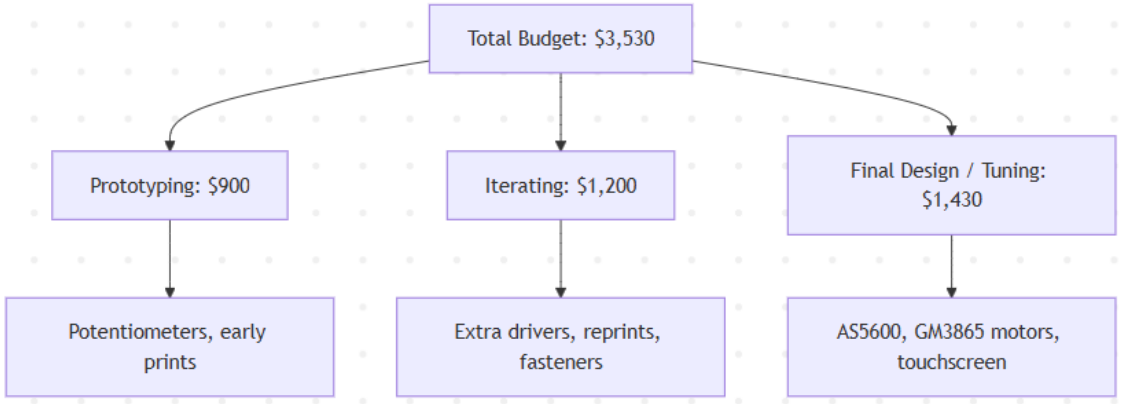

Fig. 13. Diagram of the main three phases of the team budget breakdown

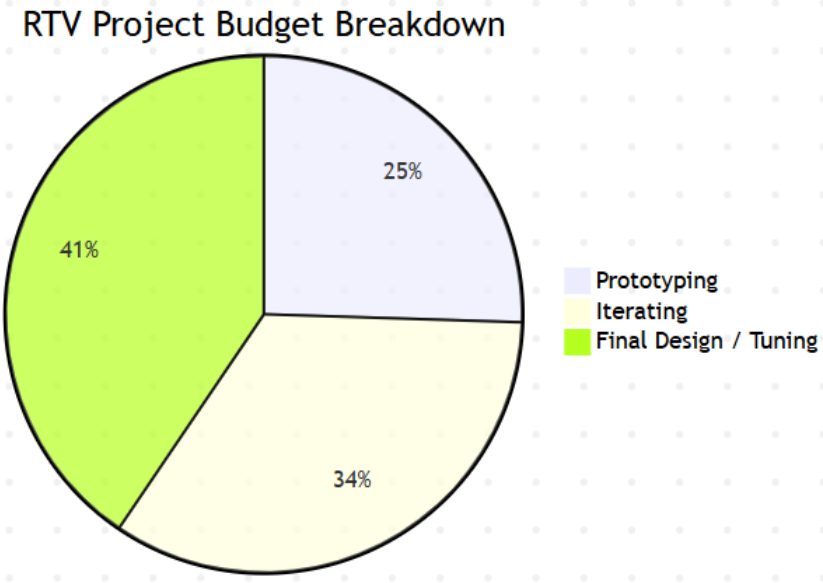

Fig. 14. Pi Chart of team budget breakdown

7.3 Bill of Materials (BoM)

Table 16. Robot 1 General Bill of Materials

Robot One				
Component	**Quantity**	**Designation**	**Cost**	**Total Cost**
520 Motors 12V	4	Mechanical	$7.98	$31.56
Wheels	included^	Mechanical	-	-
6010 bearings (6mm)	2	Mechanical	$0.75	$1.70
Aluminum Rods	3	Mechanical	$1.20	$3.60
Acrylic 4"X6"	1 pack	Mechanical	$1.60	$1.60
PLA (grams)	1 roll	Mechanical	$17.99	$17.99
Dupont Jumper Wire Set	1 Pack	Electrical	$6.98	$6.98
Header Pins	1 Pack	Electrical	$7.39	$7.39
Voltage Step-Down	1	Electrical	$1.30	$1.30
BMS Board (14.8V)	1	Electrical	$8.69	$8.69
Microcontroller (RP2040/Pico)	1	Electrical	$8.99	$8.99
LiFePO4 Battery Charger	4	Electrical	$12.99	$38.97
Protoboard Set	1	Electrical	$14.59	$14.59
Rocker Switch (On/Off)	1	Electrical	$17.99	$17.99
Motor Driver (DRV8871)	2	Electrical	$4.33	$8.66
Battery Charger	1	Electrical	$14.99	$14.99
Mag Encoder	1	Electrical	$2.60	$2.60
Longer M3 Threaded Inserts	1 pack	Mech/Shared	$9.99	$5.00
Shorter M3 Threaded Inserts	1 pack	Mech/Shared	$9.99	$5.00
M2 Threaded Inserts	1 pack	Mech/Shared	$9.99	$5.00
M3 x 12mm Socket Screws	1 pack	Mech/Shared	$8.95	$4.48
M3 x 8mm Socket Screws	1 pack	Mech/Shared	$8.95	$4.48
M2 Screw Assortment Box	1 pack	Mech/Shared	$14.99	$7.50
M3 Zinc Hex Nuts (5-piece)	1 pack	Mech/Shared	$3.75	$1.88
LCD Screen (4-inch)	1	UI	$20.99	20.99

Total per unit: $246.46

Table 17. Robot 1 General Bill of Materials

Robot Two				
Component	**Quantity**	**Designation**	**Cost**	**Total Cost**
Nema 17 Stepper Motor	1	Mechanical	$14.99	$14.99
LiFePO4 Batteries	4	Mechanical	$12.99	$38.97
PLA (grams)	1 roll	Mechanical	$17.99	$17.99
Acrylic 4"x6"	1 pack	Mechanical	$16.99	$6.80
686 Ball Bearings (10-pack)	1	Mechanical	$8.59	$0.86
Longer M3 Threaded Inserts	1 pack	Mechanical	$9.99	$5.00
Shorter M3 Threaded Inserts	1 pack	Mechanical	$9.99	$5.00
M2 Threaded Inserts	1 pack	Mechanical	$9.99	$5.00
M3 x 12mm Socket Screws	1 pack	Mechanical	$8.95	$4.48
M3 x 8mm Socket Screws	1 pack	Mechanical	$8.95	$4.48
M2 Screw Assortment Box	1 pack	Mechanical	$14.99	$7.50
M3 Zinc Hex Nuts (5-piece)	1 pack	Mechanical	$3.75	$1.88
Ping Pong Ball	1	Mechanical	$2.39	$0.27
22 AWG Hookup Wire	1 roll	Electrical	$15.29	$15.29
Dupont Jumper Wire Set	1 pack	Electrical	$6.98	$6.98
Header Pins	1 pack	Electrical	$7.39	$7.39
ToF Sensor (VL53L0X)	1	Electrical	$12.99	$12.99
Voltage Step-Down	1	Electrical	$8.69	$8.69
BMS Board (14.8V)	1	Electrical	$8.99	$8.99
Microcontroller (RP2040/Pico)	1	Electrical	$12.99	$12.99
Battery Charger	1	Electrical	$14.99	$14.99
Protoboard Set	1	Electrical	$13.59	$13.59
Rocker Switch (On/Off)	1	Electrical	$7.99	$7.99
LCD Screen (4-inch)	1	UI	$20.99	$20.99

Total per unit: $242.62

8 Design Standards

8.1 Design Standards Research

Robot 1:

Given that the interface between the metal motors and the 3D-printed chassis holds the primary mechanical risk for Robot #1, we have integrated brass heat-set inserts to maximize joint integrity. Our design is informed by ASME B18.2.8 for clearance hole diameters and ASME B1.13M for metric screw thread profiles, ensuring precise tolerances within our CAD model [6 & 7]. The M3 fastener is our primary hardware standard. We utilize 10mm screws in conjunction with deep-set threaded inserts to distribute high torque loads at the motor mounts. Similarly, we utilize 5mm screws with smaller threaded inserts for low-stress mounting of the logic components and the 4" touchscreen, ensuring a secure fit without compromising the thinner sections of the printed geometry.

In terms of safety and interaction with our target audience, we have identified the pendulum's kinetic energy as a Class 2 Mechanical Source and implemented a dual-layer safeguard. To mitigate risks inherent in a mobile pendulum system, the design implements a "Safety by Separation" strategy derived from IEC 62368-1 [4]. This is achieved by housing the Raspberry Pi Pico and high-current motor circuitry within a four-pillar internal cage, while the 4" touchscreen is mounted externally to a protective bulkhead, isolating the user from "Class 2" electrical and thermal energy sources. Furthermore, mechanical hazards such as pinch points at the pendulum pivot are addressed via a 3D-printed slip-on shroud in accordance with ASTM F963-17 Section 4.18, ensuring the device remains a "fail-to-safe" system during autonomous PID-controlled operation [6].

Additional care was taken to ensure safety and adherence to regulations. FCC Part 15 (Subpart B) regulates "Unintentional Radiators" [5]. Given that the PicoPi uses digital logic switching at high frequencies, this code ensures that our robot does not emit harmful radio-frequency interference (RFI). Our cage design acts as a basic EMI (Electromagnetic Interference) shield so that we conform to the above-mentioned code. The cage itself, and the chassis for that matter, is made of PLA filament that we run through a 3D printer, RoHS (Restriction of Hazardous Substances) ensures that the 3D printer filament and the lead-free solder used on your PicoPi/circuits do not contain toxic levels of heavy metals (Lead, Cadmium, etc.). We can ensure this is done by tracking materials used in our components. This is crucial for the "Audience-Facing" screen and parts that students may touch.

Table 18. Standard Code for Robot 1

Standard/Code	General Design Affect	Project Application
ASME B1.13M [55]	Thread standardization	Specifies the 60° form for M3 screws and brass inserts to ensure max load transfer
ASME B18.2.8 [56]	Fit and tolerances	Specifies a >1mm close fit clearance to ensure proper insert-screw connection
ASTM F963-17 [57]	Consumer/Toy Safety	Limits gap sizes at the pendulum pivot to under 5mm (via shroud) to prevent finger entrapment
IEC 62368-1 [59]	Energy Source isolation	Validates the 18 mm thick bulkhead wall separating "Class 1" logic from "Class 2" motor power.
FCC Part 15 (sub-sect. B) [60]	RFI Mitigation	Ensures the 133 MHz clock of the PicoPi does not interfere with school infrastructure
RoHS 3 [61]	Material Toxicity	Confirms that all 3D filaments and solder are lead-free (< 1000 ppm) for safe student interaction.

8.1.1 Robot 1 Annotated Bibliography:

ASME B1.13M: Metric Screw Threads: M Profile. American Society of Mechanical Engineers. This standard specifies the thread profile and standardization for metric threads. For Robot #1, this standard informs the 60° thread form used for the M3 screws and brass heat-set inserts. Adhering to this profile ensures precise tolerances within the CAD model and maximizes torque load transfer, which is critical for maintaining joint integrity at the metal motor interfaces.

ASME B18.2.8: Clearance Holes for Bolts, Screws, and Studs. American Society of Mechanical Engineers. This standard provides the recommended drill sizes and tolerances for clearance holes. In the context of this project, it is utilized to specify a close fit clearance of >1mm. This tolerance ensures a proper and secure connection between the 10mm/5mm screws and the 3D-printed chassis, facilitating high-torque motor mounting as well as the low-stress mounting of logic components without fracturing thin-walled geometries.

ASTM F963-17: Standard Consumer Safety Specification for Toy Safety. ASTM International. A comprehensive safety standard aimed at mitigating mechanical, chemical, and electrical hazards in consumer products intended for youth interaction. Specifically, Section 4.18 is applied to the pendulum system to address pinch point hazards. It dictates the implementation of the 3D-printed slip-on shroud, limiting gap sizes at the pendulum pivot to under 5mm to prevent finger entrapment and ensure the device acts as a "fail-to-safe" system.

FCC Part 15 (Subpart B): Unintentional Radiators. Federal Communications Commission. This federal regulation governs electronic devices that inadvertently emit radio frequency (RF) energy during operation. Because the Raspberry Pi Pico utilizes high-frequency digital logic switching (specifically a 133 MHz clock), this code is applied to ensure the device does not emit harmful radio-frequency interference (RFI) that could disrupt school infrastructure. The 3D-printed PLA cage design serves as a baseline electromagnetic interference (EMI) shield to help meet this requirement.

IEC 62368-1: Audio/video, information and communication technology equipment - Part 1: Safety requirements. International Electrotechnical Commission. This hazard-based safety standard focuses on energy source isolation and safeguards. It directly informs the "Safety by Separation" strategy used in Robot #1. By classifying the high-current motor circuitry and pendulum kinetic energy as a Class 2 source, the standard validates the use of an 18mm thick protective bulkhead wall to isolate these hazards from the Class 1 logic components (the 4” touchscreen), keeping the user safely separated from electrical and thermal risks.

RoHS 3 (Directive 2015/863): Restriction of Hazardous Substances. European Union. This directive restricts the use of specific hazardous materials, such as heavy metals, in electrical and electronic equipment. For this project, it serves as the benchmark for material toxicity, confirming that the PLA filament used for the chassis and cage, as well as the solder for the PicoPi circuits, are lead-free (<1000 ppm). Material tracking ensures that the "Audience-Facing" screens and touchpoints are entirely safe for student interaction.

8.1.2 Robot 2:

Robot #2, ball-and-beam system, is an audience-facing electromechanical device intended for educational demonstration and interaction. As such, applicable standards, codes, and regulations were identified and incorporated to ensure mechanical integrity, fastener compatibility, electrical safety, and user protection. While the primary analytical work for Robot #2 focused on system dynamics and actuator sizing, relevant standards guided hardware selection, interface design, and safety mitigations throughout the mechanical design process.

The stepper motor is mounted directly at the beam pivot and transmitting torque through an aluminum pin, attached to the motor; into a 3D-printed PLA beam. The motor-to-beam interface represents the primary mechanical

load path and associated mechanical risk. Metric fastener standards were therefore applied to ensure reliable torque transmission, predictable joint behavior, and compatibility with commercially available hardware.

The beam is attached to a hub called the “Center Hub” using M3 fasteners, whose geometry and tolerances are governed by ASME B1.13M (metric screw thread profiles) and ASME B18.2.8 (metric clearance hole dimensions). These standards informed CAD hole sizing, fastener selection, and the load assumptions used in the factor-of-safety calculations. By adhering to standardized M3 geometry, the design ensures proper fit, consistent load sharing among fasteners, and repeatable joint performance under cyclic loading conditions [55], [56].

To mitigate the risk of shear-out and bearing failure in printed plastic, the design explicitly avoids transmitting torque directly through a printed D-shaped shaft interface on the beam. Instead, torque is transferred through a standardized aluminum pin, consistent with best practices for polymer–metal interfaces subject to repeated loading.

The beam and structural components of Robot #2 are fabricated from PLA filament using fused deposition modeling (FDM). While PLA components are not governed by a single structural design code, their use is consistent with guidance provided in ASTM F2792, which defines terminology and general practices for additive manufacturing processes. Material properties used in analytical calculations (such as density and stiffness assumptions) were derived from manufacturer datasheets and validated through conservative assumptions [57].

The use of PLA is further justified by the extremely low applied loads associated with the ball-and-beam system (ball mass ≈ 2.7 g), which result in large factors of safety even under worst-case loading scenarios. This supports the selection of lightweight printed components while maintaining structural adequacy.

The intension of Robot 2 is to demonstrate it in an educational environment; mechanical hazards associated with moving parts were considered. Beam motion is intentionally limited to ±15°, reducing the risk of high-speed motion or projectile behavior. This design choice aligns with general mechanical safety principles outlined in ASTM F963-17, which addresses accessible moving components and pinch-point hazards in devices intended for user interaction [54].

All rotating and translating components are either low-energy or shielded by geometry, and no exposed pinch points exist near the beam pivot due to centralized motor placement and hub-based torque transfer. These measures ensure the system remains fail-safe during autonomous operation and user observation.

Robot #2 employs a stepper motor driven by low-voltage electronics and digital control hardware. As an unintentional radiator using high-frequency digital logic, the system is subject to FCC Part 15 (Subpart B), which regulates electromagnetic interference. The compact wiring layout, short motor leads, and grounded aluminum components reduce the likelihood of radiated emissions interfering with nearby equipment [60].

Additionally, all electronic components and 3D-printed materials are selected to comply with RoHS 3 (EU Directive 2015/863), ensuring that lead, cadmium, and other restricted substances remain below permissible thresholds. This is particularly important given the robot’s educational use and potential for direct student interaction [59].

Table 19. Standard Code for Robot 2.

Citation	Standard / Code	General Design Impact	Application to Robot 2
[44]	ASTM F963-17	Mechanical safety / pinch hazards	Informs safe beam motion limits and elimination of exposed pinch points
[55]	ASME B1.13M	Metric thread geometry	Defines M3 screw thread profiles used for hub-to-beam attachment
[56]	ASME B18.2.8	Fastener fit and tolerances	Specifies clearance hole sizing for M3 fasteners in printed beam
[57]	ASTM F2792	Additive manufacturing	Provides framework for terminology and material assumptions in FDM PLA parts

		practices	
[58]	FCC Part 15 (Subpart B)	EMI regulation	Ensures digital electronics do not emit harmful RF interference
[59]	RoHS 3	Material toxicity limits	Confirms PLA filament and solder are safe for audience interaction

8.1.3 Annotated Bibliography:

[54] ASTM F963-17 – Standard Consumer Safety Specification for Toy Safety
Citation: ASTM International. (2017). *ASTM F963-17: Standard Consumer Safety Specification for Toy Safety*

Annotations:T he safety requirements for toys which include but are not limited to mechanical hazards, flammability, and toxicology. These requirements involve consumer products that may be handled by children. Ensuring that this is compliant with the U.S. safety expectations, the material choice has been taken into consideration for hazard prevention.

[55] ASME B1.13M – Metric Screw Threads: M Profile

Citation: American Society of Mechanical Engineers. *ASME B1.13M: Metric Screw Threads—M Profile.*

Annotation: The geometry, tolerances, and dimensional limits for the metric screw threads. This solidifies that the threaded components in the design are compatible and manufacturable in a product.

[56] ASME B18.2.8 – Metric Fasteners: Clearance Holes
Citation: American Society of Mechanical Engineers. *ASME B18.2.8: Metric Fasteners—Clearance Holes.*
Annotations: Clearance hole size for metric fasteners are standardized for the dimensioning in CAD models and drawings to ensure proper assembly tolerances. This also curates the BOM fastener compatibility. [57] ASTM F2792 – Standard Terminology for Additive Manufacturing Technologies
Citation: ASTM International. *ASTM F2792: Standard Terminology for Additive Manufacturing Technologies.*
Annotations: Using additive manufacturing is the focus for this standard. This ensures that the language across documents, manufacturing notes, and overall communication between individuals participating in the design process are the same. This is useful when the 3D printing process and specifications are needed to replicate the process of the product.

[58] FCC Part 15, Subpart B – Unintentional Radiators
Citation: Federal Communications Commission. *FCC Part 15, Subpart B—Unintentional Radiators.*

Annotations: Sets limits on the electromagnetic emissions form the electrical devices in use that radiate radio frequency (RF) energy. This affects the design enclosure where the electrical components are housed. Furthermore, grounding, shielding, and printed circuit board (PCB) layout are also checked for its' compliance with the U.S. regulatory requirement [59] EU Directive 2015/863 (RoHS 3) – Restriction of Hazardous Substances

Citation: European Union. (2015). *Directive 2015/863 (RoHS 3): Restriction of Hazardous Substances.*
Annotations: Restrictions of hazardous materials: lead, mercury, cadmium, and specific flame retardant are restricted with RoHS 3 testing in electrical equipment. The testing aids in the selection of materials, environment compliant, and supplier verification to be docile in the BOM.

[60] IECEE Standard IEC 62368-1:2023: Audio/video, information and communication technology equipment – Part 1: Safety requirements
Citation: IECEE. (2023). IEC 62368-1:2023: Audio/video, information and communication technology equipment – Part 1: Safety requirements
Annotations: Product safety standard that classifies energy sources, prescribes safeguards against those energy sources, and provides guidance on the application of, and requirements for, those safeguards.

8.2 Design Standards Used

8.2.1 Robot 1 & 2:

I. ASTM F963-17 – Standard Consumer Safety Specification for Toy Safety [54]:
   a. Purpose: Safety requirements for toys to ensure the safety of children during usage by reducing mechanical hazards, sharp edges, small parts, flammability, and certain chemical exposure.
   b. Supporting Evidence: The enclosure for the geometry avoids small detachable parts and sharp edges with robot 1 and 2's final design by following the dimensional guidance from ASTM F963-17. A safety switch that has an on/off mode to ensure the proper deactivation of the system at any point of the use of the robot. Experiment 1: Safety and Dimension describe the procedure of supporting this standard. See *section 11.2.1.*

II. ASME B1.13M – Metric Screw Threads: M Profile [55]:
   a. Purpose: Specifies dimensions, tolerances, and profiles for metric screw threads to ensure the proper fit between threaded components
   b. Supporting Evidence: The threaded holes in the CAD models of robot 1 and 2 and drawings uses dimensions and tolerances greater or less than 0.02mm taken from the ASME B1.13M and this shows the standard metric fasteners will assemble correctly, and this shows that the design follows the mechanical practices. See *CR08*.

III. ASME B18.2.8 – Metric Fasteners: Clearance Holes [56]:
   a. Purpose: Recommends the clearance of hole sizes for metric fasteners using values from the ASME B18.2.8 that can be passed through the materials without interference.
   b. Supporting Evidence: *See sections 7.2 & 7.3.*

IV. ASTM F2792 – Standard Terminology for Additive Manufacturing Technologies [57]:
   a. Purpose: Manufacturing; 3D printing processes, materials, and features.
   b. Supporting Evidence: See sections *7.2 & 7.3.*

V. FCC Part 15, Subpart B – Unintentional Radiators [58]:
   a. Purpose: Electromagnetic emissions from electrical components that may interfere with other equipment and radiate RF energy.
   b. Supporting Evidence: See section *6.3.*

VI. EU Directive 2015/863 (RoHS 3) – Restriction of Hazardous Substances [59]:
   a. Purpose: Restricts hazardous materials in electrical components and equipment to reduce environmental and health impacts.

b. Supporting Evidence: See section *7.3.*

VII. IECEE Standard IEC 62368-1:2023: Audio/video, information and communication technology equipment – Part 1: Safety requirements

a. Purpose: Defines minimum required separation of class 1 and class 2 power sources

b. The Base plate of the Frame for Robot 1 serves as a bulkhead between a number of class 1 electrical and thermal power sources, the various electrical components used to control the system, and class 2 electrical and thermal power systems, the four motors moving the robot, and meets the minimum required dimensions to separate the classes of power sources specified by IEC 62369-1:2023. See section

9 Design Validation and Initial Prototyping for Both Systems

9.1 Failure Modes and Effects Analysis (FMEA) for Inverted Pendulum

Table 20: FMEA for Robot 1

Sub assembly	Component	Function	Potential Failure Mode	Potential Effect(s) of Failure	S	Potential Cause(s) / Mechanisms	O	Current Design Controls / Tests	D	RPN	Recommended Action (Implemented)
Mechanical	Pendulum Robot Frame	Support for all subsystems	Frame cracks, warps, or misaligns	Robot tilts, components detach or misalign	9	Weak material, stress concentration, impact	4	Visual inspection, low-speed balance tests	3	108	Frame reinforced with additional support structures: Walls, Horizontal beams on top of walls
Mechanical	Motor Bracket	Secure motors to frame	Bracket loosens or fractures	Motors shift, misalignment in drive system	8	Vibration, weak mounting points	4	Torque tests, visual inspection	3	96	No action necessary, Metal Motor Brackets provided with motors proved sufficient
Mechanical	Pendulum Bearings	Support pendulum rotation	Bearing seizes or adds friction	Pendulum movement restricted, poor control	8	Dust ingress, poor alignment, wear	3	Rotation smoothness test	4	96	Used sealed bearings; ensured alignment and lubrication
Mechanical	Motor Bracket Screws	Fasten brackets to frame	Screws loosen or strip threads	Motor misalignment or detachment	8	Vibration, over-torque	4	Visual inspection, torque checks	3	96	Metal threaded inserts used in base to provide solid anchoring for motors
Pendulum	Pendulum Assembly	Provides center arm for balance, supports potentiometer	Arms bend or joint loosens	Pendulum swings unevenly or angle changes unpredictably	9	Weak joint connection, fatigue	4	Manual deflection test	3	108	Strengthened joints, added lip to pendulum Shoulder Brackets to ensure arm alignment
Pendulum	Potentiometer	Measures pendulum angle	Incorrect or unstable readings	Robot miscalculates angle, loses balance	8	Loose mounting, electrical noise, wear	3	Calibration test, shielding wires	4	96	Potentiometer mount redesigned to maximize strength, calibrated code for offset
Motors	L-Type 520 Motors	Provide motion and balancing torque	Motor stalls or overheats	Robot falls or oscillates uncontrollably	10	Overload, friction, underpowered motor	5	Bench test under load	3	150	No action necessary, selected motors never stalled or overheated during testing
Motors	67.5 mm Wheels	Transfer motor torque to ground	Wheels slip or detach	Robot cannot move or balance	9	Loose fit, worn tires, low friction	4	Visual inspection, traction test	3	108	No action necessary, Wheels provided with motor had sufficient grip throughout duration of testing

Control	Arduino	Processes sensor data, controls motors	Software crash or voltage reset	Robot stops or behaves erratically	10	Power fluctuation, coding bug	3	Unit testing, watchdog timer, battery monitoring	4	120	Switched to Raspberry Pi to increase system responsiveness
Battery	Battery	Supplies system voltage/current	Battery drains mid-operation	Robot shuts off mid-test	9	Low capacity, poor contact, over-discharge	5	Voltage check before use	3	135	LiFeP04 Battery capacity proved sufficient during testing
Other (Tool)	Breadboard	Distributes circuit connections	Loose or intermittent connections	Random resets or inconsistent control	8	Poor contact, vibration	4	Visual inspection, continuity test	3	96	Transitioned to soldered PCB; Designed custom PCB for system

9.2 Failure Modes and Effects Analysis (FMEA) for Ball-on-Beam

Table 21: FMEA for Robot 2

Subassembly	***Component***	***Function***	***Potential Failure Mode***	***Potential Effect(s)***	***S***	***Potential Cause(s)***	***O***	***Current Controls / Tests***	***D***	***RPN***	***Recommended Action (Implemented)***
Sensing	*VL53L0X ToF Sensor*	*Measure ball distance*	*Ambient light interference*	*Tracking errors; unstable PID*	*7*	*Classroom lighting; surface reflections*	*2*	*Live data logging; isolated laser timing*	*1*	***14***	*Implemented VL53L0X Time-of-Flight sensor to replace standard optical tracking, isolating readings from room lighting.*
Sensing	*Sensor Mount*	*Align sensor laser*	*Physical shifting / Misalignment*	*Laser hits beam wall instead of ball*	*7*	*Vibration from motor; loose tolerances*	*3*	*Physical inspection during operation*	*2*	***42***	*Designed a custom, tight-tolerance 3D-printed recess to rigidly lock the sensor PCB exactly parallel to the beam axis.*
Mechanical	*Base Chassis*	*Support system*	*Fracture during transport*	*Structural failure; system collapse*	*8*	*Thin 3D print walls; high-impact drops*	*2*	*36-inch physical drop test*	*2*	***32***	*Thickened standard PLA walls and utilized heat-set threaded inserts to eliminate stress fractures.*
Mechanical	*Beam Track*	*Confine ball movement*	*Ball falls off the side of beam*	*Demonstration interrupted; system stall*	*6*	*High angular acceleration; uneven rolling*	*4*	*Observational tracking limits*	*1*	***24***	*Engineered a U-channel profile into the top of the beam with raised PLA side-rails to physically contain the ball.*

Mechanical	*Motor Hub*	*Transfer rotational torque*	*Hub slipping on motor shaft*	*Loss of zero-position; immediate PID failure*	*9*	*Smooth circular shaft; inadequate friction*	*2*	*Rotational load testing*	*2*	***36***	*Utilized a NEMA 17 with a flat D-shaft and integrated a metal set-screw into the printed hub to physically lock rotation.*
Actuation	*NEMA 17 Stepper*	*Tilt beam*	*Mechanical slop / rotational jitter*	*Uncontrollable ball oscillation*	*7*	*Linkage arm play; low step resolution*	*2*	*Visual oscillation tracking*	*2*	***28***	*Integrated direct-drive shaft (eliminating linkage arms) and applied 1/8 micro-stepping to ensure perfectly smooth actuation.*
Actuation	*Stepper Driver*	*Deliver motor current*	*Motor/Driver overheating*	*Thermal shutdown; skipped steps*	*7*	*Continuous 90-minute holding torque*	*3*	*Thermal monitoring during runtime test*	*2*	***42***	*Tuned the VREF potentiometer on the driver to reduce holding current to the minimum required threshold, preventing thermal overload.*
Power	*Buck Converter*	*Regulate 14.8V down to logic*	*Voltage drop-off / Brownout*	*Microcontroller resets; loss of control*	*8*	*Extended 90-minute demonstrations*	*2*	*Continuous 90-min runtime test*	*2*	***32***	*Integrated a dedicated 5V/3.3V buck converter to safely step down the LiFePO4 array, ensuring sustained logic voltage.*
Power	*Internal Wiring*	*Route power/signals*	*Wire disconnects*	*Complete subsystem failure*	*8*	*Transport vibrations; K-12 physical handling*	*3*	*Continuity checks; physical shake test*	*2*	***48***	*Eliminated breadboards in the final assembly; transitioned to soldered connections and secure headers to survive physical transit.*

Control	*RP2040 Pico*	*Process PID loop*	*Processing lag / software stall*	*System fails to react in time*	*8*	*Code inefficiencies; slow baud rate*	*2*	*Software stress testing; sample rate checks*	*2*	***32***	*Upgraded to dual-core RP2040 to handle rapid sensor I2C filtering and UI touchscreen inputs simultaneously without bottlenecking.*
Control	*PID Software*	*Compute error*	*Integral Windup*	*Extreme overshoot when ball is touched*	*7*	*User physically holds ball; I-term accumulates*	*4*	*Intentional user interference testing*	*1*	***28***	*Coded an anti-windup clamp into the software to freeze the Integral term if the physical error exceeds the beam's geometric limit.*

9.3 Initial Prototyping

9.3.1 Robot 1 Prototype

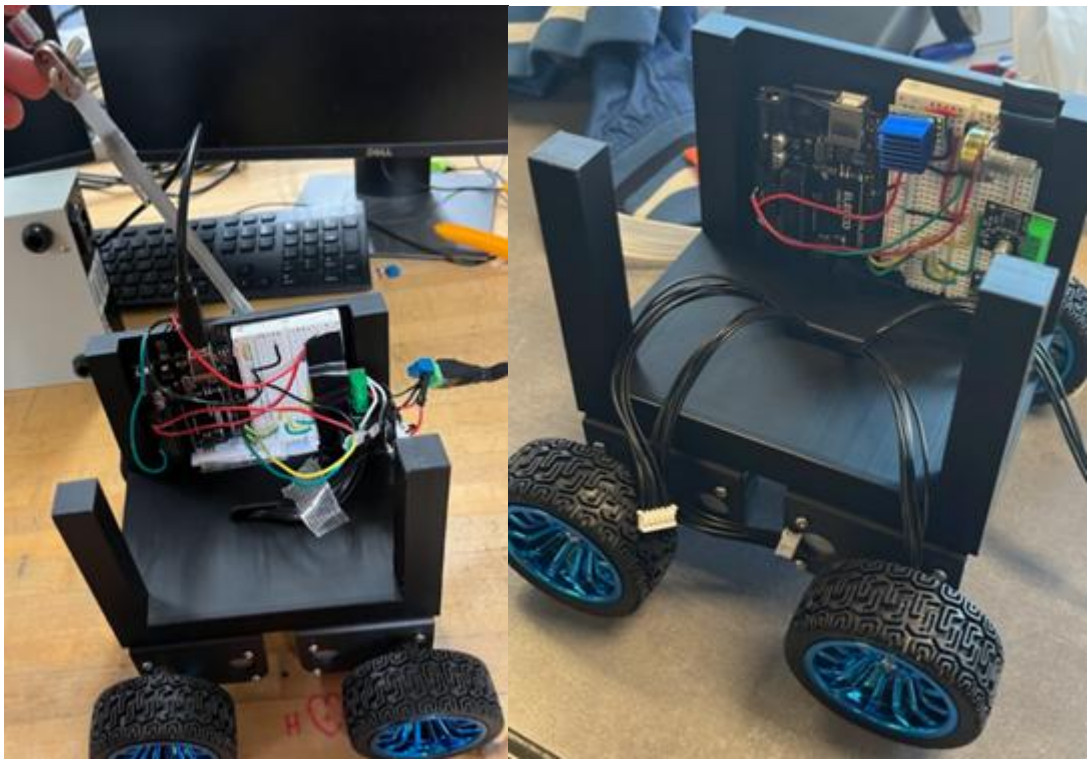

Figure 15 & 16: Early Prototype of Robot 1 with the potentiometer and Arduino

The initial Phase 1 prototype/proof-of-concept to evaluate the accuracy of our theoretical modeling and virtual simulations. The system set out to answer three critical questions: determine if the electrical components could connect with minimal noise and high resolution, if the 3D-printed housing could hold all components together, and whether or not the motors could be controlled accurately enough to run the PID controller.

Physical testing of this prototype yielded highly definitive data that necessitated a major system redesign. Initially the potentiometer read well and could measure the correct angles, however, the accuracy was lacking for the speeds and angles we were hoping for. The next issue we ran into was trying to incorporate the touchscreen on the Arduino module which ended up not being able to run all the appropriate programs at the correct frequencies and reliably. Finally, a massive issue in physically mounting a magnetic encoder along the axis of rotation of the pendulum was difficult when on the exterior. To resolve the discovered vulnerabilities, the team implemented four major design iterations:

- **Iteration 1 (Potentiometer)** We eliminated the potentiometer and incorporated a high-resolution magnetic encoder that could read and transfer data much more accurately and at higher frequencies.
- **Iteration 2 (Raspberry Pi Pico):** To eliminate the bandwidth issues, we completely rehauled our microcontroller circuit design base from an Arduino UNO to a Raspberry Pi Pico in order to better allocate memory to the correct programs and run all the necessary components.
- **Iteration 3 (Chassis Redesign):** The next big issue came after solidifying the circuit which involved creating divots and places for the main components to rest in order to avoid any crossing wires and organize the wiring better. This increased the size of the robot but also eliminated other unnecessarily thick areas essentially optimizing the space.
- **Iteration 4 (Interior Magnetic Encoder):** The difficulties of the magnetic encoder were solved by cutting the pendulum arm into 4 sections and running the sensor inside the robot along the axis of the rotation. The 4 sections were built around the encoder allowing for a safer and more discrete look and function.

9.3.2 Robot 2 Prototype

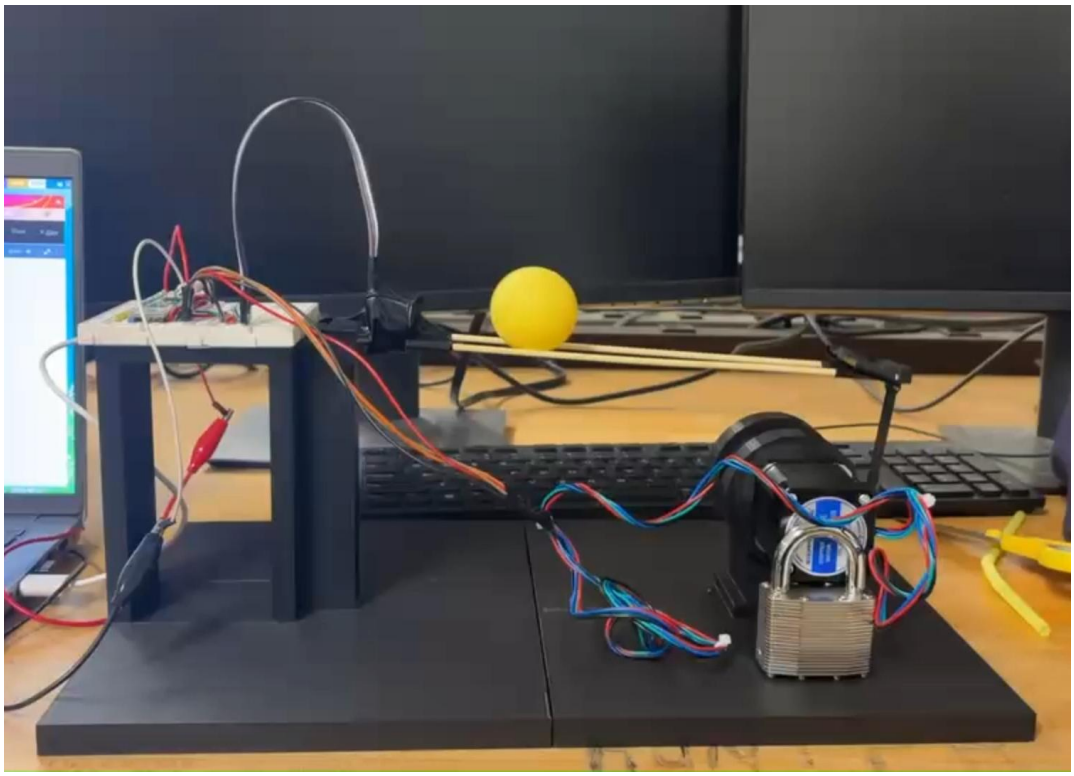

Figure 17: Early Prototype of the Offset-Linkage Ball-on-Beam

The initial Phase 1 prototype was constructed as a proof-of-concept to evaluate the fundamental feasibility of a stepper-driven balancing system. Specifically, the team utilized this build to answer three critical engineering questions: whether a NEMA stepper motor could provide the necessary responsiveness when connected via an offset, 3-part 3D-printed kinematic linkage; whether a standard, low-cost HC-SR04 ultrasonic sensor could accurately track a small, spherical ping-pong ball; and whether it was viable to 3D-print the entire supporting chassis as a single "monolithic" piece to reduce assembly time, utilizing simple wooden skewers to act as the track.

Physical testing of this prototype yielded highly definitive data that necessitated a major system redesign. While the stepper motor itself proved sufficiently responsive, the mechanical linkage system was deeply flawed. The 3-part crank and connecting rod introduced severe mechanical backlash (slop) at the joints, and utilizing a stationary hinge on one end of the beam created a non-linear relationship between the motor's step angle and the beam's actual tilt angle, complicating the control mathematics. Furthermore, the ultrasonic sensor was entirely ineffective for this application; its wide acoustic beam width caused it to catch false echoes off the wooden skewers and the surrounding environment rather than isolating the small surface area of the ball. Finally, the monolithic printing strategy proved to be a critical manufacturing error. During testing, if a single hinge or mount fractured, the entire robot had to be discarded and reprinted, resulting in unacceptable material and time costs.

The failures and observations from this early prototype directly informed the highly successful architecture of the final Robot 2 build. To resolve the discovered vulnerabilities, the team implemented four major design iterations:

- **Iteration 1 (Sensing Pivot):** The ultrasonic sensor was entirely scrapped and replaced with a VL53L0X Time-of-Flight (ToF) sensor. This utilized a focused infrared laser, completely eliminating false echoes and providing 1.0 mm resolution regardless of the beam's geometry.

- **Iteration 2 (Actuation Pivot):** To eliminate the mechanical slop of the 3-part linkage and drastically simplify the control mathematics, the team completely redesigned the physical geometry. The stationary hinge was removed, and the axis of rotation was moved to the exact dead-center of the beam. The beam was then mounted *directly* to the stepper motor shaft (Direct-Drive), eliminating linkage errors and creating a perfectly symmetrical mathematical model.
- **Iteration 3 (Manufacturing Pivot):** The monolithic printing strategy was abandoned in favor of a modular chassis. The final base was segmented into distinct parts fastened together using brass heat-set threaded inserts. This allowed the team to rapidly swap and reprint specific mounts or walls without re-manufacturing the entire robot.
- **Iteration 4 (Beam Pivot):** The flimsy wooden skewers were replaced with a custom-designed, 3D-printed U-channel beam featuring raised sidewalls to provide a consistent, straight rolling surface for the ball.

9.4 Other Engineering Calculations

9.4.1 Other Engineering Calculations – Colin Parsinia & Andres Gonzales

This calculation corresponds to the final selection of our power management/delivery system and informs safety measures to ensure the electrical and mechanical systems work together seamlessly and safely. The main components under investigation are as follows: batteries, battery charging, battery management system, power to logic/motor split, and wire/connections. The risks paired with oversight in our electrical load analysis mainly affect our logic (PiPico microcontroller) and our reliability.

9.4.1.1 Electrical Load Analysis

This high FoS was intentionally chosen to ensure that even as the batteries age (and internal resistance increases) or if a motor develops a mechanical jam, the robot will remain powered. This informed the selection of the 30A BMS over a cheaper 15A or 20A alternative, prioritizing demonstration reliability over cost.

$$I_{total} = 4 \cdot I_{stall} + I_{Logic} \rightarrow \quad (7)$$

$$4 \cdot 3.2 + 0.3 = 13.1\,Amps \quad (8)$$

$$FoS = 2.29$$

This FoS additionally informed our design to protect the RP2040 logic from theV_{sag} caused by 13.1A surges, we implemented a 3.3V Buck Converter with a high input voltage range to ensure logic stability even if the battery voltage dips.

Using the updated numbers, we can solve for the voltage sag which can cause issues to our logic if not properly regulated. The nominal voltage from the 4 motors is about 12.8V and the estimated internal resistance from the components and wiring is about 0.02 ohms and 0.01 ohm per battery cell gives the following:

$$V_{sag} = V_{nom} + (I_{total} \cdot R_{int-resis.}) \rightarrow 12.01V \quad (9)$$

The voltage drop for a 4 motor stall calculated with the product of the total current and the system resistance yield:

$$\Delta V = I_{total} \cdot R_{sys} = 13.1\,A \cdot 0.06\,\Omega \quad (10)$$

The factor of safety calculation then becomes:

$$FoS = \frac{12.01\,V}{5\,V} = 2.4 \quad (11)$$

The standard rating for the H-Bridge DRV8871 IC was found in the data sheets to be about 3.6A and the motor stall draw, measured at 12V, was estimated to be about 3.2A average. We have to test this with all the components mounted on, but with what we have calculated we find a FoS of:

$$FoS = \frac{I_{peak}\,(3.6A)}{I_{motor\ stall}\,(3.2A)} = 1.12 \quad (12)$$

A Factor of Safety of 1.12 is relatively "tight" in power electronics. Because the driver is operating so close to its maximum capacity during a stall, this informed our design to include active cooling or heat sinks on the DRV8871 chips. Without these, the driver would reach its thermal shutdown temperature ($175^{\circ}C$) long before the motor itself failed. We have further tests to perform to ensure a higher FoS. This, however, is not enough, we plan to add a programmed “buffer” by limiting the PWM duty cycle to 90% to further protect our logic.

Table 22: Electrical Sub-System FoS Comparison

Sub-System	Part	Load Scenario	Material/ Spec	Method of FoS	Min. FoS
Power Logic	30A BMS	Simultaneous 4-motor stall at 100% PWM	Lithium BMS	$\frac{BMS\ Trip\ Rating\ (30A)}{Calculated\ Peak\ Load\ (13.1A)}$	2.29
Power Logic	3.3V Buck Converter	Voltage Sag during motor transients	Euogeudel Module	$\frac{Calculated\ V_{sag}(12.01V)}{Min.\ Input\ Req.\ (5V)}$	2.4
Drive Train	Motor Driver	Continuous Motor Stall	DRV8871 IC (H-bridge)	$\frac{Peak\ Current\ Limit(3.6A)}{Measured\ Motor\ Stall\ (3.2A)}$	1.12

The electrical load analysis directly dictated the robot's power architecture, transitioning the design into a dual-rail system that isolates sensitive logic from mechanical noise. By calculating a peak system draw of 13.1A against the 30A BMS, we established an FoS of 2.29 to prevent safety trips during high-torque maneuvers. Additionally, the 0.786V voltage sag calculated during 4-motor stalls informed the selection of a 3.3V Buck Converter, providing a Headroom FoS of 2.40 to ensure the RP2040 and touchscreen remain stable under maximum stress. Crucially, the narrow 1.12 FoS identified for the DRV8871 drivers informed a specialized thermal strategy; we integrated finned aluminum heat sink and a software-defined 90% PWM cap to increase the thermal safe operating area. This multi-layered approach ensures the system can sustain peak stall currents without triggering thermal shutdown or logic brownouts.

9.4.2 Other Engineering Calculations for Robot 2– Freddy Rivera & Florence Fasugbe

This section summarizes the load analyses, motor validation calculations, and operational estimates performed for Robot 2’s ball-on-beam system. All calculations were performed under conservative worst-case assumptions to confirm mechanical feasibility, establish safe operating limits, validate actuator selection, and verify compliance

with the project's Engineering Requirements.

Note: Early-stage geometric parameters assumed a beam length of 254 mm (10 inches) during initial design. The finalized SolidWorks CAD model specifies a beam length of 290.8 mm, yielding a maximum ball travel radius of: $r_{\max} = 0.1454$ m from the center pivot to the end-wall. All results presented in this section reflect the finalized geometry.

9.4.2.1 System Parameters

The following parameters were used consistently across all Robot 2 analyses and reflect the final built system:

- **Beam Length (L):** 290.8 mm (0.2908 m)
- **Maximum Ball Radius from Pivot (r_max):** 145.4 mm (0.1454 m)
- **Ball Mass (m_b):** 0.0027 kg
- **Ball Radius (R):** 0.020 m
- **Ball Moment of Inertia:**

$$J_b = \frac{2}{3} m_b R^2 = 7.20 \times 10^{-7} \text{ kg·m}^2$$

- **Beam Moment of Inertia (J_beam):** 3.4×10^{-4} kg·m^2
- **Gravity (g):** 9.81 m/s^2
- **Motor Model:** StepperOnline 17HS19-2004S1 (NEMA 17)
- **Motor Rated Holding Torque:** 0.59 N·m
- **Motor Rated Current:** 2.0 A
- **Motor Operating Current:** 1.5 A
- **Supply Voltage:** 13.3 V
- **Battery Capacity:** 7,200 mAh
- **Microstepping Mode:** 1/8 step (TMC2209 driver)

9.4.2.2 Plant Model Summary

The governing equation of motion for the ball-on-beam system was derived using Lagrangian [38] mechanics, modeling the ping-pong ball as a thin hollow sphere. After applying the small-angle approximation ($\sin\theta \approx \theta$), the simplified plant equation is:

$$\ddot{x} = -\frac{3}{5} g\theta$$

The plant gain is:

$$K_{\text{plant}} = -\frac{3}{5}(9.81) = -5.886 \text{ m/s}^2 \text{ per rad}$$

This means for every 1 radian of beam tilt, the ball accelerates at 5.886 m/s^2.

9.4.2.3 Available Motor Torque at Operating Conditions

$$T_{\text{available}} = \left(\frac{1.5}{2.0}\right)(0.59) = 0.44\ \text{N·m}$$

This value is used as the baseline for all factor of safety calculations.

9.4.2.4 Load Case 1: Static Torque Requirement

$$T_{\text{required}} = m_b g r_{\max}$$
$$T_{\text{required}} = (0.0027)(9.81)(0.1454) = 0.00385\ \text{N·m}$$
$$\text{Factor of Safety} = \frac{0.44}{0.00385} \approx 114$$

This confirms the NEMA 17 [13] motor is more than sufficient for worst-case static loading.

9.4.2.5 Load Case 2: Maximum Allowable Angular Acceleration

$$\ddot{\theta}_{\max} = \frac{g}{r_{\max}} = \frac{9.81}{0.1454} = 67.47\ \text{rad/s}^2$$

Applying a safety factor of 2:

$$\ddot{\theta}_{\text{limit}} = \frac{67.47}{2} = 33.7\ \text{rad/s}^2$$

9.4.2.6 Total Rotational Inertia

$$J_{\text{total}} = J_{\text{beam}} + m_b r_{\max}$$
$$J_{\text{total}} = 3.4 \times 10^{-4} + (0.0027)(0.1454^2)$$
$$J_{\text{total}} = 3.97 \times 10^{-4}\text{kg·}m^2$$

9.4.2.7 Required Dynamic Torque

$$T_{\text{dynamic}} = J_{\text{total}}\ddot{\theta}_{\text{limit}}$$
$$T_{\text{dynamic}} = (3.97 \times 10^{-4})(33.7) = 0.0134\text{N·m}$$
$$\text{Factor of Safety} = \frac{0.44}{0.0134} \approx 33$$

This confirms the motor can comfortably achieve the required acceleration.

9.4.2.8 Load Case 3: Maximum Recoverable Beam Angle (Rolling Without Slip)

$$\theta_{\max} = \arctan\left(\frac{5}{2}\mu_s\right)$$
$$\theta_{\max} = \arctan(0.375) = 20.5°$$

Any beam angle below this ensures rolling without slipping.

9.4.2.9 Battery Runtime Estimate

$$\text{Runtime} = \frac{7200\ \text{mAh}}{1500\ \text{mA}} = 4.8\ \text{hours} = 288\ \text{minutes}$$

This exceeds the requirement of 30 minutes.

9.4.2.10 Structural Factor of Safety Summary

Table 23: FoS for Robot 2

Load Case	Parameter Checked	Required	Available	Factor of Safety
Static (ball at beam end)	Motor holding torque	0.00385 N·m	0.44 N·m	~114
Dynamic (software accel limit)	Motor dynamic torque	0.0134 N·m	0.44 N·m	~33
M3 Screw Shear	Shear stress	3.43 MPa	~150 MPa	~44
PLA Bearing Stress	Crushing stress	1.12 MPa	~25 MPa	~22

All factors of safety are well above acceptable minimums.

9.4.2.11 Design Implications

The calculations presented in this section collectively validated the core mechanical and electrical architecture of Robot 2. The negligible static torque demand confirmed that direct-drive motor placement at the pivot axis was structurally viable, eliminating linkage complexity and backlash. The large dynamic torque margin established that beam motion would be governed by software acceleration limits rather than hardware constraints, enabling smooth closed-loop control. The rolling slip analysis justified the physical hard-stop geometry, and the battery runtime estimate confirmed compliance with ER02 by a substantial margin. High structural factors of safety throughout confirmed that lightweight 3D-printed PLA components are appropriate for this application, directly supporting the project's objective of producing a low-cost, mass-producible educational platform.

9.5 Future Testing Potential

The testing phase covered all major performance and safety checks, overall the results show that the robots meet the core engineering requirements tied to durability, battery life, safety, control accuracy, and cost. The drop test confirmed the 3D-printed chassis can handle a 36-inch fall without structural failure, supporting the kid-friendly and durability requirements. With battery endurance testing, it shows that the $LiFePO_4$ packs provide well over the required 30 minutes of runtime, proving the systems truly operate as battery-powered platforms. Physical safety checks such as weight, dimensions, edge radii, and pinch-point clearance, fall within the expected limits equates that both robots comply with the ASME safety standards. The interface tests verify that the touchscreen and the emergency switch behav correctly, which satisfies the interactive-interface requirement. Furthermore, the control-loop testing shows that both robots can settle back to a stable state in under five seconds, confirming the PID balancing requirement. For Robot #2, the ToF sensor calibration stayed within the allowed error range, proving the control hardware is accurate enough for educational use. Finally, the BOM audit demonstrates that the per-unit cost stays under the required limit and meets the inexpensive manufacturing requirement. Altogether, these experiments show that the engineering requirements map cleanly to the customer requirements, and passing them verifies that the robots function as safe, durable, low-cost educational props for outreach.

10 Final Hardware

10.1 Final Physical Design – Robot #1

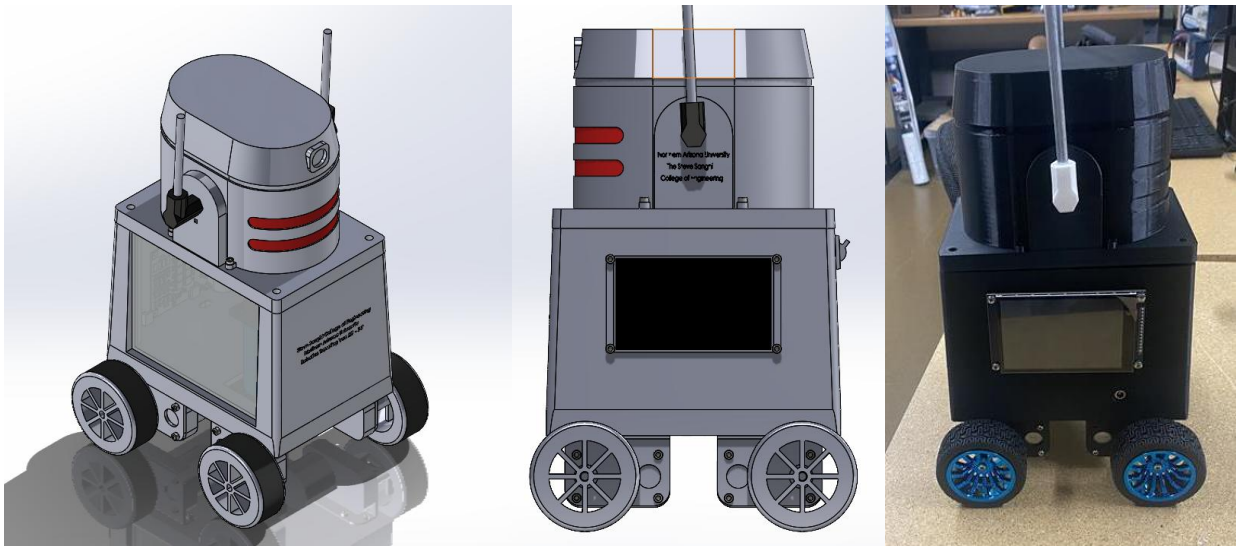

Figures 18-20: From left 2 right, Isometric Cad View of Robot 1, Side Cad View of Robot 1, Actual side view of robot 1

The final design of robot 1 is the result of many iterations and tests to fully refine the design to make it sleek and optimize its functionality. The Strong Top and Bottom Frames in combination with the Pendulum Shell fabricated from TPU plastic ensure the robot can endure all the rigors of regular use during outreach events, the touchscreen offers an avenue for interaction with the robots system, the exterior allows students to inspect the internal systems that allow the robot to function, and the wheels provide the necessary force to balance the system. With proper electrical and code refinement the robot will be able to perform its function as an interactive inverted-pendulum robot to be used to interest students in NAU's engineering program.

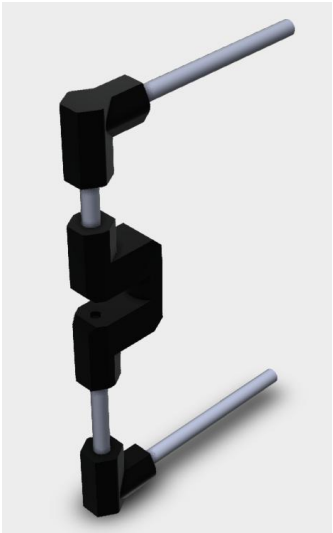

Figure 21: Final Pendulum Sub-Assembly

The major sub-assembly of this robot is the Pendulum itself, which went through multiple design iterations

throughout the course of the project. Initially the idea for the pendulum was to have a single aluminum rod that a pass-through potentiometer would be mounted on, but due to the lack of properly sized pass through potentiometers, the pendulum was re-worked to have a similar design to the final, but was scrapped along with the original frame design seen in the below figure

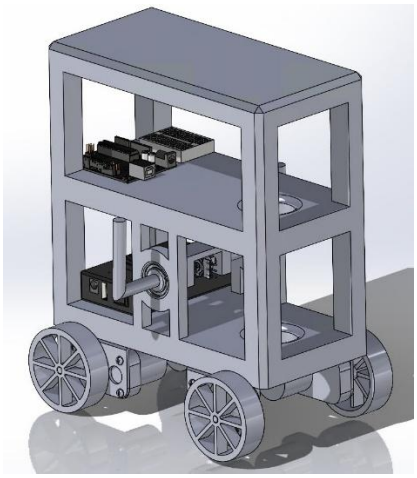

Figure 22: Final Robot 1 Design from Semester 1 with original segmented beam

To Briefly discuss why these designs were scrapped, the Entire Frame design was scrapped as it was originally designed to maximize the dimensions we were given as many of the electrical components had yet to be fully decided on so their exact dimensions were unknown, but once they were selected the entire frame was redesigned to minimize dimensions as much as possible to reduce 3D printing costs. The original Pendulum design was scrapped as at the time a physical potentiometer was being used, but it was later determined that the physical potentiometer lacked the necessary precision so it was swapped out with a magnetic potentiometer. With the addition of the magnetic potentiometer, it was decided to return to the initial idea of having the beam be a single solid piece of metal that was bent at either end with the potentiometer mounted at one side of the pendulum, but this idea was soon revise due to learning that a magnetic potentiometer needs to be able to clearly read the magnetic poles. This led to the idea of creating 3D printed brackets to connect the external arms with the connecting axis, as a slot could be added to put a magnet in to properly read the angle of the beam with the magnetic potentiometer. This design received a few iterations, but was eventually scrapped after realizing that there was no space in the potentiometer mount for wiring without compromising its structural integrity, and having exposed wiring would violate safety standards, so it was eventually decided to return to the original pendulum design of a center bracket in which the magnetic potentiometer could be positioned, and a slot for the magnet to be placed, resulting in the final design seen above.

Breaking down the components of the Final Pendulum Sub-Assembly, it can be divided into the 3D printed Parts, and the machined aluminum rods. Starting with the elbow brackets, these came about as part of the switch to the magnetic potentiometer, as a result of realizing the magnetic potentiometer needed to be parallel to a magnet, and the realization that there was no easy way to bend an aluminum rod to a 90 degree angle.

Figure 23: Pendulum Elbow Bracket

Originally, both holes in the Arm Bracket were perfectly circular, but it was soon realized that this would cause misalignment of the pendulum arms as the brackets could rotate independently of each other. The lip was added to the horizontal hole, and a similar lip was machined into each end of each segment of the interior pendulum beams as can be seen in the example pictured below.

Figure 24: Interior beam segment with machined lips

The last major component of the Beam Subassembly is also the last designed, being the interior bracket which is concealed by the Pendulum Shell in the final design. As mentioned previously the center bracket was one of the first concepts generated for the beam, and despite being initially dismissed with the redesign, managed to return in the final design out of the necessity to enclose all electrical components of the design.

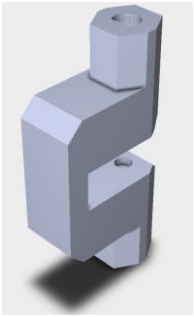

Figure 25: Interior Bracket of Pendulum

Moving from the Pendulum Sub-Assembly to the Major components of the Final Assembly and starting from the top up, The Pendulum Shell came out of the desire to make the robot more visually appealing, while also offering additional structural stability. The design itself is inspired by the robot designs found in Star Wars, which is well known for its appealing robot designs. As was mentioned previously it was also printed out of TPU filament due to its more elastic properties, the hope being that is flexible structure would reduce the impact of the robot falling on its head.

Figure 26: Pendulum Shell

The next major component of the Final Assembly was the top frame of the robot, which contains the rounded arms that hold up the pendulum sub-assembly. The top and the bottom frame were initially one solid piece, but after printing this single-part frame, there were numerous printing errors that severely negatively affected the quality of the frame, so it was decided to separate the frame into 2 solid pieces that were better designed for 3D printing. Once the frame was separated, the top frame remained mostly unchanged except for some minor dimensioning adjustments, some holes cut for threaded inserts to better hold the potentiometer mount, and the addition of a hole for the potentiometer wiring.

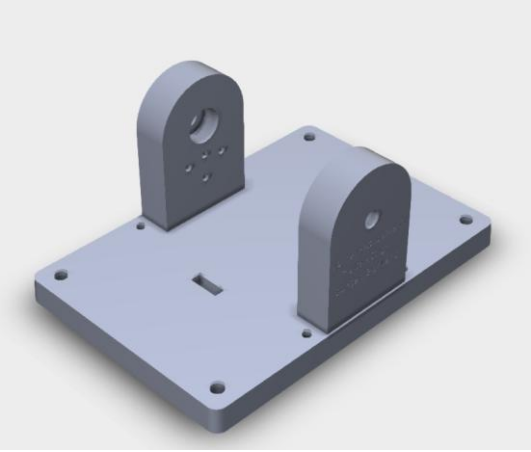

Figure 27: Robot 1 Frame Top

On the topic of the Magnetic Potentiometer mount, it was another part that received numerous iterations over

the second semester, most adjustments being to increase the dimensions of the shaft connecting the square head that holds the potentiometer to the top frame, the addition of screw holes for further structure support, and finally some holes for wiring out of the back of the magnetic potentiometer mount.

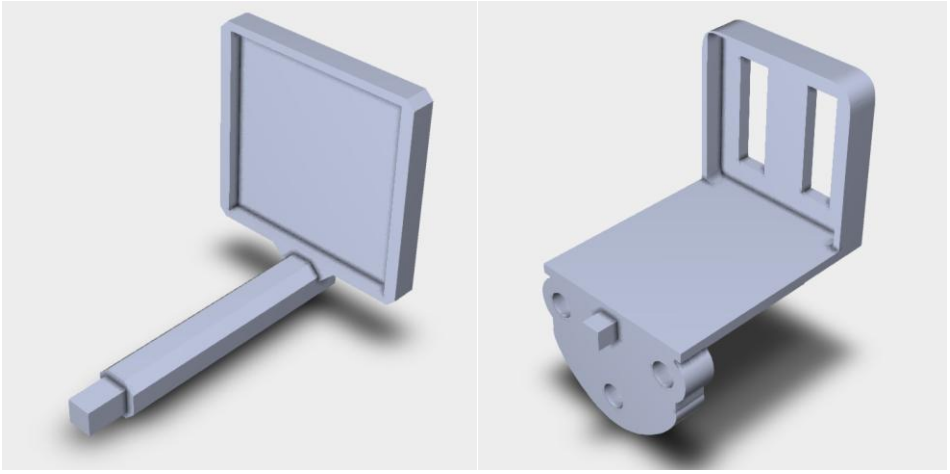

Figures 28 & 29: Original Magnetic Potentiometer mount (Left), & Final Design (Right)

Lastly, The bottom Frame was another heavily iterated part, as it originally comprised the whole frame along with the Top frame as was mentioned previously. Over it the project, it also received a number of iterations, including the addition of the external sloped walls, numerous holes to allow for the various externally mounted components to connect to the PID control systems mounted inside, a square divot on one side to better hold the battery, a slot to hold the acrylic window in the previously open side, a few structures to hold the electrical components and wiring, some additional divots to allow more space for the sizable PID control system that was encroaching into the walls, rounded interior edges on the columns to prevent damage to wiring, and lastly some additional length to give more space to the internal wiring.

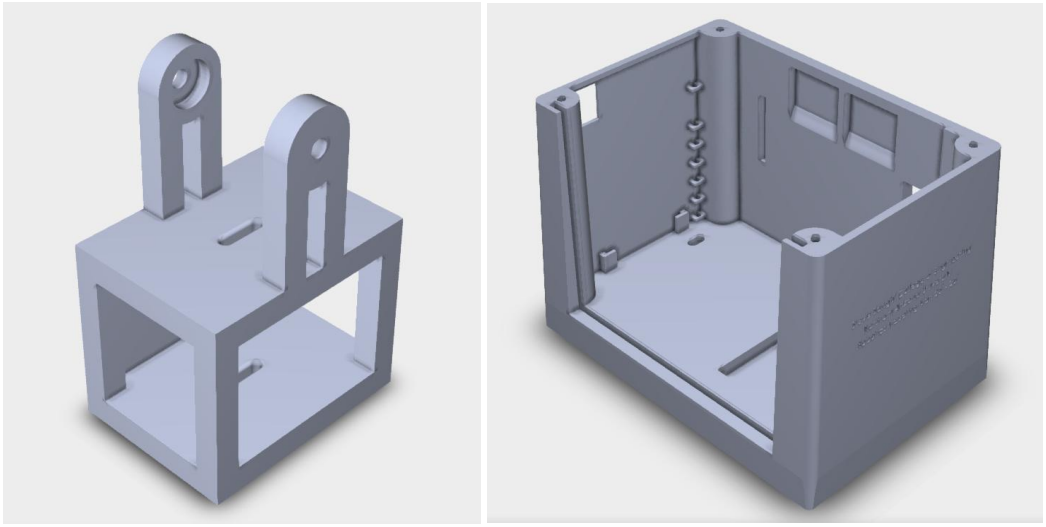

Figures 30 & 31: Original Minimized Robot 1 Frame (Left) and Final Bottom Frame (Right)

Through all the iterations, the final design of Robot #1 has made all the necessary cuts, modifications, and additions to perform its function, satisfy safety standards, all while maintaining a professional aesthetic design.

10.2 Final Physical Design – Robot #2

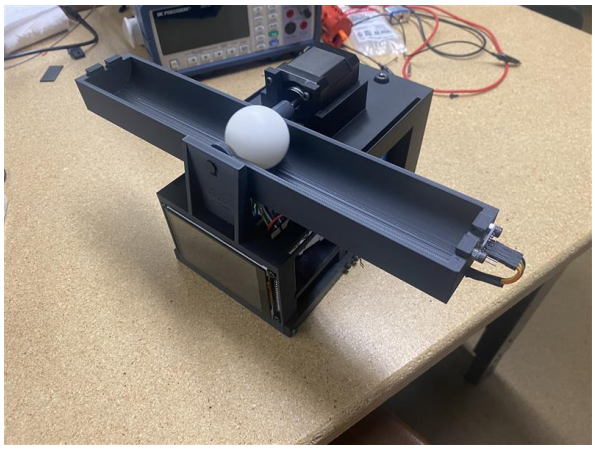

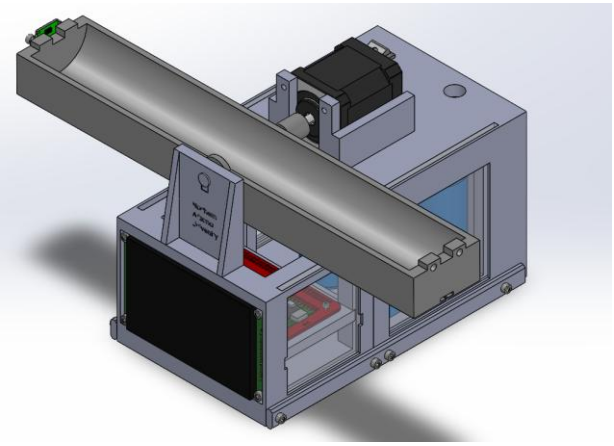

Figure 32 & 33: Full Assembly of Physical Robot 2 and SolidWorks CAD Isometric View

The final physical architecture of the Ball-on-Beam system is a highly optimized, modular, 3D-printed assembly designed specifically for K-12 outreach. At the top level, the system consists of a hollow-core structural base split into two primary sub-assemblies: the Motor Holder and the Center Hub. These two halves are rigidly mated at the floor utilizing custom "railroad-inspired" structural tie plates. Suspended directly above this base is the active tracking beam. To prevent the system's weight from acting as a cantilevered load solely on the motor, the beam utilizes a split-axis mounting strategy, with one end of the rotational axis is driven directly by the stepper motor, while the opposite end is supported by a passive shaft and bearing system integrated into the Center Hub wall. This disperses the rotational load evenly across the chassis while leaving the center of the beam completely unobstructed for the ball to roll freely.

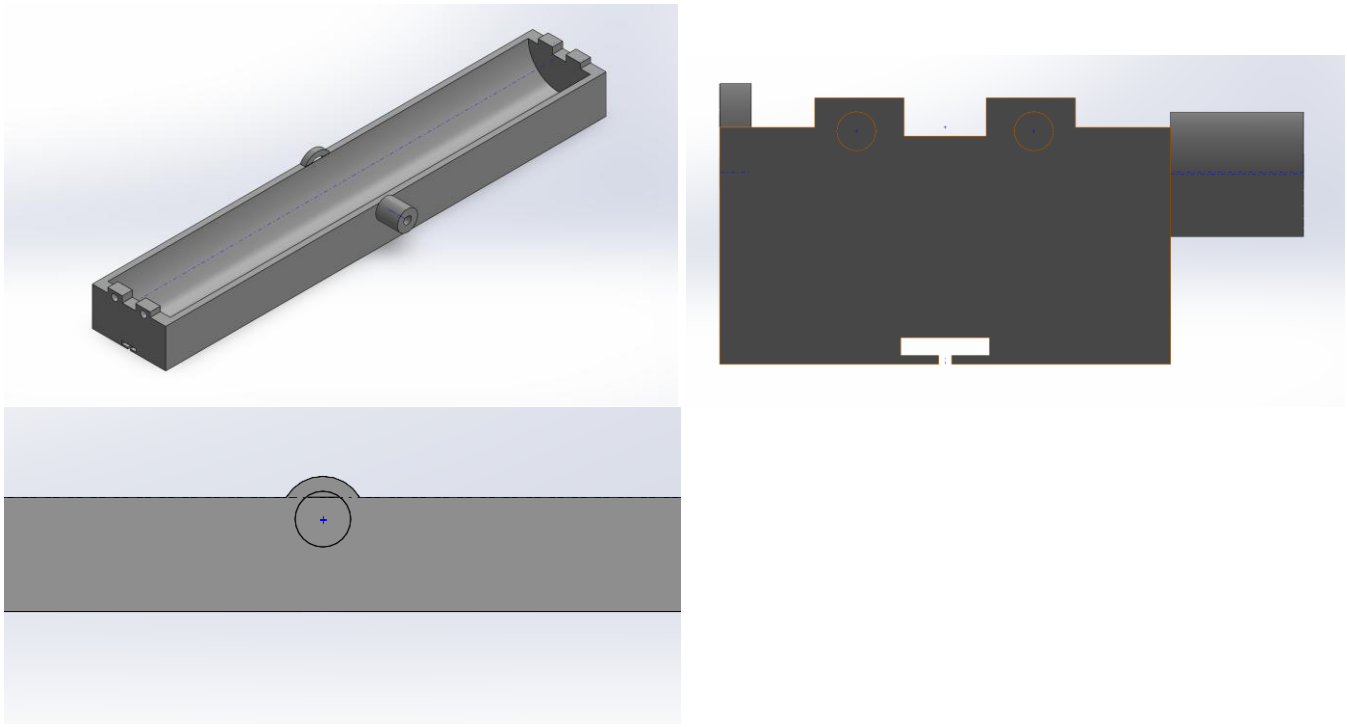

Figure 34-36: View of the Beam CAD and close up look at wire channel and bearing mount

The beam was iterated from a simple flat track into a precision U-channel trough. The curvature of the trough was explicitly designed to match exactly half the diameter of the ping-pong ball, ensuring the ball naturally self-centers along the axis of the Time-of-Flight sensor. To manage cable fatigue during continuous rotation, a slit was modeled along the underside of the beam, allowing sensor wires to be tucked safely inside the channel and exit near the center pivot point, preventing them from snagging during operation. The two ends of the beam feature distinct mounting topologies: the drive-side features a tightly toleranced D-shaft sleeve that mates directly with the NEMA 17 stepper motor shaft, while the support-side features a recessed housing that accepts a mechanical bearing, which rides on a static shaft protruding from the Center Hub wall.

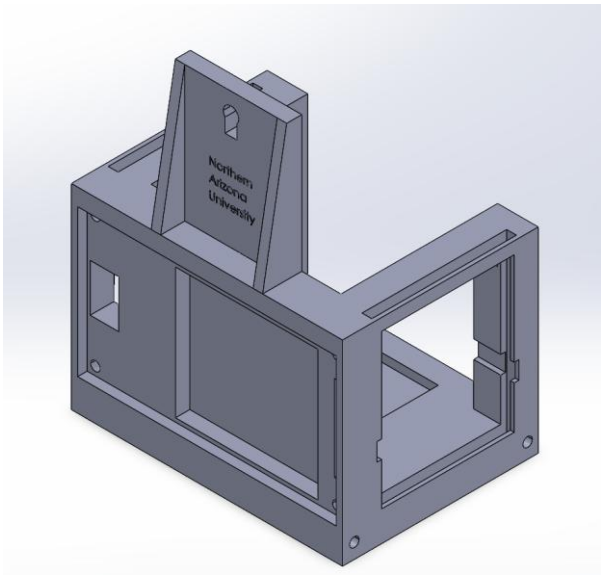

Figure 37: Isometric View of the Center Hub CAD

The Center Hub serves as both the primary electronics housing and the passive structural support for the beam. The top of the hub features an extruded vertical wall with a custom shaft plug that mates with the beam's bearing. A critical design iteration was setting the overall height of this wall geometry just below the beam's maximum travel arc, causing it to act as a precise physical hard-stop at ±20°. This eliminates any possibility of the beam over-rotating due to a software fault, serving as a passive mechanical failsafe entirely independent of the control system. Internally, the hub is hollowed out with dedicated, tiered mounting shelves for the electronics, the top shelf secures the microcontroller, while a custom slit directly below it houses the Battery Management System. The front face features a flush-mounted recessed cut-out into which the interactive touchscreen UI slides and is secured with mounting screws.

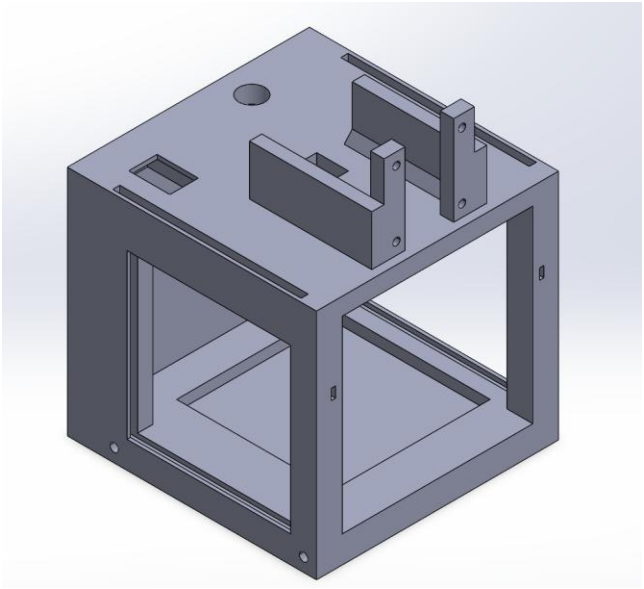

Figure 38: Isometric View of the Motor Holder CAD

Located opposite the Center Hub, the Motor Holder sub-assembly is designed to securely anchor the actuation and power systems. The top pocket is dimensionally matched to the NEMA 17 stepper motor, utilizing the motor's front mounting screw pattern to lock it rigidly into the PLA wall and eliminate rotational rattling under dynamic loading. Below the motor, the structure is hollowed out to serve as the primary battery compartment, intentionally locating the heavy LiFePO4 cells low to the ground to maintain a stable center of gravity. The roof of the Motor Holder features two dedicated cut-outs for the main power switch and charging cable port, deliberately positioning the user power controls away from the moving beam as a safety measure.

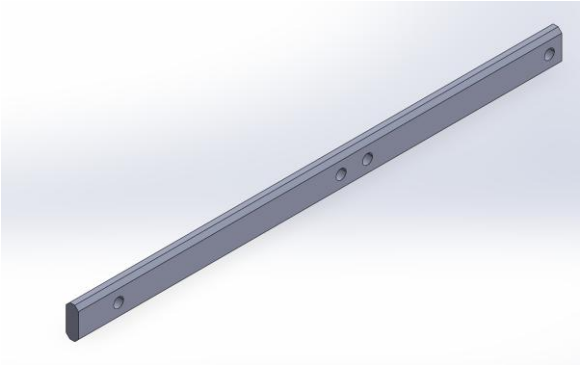

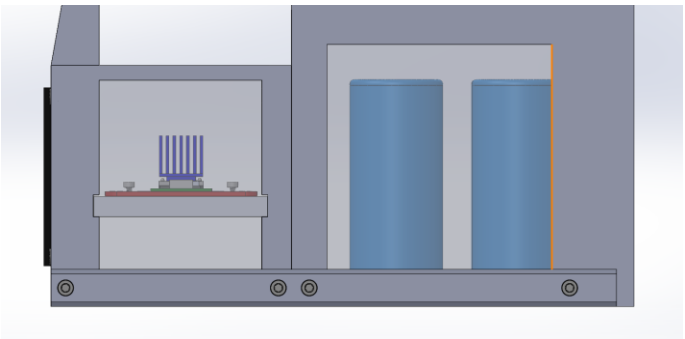

Figure 39 & 40 CAD View showing the bottom tie plates and the side window slots

To rigidly lock the Center Hub and Motor Holder together into a single chassis, the team designed custom "railroad" structural tie plates. These rectangular plates bridge the two halves at the floor level, utilizing four M3 screws threaded into brass heat-set inserts to pull the assembly tightly together. Finally, to satisfy the K-12 engagement requirement, the hollow sides of both sub-assemblies feature slotted tracks that accept clear acrylic viewing windows. This design iteration ensures all internal wiring, the BMS, and the battery array are fully protected from physical damage while still allowing students to directly observe the internal circuitry of the robot during operation.

11 Final Testing

11.1 Top level testing summary table

Table 24: Top Level Testing Summary Table

Experiment / Test	***Relevant DRs***	***Testing Equipment Needed***	***Other Resources***
EXP1: Safety & Dimensions	*ER1 - Overall Dimensions* *ER4 - Electrical Safety* *ER8 - Sharp Edge Radii* *ER9 - Pinch Clearance* *CR1 - Operating Space* *CR4 - Kid-Friendly*	*Calipers, CPSC safety gauge*	*Lab workspace*
EXP2: BOM Audit	*ER6 - Manufacturing Cost* *CR6 – Inexpensive*	*Excel BOM spreadsheet, purchasing receipts*	*Market Comparison Data*
EXP3: Chassis Drop Test	*ER5 - Drop Test* *CR4 - Kid-Friendly* *CR5 – Durability*	*36-inch desk/table, measuring tape, camera*	*Hard classroom floor*
EXP4: Battery Endurance	*ER2 - Power Run Time* *CR2 - Battery Powered*	*Stopwatch, digital multimeter, Excel*	*Fully charged LiFePO4 batteries*
EXP5: Interface & Control	*ER3 - Control Hardware* *ER7 - PID Settling* *ER10 - Emergency Stop* *ER11 - Visual Feedback* *CR3 - Active Balancing* *CR7 - Interactive Interface* *CR8 - Educational Props*	*Raspberry Pi logic analyzer, Touchscreen GUI, E-Stop circuit*	*Client testing parameters*
EXP6: PID Stability	*ER7 - PID Settling Time* *CR3 - Active Dynamic Balancing*	*Stopwatch, video recording device*	*Level surface*
EXP7: Sensor Calibration	*ER3 - Control Hardware* *CR8 - Educational Props*	*Centimeter ruler, protractor, tape markers*	*None*

Table 23 is the Top level Testing Summary for the final round of testing performed on both robots, except for experiment 3: the chassis drop test which was only performed on Robot 1. The first column of the table lists each experiment performed, the second column lists what design requirement each experiment is designed to prove the robots satisfy, the third column describes the tools directly used to acquire data in each experiment, and the last

column includes and other resources necessary to perform to the associated experiment.

11.2 Detailed Testing Plan

11.2.1 Test 1: Safety & Dimensions

11.2.1.1 Summary

The first test performed was conducted to verify that both robots designs had no dangerous elements such as exposed wiring, thin recesses on moving parts that could pinch skin, no sharp edges, and was overall safe to operate in direct contact with children ages K-12 following CPSC standards, while remaining compact in overall design.

11.2.1.2 Procedure

The procedure for the test involved using calipers and the CPSC safety gauge to inspect any potential points of risk on each robot and ensure they were compliant with CPSC standards, as well as measuring the overall dimensions of both robots to ensure they remained within a 12 in. x 12 in. x 12 in. cube.

11.2.1.3 Results

After performing the experiment, it was found that there were no outstanding violations of the CPSC guidelines, and both robots overall dimensions remained within the 12 inch cube maximum.

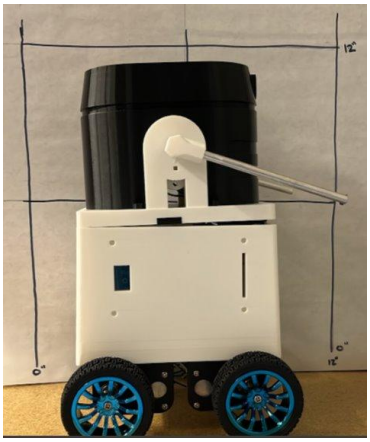
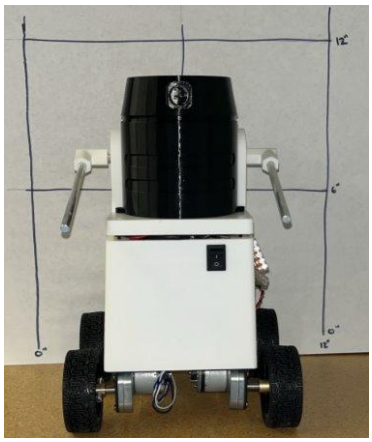
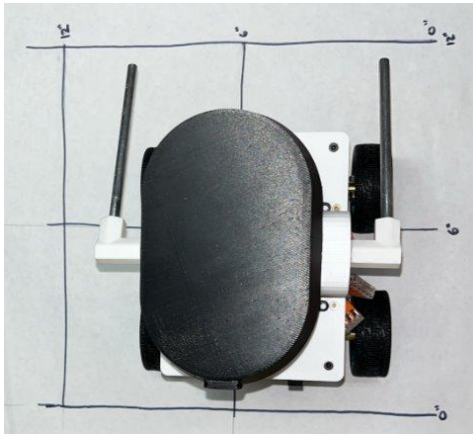

Figures 41-43: Left to Right - Profile, Front, and Top views of Robot #1 Verifying dimensions under 12 inches

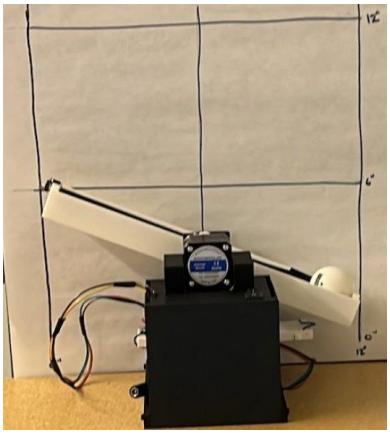
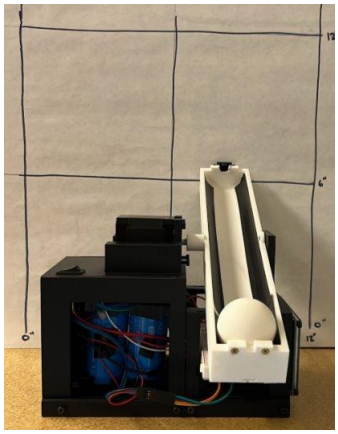
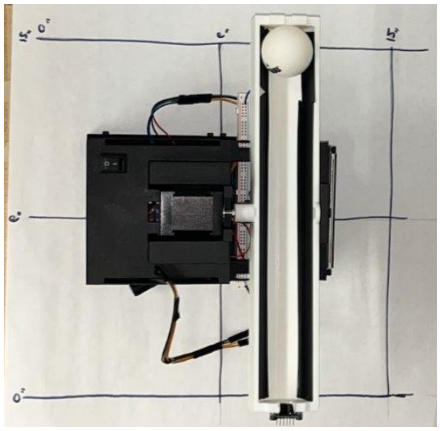

Figures 44-45: Left to Right - Profile, Front, and Top views of Robot #2 Verifying dimensions under 12 inches

11.2.2 Test 2: Bill of Materials Audit

11.2.2.1 Summary

The Second Test performed was an Audit of all materials used in the construction of the final version of each robot to fully evaluate the cost of each robot to verify the exact manufacturing costs of each and if they remained cheaper than similar devices on the market today.

11.2.2.2 Procedure

The Test was performed by looking at the receipts for each component purchased and compiling them on a spreadsheet so they could be summed for the total value. That value was then compared to the price of similar devices found online.

11.2.2.3 Results

Robot #1 was found to have an overall manufacturing cost of $241.90 dollars, which offers consumers 48% savings compared to similar robot models available for purchase, while Robot #2 was found to have an overall manufacturing cost of $244.06 dollars, which offers consumers 49% savings compared to similar robot models available for purchase. See Appendix 15.1 and tables 16 and 17 for more details.

11.2.3 Test 3: Chassis Drop Test

11.2.3.1 Summary

The third test performed was exclusively performed on Robot #1 as due to the mobile nature of the robot, it is at risk of rolling of tables during active operation, and as such should be able to survive the forces imposed by such falls

11.2.3.2 Procedure

The chassis for Robot #1 was assembled including major structural elements and major sources of weight, in this case being the motors, wheels, and the battery. Other electrical components were excluded at time of testing due to limited resources meaning such components could not be risked in testing, and their weight was also determined to be negligible in affecting the outcome of the test. With the assembled frame loaded with major sources of weight, the robot was dropped at various angles from a height of 34 inches. The first angle was on the robots front, pushed off a table in such a way to mimic it rolling off a table during operation, while the second was on the robots side, and finally the robots top. After each drop condition the robot was visually inspected for any fractures or deformations in its frame.

11.2.3.3 Results

At each angle of impact, Robot #1's frame showed no signs of deformation or fracture, verifying the robots ability to survive the most adverse conditions it may encounter during average operation.

11.2.4 Test 4: Battery Endurance

11.2.4.1 Summary

The fourth test performed was designed to verify that both robots could operate on battery power alone and for 30 minutes continuously, which was determined to be equivalent to the amount of intermittent use the robots would see during an outreach event

11.2.4.2 Procedure

Both robots were activated with fully charged batteries and run continuously over a period of time measured by a stopwatch, while the voltage draw was measured with a multimeter. This data was then imported into an excel sheet so the power burn rate of both robots could be determined and compared to the standard LiFeP04 Battery discharge curve model to evaluate the lifespans of both robots.

11.2.4.3 Results

As can be seen in Figure X below, both robots far exceed the required operating time of 30 minutes required for average operation during outreach events

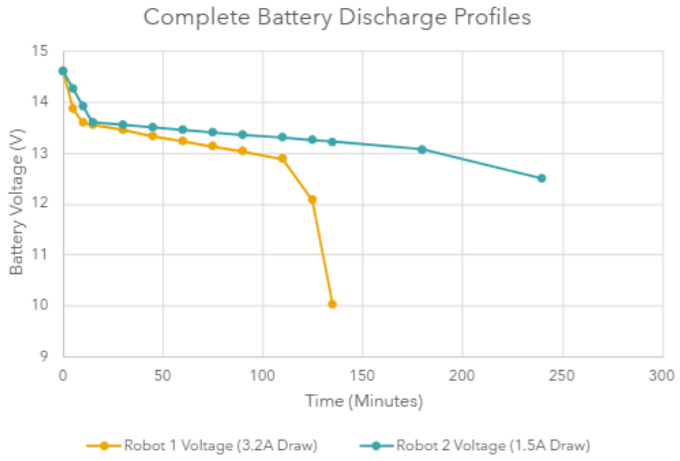

Figures 46: Graph depicting Battery discharge over time for both robots

11.2.5 Test 5: Interface & Control

11.2.5.1 Summary

The fifth test performed was designed to verify the system could function successfully with touch-screen integration, aspects of the robots function could be successfully changed through the touch screen, and that the emergency stop severs power immediately as part of the safety requirements.

11.2.5.2 Procedure

The PID control systems were activated including the touch screen which was then both visually inspected to verify the appropriate values were displayed, and the programed buttons were tested to verify functionality, then the emergency stop switch was flipped to very immediate cessation of operation.

11.2.5.3 Results

The touch screen was verified to display the correct information, the programed buttons on the touch screen were verified to be functional, and robot function ceased immediately upon flipping the power switch, satisfying all interactivity and safety requirements.

Figures 47: Touch screen display for Robot 2

11.2.6 Test 6: PID Stability & Settling

11.2.6.1 Summary

The sixth test is designed to verify the robot is capable of performing its intended function of brining the system into balance in a reasonable time frame of under 15 seconds. Due to the descoping of Robot #1's functionality it was exempt from this test.

11.2.6.2 Procedure

Robot #2 was activated and the system was allowed to reach equilibrium, in this case the ball staying at the center of the beam. The ball was then displaced from the center and a stopwatch was used to measure the time required for the ball to reach a state of equilibrium at the center of the beam. The test was then repeated 5 times to find the average time necessary for the system to settle.

11.2.6.3 Results

Robot #2 was found to take about 8.93 seconds on average to re-settle the ball at the center of the beam after being displaced, successfully falling under the required 15 second time limit.

11.2.7 Test 7: Sensor Calibration

11.2.7.1 Summary

The seventh test was performed to verify the sensor systems and calculations being utilized were properly reading the moving elements of the system, for Robot #1 the magnetic potentiometer reading the angle of the pendulum, and for Robot #2 the Time of Flight sensor reading the distance of the ball along the length of the beam. In both cases the sensors must have at most 5% error in the data being measured

11.2.7.2 Procedure

For Robot #1, a protractor was used to compare the actual angle of the beam to the angle being measured by the magnetic potentiometer while the pendulum was held at 45 degree increments starting from 0 degrees (Holding the beam flat on the left). For Robot #2 a ruler was used to measure the distance from the Time of Flight sensor to various points on the beam which were then marked so the ball could be held at that distance and the sensor measurement could be compared to the actual. The points marked were each end of the beam, the center of the beam, and the midpoints between each and of the beam and the center.

11.2.7.3 Results

Each measurement from either sensor was recorded and an error calculation was performed with the actual measurement at each point, the results for which can be seen in the below tables.

Table 25: Magnetic Encoder Error Data for Robot #1

Magnetic Encoder Calibration			
Physical Angle	**Raw Output**	**Calibrated (+56.0°)**	**% Error (180° FSR)**
0° (Flat Left)	-54.4°	1.6°	0.89%
45°	-9.3°	46.7°	0.94%
90° (Upright Center)	34.0°	90.0°	0.00%
135°	84.0°	140.0°	2.78%
180° (Flat Right)	127.2°	183.2°	1.78%

Table 26: Time of Flight Error Data for Robot #2

Time-of-Flight (ToF) Sensor Calibration			
Physical Mark	**Raw Reading**	**Calibrated (−2.3 cm)**	**Tracking Error**
0 cm (Close End)	2.3 cm	0.0 cm	0.00%
7.28 cm (1st Quarter)	9.5 cm	7.20 cm	1.10%
14.55 cm (Middle)	17.1 cm	14.80 cm	1.70%
21.83 cm (3rd Quarter)	23.5 cm	21.20 cm	2.90%
29.10 cm (Far End)	30.2 cm	27.90 cm	4.10%

12 Future work

With all tests completed, Robots #1 and #2 are currently in very different stages of development, but both have similar paths moving forward. Starting with Robot #1, while its current descoped state has been approved by the client as acceptable, it is still not the desired state for Robot #1 and there is a fair amount of work that must be done in order to reach that point. First and foremost, the electrical system needs finalization, as in its current state it is still running on a breadboard rather than the designed printed circuit board. Due to delays outside of the team's control, the order for the PCB's for both robots was unable to be filled and a finalized electrical system couldn't be completed. Due to the more mobile nature of Robot #1, the breadboard is incapable of holding the circuit together while the robot is operating as intended, meaning testing the systems code was impossible to test, and the only functions that could be tested were the sensitivity of the magnetic encoder and the motors moving in response to the pendulum's current angle. Once a proper electrical system is established, the code to balance the pendulum can properly be tested, tuned, and refined to a state of smooth operation, at which point the integration of the touch screen and the interactive aspect of the robot can be further developed. Additionally, if the code struggles to balance the system due to the low mass of the pendulum, as the client suggested, the length of the pendulum could be increased to both increase the mass of the pendulum, as well as increase the distance between the center of mass of the pendulum and the axis of rotation, which should greatly reduce the required speed necessary to rotate the pendulum. Once the pendulum system is properly developed and the code is finely tuned, the final aesthetic adjustments can be made to ensure the robots look clean and well organized. This process would involve proper wire management and may require the introduction of additional features to the frame of the robot to achieve said wire management. Once those steps are completed, the robot should be in a state fully satisfying the clients desires for the product, and it can be used in outreach events.

Moving to Robot #2, as mentioned previously, it is in a much better position, being fully functional and capable of balancing the ball at the center of the beam in under 15 seconds, and has already been displayed at an outreach event. This doesn't mean that more steps can be taken to further improve the final product, first and foremost being the finalization of the electrical systems. Similarly to Robot #1, Robot #2 was unable to have its electrical systems finalized due to not receiving the designed printed circuit board, and it too is currently running on a Breadboard. Unlike Robot #1 however, the stationary nature of Robot #2 means that more advanced testing could be performed to get it to the current state of functionality. With the electrical systems finalized, the balancing code could use additional refinement, as at the current time while Robot #2 is able to balance properly the beam tends to move more sporadically as the ball reaches the center of the beam rather than smoothly making small adjustments until the ball stops moving. Additional time spent modifying and testing the balancing code should be able to bring the beam's operation to the clients desired state of smoothness. Lastly, once all systems are finalized and refined, Robot #2 can receive the same aesthetic adjustments mentioned for Robot #1 to improve the overall appearance of the robot to fit the client's desire for a professional design.With the remaining steps laid out, any future teams who might be brought on to complete the last remaining work needed should have a clear set of goals to work off of and fulfill the clients original request for two fully functional, interactive, professionally designed robots for use at student outreach events.

13 Conclusion

The purpose of this capstone project is to design and build two highly interactive educational robots that can travel as outreach demonstrations for NAU. This is sponsored by Dr. Michael Shafer and the project focuses on creating low-cost and robust teaching platforms that visually communicate core control-system concepts and STEM interest among younger students. The functions of the corresponding robots are:

- Robot #1 – Inverted Pendulum: Highlights Lagrangian motion, mobility, and spatial tracking using magnetic encoders. Active PID balancing was removed from scope to emphasize structural durability and dependable component performance.
- Robot #2 – Ball-on-Beam: A single-axis that is a direct drive system that provides a clear, hands-on demonstration of how an active PID feedback control works.

The project had a $5,000 budget, and the main requirement was for it to be mass producibility for future deployment. The team met this by using off the shelf electronics and standard 3D-printed PLA, which achieved a scalable per-unit cost of under $300. Over the academic year, the work progressed from theoretical modeling to fully functional hardware capable of withstanding the demands of K–12 outreach environments.

The project criteria established the importance of performance, safety, and durability for each platform. The two robots must satisfy these functions to be a NAU outreach tool. The systems must effectively translate from mathematical equations to behavior that is observable in physical motion. Through dynamic tracking or active feedback control loops towards K-12 students. Students must also be able to safely adjust system variables through the onboard touchscreens without relying on external computers. To survive the wear and tear of a K–12 environment, both robots utilize thickened 3D-printed PLA architectures and robust mechanical fasteners to ensure high resilience during repeated transportation and hands-on demonstrations. Each platform must operate fully without relying from wall power which is achieved through the 14.8V $LiFePO_4$ battery. This can power robots over 90 minutes of continuous use. The unit cost must remain strictly below the $300 target to support mass production for future NAU RTV deployments. Overall, the success of the robots has been confirmed through final physical testing, performance analysis, and client evaluation, verifying that the completed platforms meet the required safety, durability, and cost metrics for long-term engineering outreach.

With testing complete, Robots #1 and #2 stand at different stages of development, but they share a clear path forward. Robot #1's current state has been approved by the client, yet significant work remains to reach the intended final design. The electrical system still requires full implementation, such as delays in PCB manufacturing, preventing proper code testing, and limiting validation to encoder sensitivity and basic motor response. Once the finalized PCB is integrated, the balancing code can be properly tuned with the touchscreen interface, and mechanical adjustments such as increasing pendulum length and mass can be emphasized to improve stability. After functional refinement and wire management updates will bring Robot #1 to the client's desired professional standard for outreach use.

Robot #2 is already fully functional by being capable of balancing the ball at center in under 15 seconds and has successfully appeared at an outreach event. However, like Robot #1, it still requires completion of its electrical system once the PCB becomes available. With that in place, its balancing algorithm can be further refined to eliminate the remaining jolting of the beam motion and achieve smoother and more controlled operation. These remaining steps provide a clear roadmap for future teams that ensures they can finalize both platforms and fully satisfy the client's request for two complete, interactive, professionally finished robots for NAU's student outreach events.

14 REFERENCES

[1] ASME, Machine Screws, Tapping Screws, and Metallic Drive Screws (Metric Series), ASME B18.6.3-2024, 2024.
[2] ASME, Metric Screw Threads: M Profile, ASME B1.13M-2005 (R2020), 2020.
[3] IEC, Audio/video, information and communication technology equipment - Part 1: Safety requirements, IEC 62368-1:2023, 2023.
[4] ASTM, Standard Consumer Safety Specification for Toy Safety, ASTM F963-17, 2017.
[5] R. H. Bao and T. X. Yu, "Collision and rebound of ping pong balls on a rigid target," *Materials and Design*, Aug. 2015
[6] ASME B1.13M, *Metric Screw Threads: M Profile*, American Society of Mechanical Engineers.
[7] ASME B18.2.8, *Metric Fasteners—Clearance Holes*, American Society of Mechanical Engineers.
[8] ASTM F2792, *Standard Terminology for Additive Manufacturing Technologies*, ASTM International.
[9] Federal Communications Commission, *FCC Part 15, Subpart B—Unintentional Radiators*, United States.
[10] European Union, *Directive 2015/863 (RoHS 3): Restriction of Hazardous Substances*.
[11] "6mm shaft (stainless steel, 300mm length)," goBILDA®, https://www.gobilda.com/2100-series-stainless-steel-round-shaft-6mm-diameter-300mm-length/?setCurrencyId=1&sku=2100-0006-0300&gad_source=1&gad_campaignid=12299979486&gbraid=0AAAAAC78-tMzDwozKfjmjjBsbseH63RUZ&gclid=CjwKCAiA4KfLBhB0EiwAUY7GAaYI04A7y_dibxvlOUKvH0Tk_2K4rFEhsymQhzsrxSGyXU8zW-9DnhoCYmEQAvD_BwE (accessed Jan. 25, 2026).
[12] B. Cazzolato, *Modeling and Control of the Ball and Beam System*, University of Adelaide, Sept. 2007.
[13] StepperOnline, "NEMA 17 Bipolar Stepper Motor, 59 N·cm Holding Torque (17HS19-2004S1)." [Online]. Available: https://www.omc-stepperonline.com/nema-17-bipolar-59ncm-84oz-in-2a-42x48mm-4-wires-w-1m-cable-connector-17hs19-2004s1
[14] J. Glower, *ECE 463/663: Modern Control – Ball and Beam System Lecture Notes*, BISON Academy, Dept. of Electrical and Computer Engineering, North Dakota State University, Spring 2026.
[15] R. C. Hibbeler, *Engineering Mechanics: Dynamics*, 14th ed. Boston, MA, USA: Pearson Education, 2016.

[23] N. Hammje, "Ball-Balancing Bot Uses OpenCV on a Raspberry Pi to Stop a Ball Dead in Its Tracks," Hackster.io, 2024. [Online]. Available: https://www.hackster.io/news/nicolas-hammje-s-ball-balancing-bot-uses-opencv-on-a-raspberry-pi-to-stop-a-ball-dead-in-its-tracks-f8748c394bde. [Accessed: Oct. 5, 2025].
[24] J. Sirgado, "Magnet Levitation with Arduino," Arduino Project Hub, 2022. [Online]. Available: https://projecthub.arduino.cc/jsirgado/magnet-levitation-with-arduino-233746. [Accessed: Oct. 5, 2025]. [25] "Wheelbot: A Symmetric Unicycle That Balances Using Reaction Wheels," TechXplore, 2022. [Online]. Available: https://techxplore.com/news/2022-08-wheelbot-symmetric-unicycle-reaction-wheels.html. [Accessed: Oct. 4, 2025].
[26] A. Md. K. Alam, M. R. Karim, and S. M. M. Hasan, "Stabilising a cart inverted pendulum system using pole placement control method," in Proc. 3rd Int. Conf. on Electrical Information and Communication Technology (EICT), Khulna, Bangladesh, 2017, pp. 1–6. doi: 10.1109/EICT.2017.8168481.
[27] D. J. Block, K. J. Åström, and M. W. Spong, The Reaction Wheel Pendulum. Morgan & Claypool Publishers, 2007.
[28] R. Gajamohan, M. Muehlebach, T. Widmer, and R. D'Andrea, "The Cubli: A Cube That Can Jump Up and Balance," in IEEE/RSJ Int. Conf. on Intelligent Robots and Systems (IROS), Tokyo, Japan, 2013, pp. 3722–3727. doi: 10.1109/IROS.2013.6696915.
[29] J. R. Wertz, Spacecraft Attitude Determination and Control. Springer, 1978.
[30] B. Wie, Space Vehicle Dynamics and Control, 2nd ed. AIAA, 2008.
[31] University of Michigan, "Ball & Beam: System Modeling," Control Tutorials for MATLAB and Simulink (CTMS). [Online]. Available: https://ctms.engin.umich.edu/CTMS/index.php?example=BallBeam&section=SystemModeling. [Accessed: Sept.

10, 2025].
[32] B. Cazzolato, “Derivation of the Dynamics of the Ball and Beam System,” Univ. of Adelaide, School of Mechanical Engineering. [Online]. Available: https://www.researchgate.net/publication/235898231. [Accessed: Sept. 14, 2025].
[33] K. C., “Inverted Pendulum: Control Theory and Dynamics,” Instructables, 2025. [Online]. Available: https://www.instructables.com/Inverted-Pendulum-Control-Theory-and-Dynamics/. [Accessed: Sept. 14, 2025].
[34] S. Sackett, “Self-Balancing Inverted Pendulum Robot,” Shay Sackett’s Project Portfolio. [Online]. Available: https://www.shaysackett.com/inverted-pendulum-robot/. [Accessed: Sept. 11, 2025].
[35] B. T. Williams, “Self-Balancing Robot Using PID Packs Other Punches,” Elektor Magazine, Oct. 5, 2022. [Online]. Available: https://www.elektormagazine.com/news/self-balancing-robot-using-pid-packs-other-punches. [Accessed: Sept. 14, 2025].
[36] University of Michigan, “DC Motor Speed: System Modeling,” Control Tutorials for MATLAB and Simulink (CTMS). [Online]. Available: https://ctms.engin.umich.edu/CTMS/index.php?example=MotorSpeed&section=SystemModeling. [Accessed: Sept. 11, 2025].
[37] University of Michigan, “Ball and Beam: System Modeling (CTMS).” [Online]. Available: https://ctms.engin.umich.edu/CTMS/index.php?example=BallBeam&section=SystemModeling. [Accessed: Sept. 10, 2025].
[38] S. Anand and R. Prasad, "Dynamics and control of ball and beam system," International Journal on Recent and Innovation Trends in Computing and Communication, vol. 5, no. 5, pp. 1332–1339, May 2017.
[39] Acrome, “Ball and Beam,” Acrome Control Systems, 2024. [Online]. Available: https://acrome.net/product/ball-on-beam. [Accessed: April 19, 2026].
[40] Microsoft, “Project Moab,” Microsoft Autonomous Systems, 2024. [Online]. Available: https://www.microsoft.com/en-us/ai/bonsai-moab. [Accessed: April 19, 2026].
[41] “Arduino Ball and Beam PID Controller,” Instructables, 2020. [Online]. Available: https://www.instructables.com/Arduino-Ball-and-Beam-PID-Controller/. [Accessed: April 19, 2026].
[42] STMicroelectronics, “VL53L0X: World's smallest Time-of-Flight ranging and gesture detection sensor,” STMicroelectronics Datasheet, 2024. [Online]. Available: https://www.st.com/en/imaging-and-photonics-solutions/vl53l0x.html. [Accessed: April 19, 2026].
[43] Raspberry Pi Ltd, “Raspberry Pi Pico Documentation,” Raspberry Pi Microcontrollers, 2024. [Online]. Available: https://www.raspberrypi.com/documentation/microcontrollers/raspberry-pi-pico.html. [Accessed: April 19, 2026].
[44] IEEE Standard for Ontologies for Robotics and Automation (ORA): Core Ontologies for Robotics and Automation (CORA), IEEE Std 1872.1-2024, pp. 1–84, May 2024. doi: 10.1109/IEEESTD.2024.10557945.
[45] S. O. Fadlallah and K. M. Goher, “Bacterial foraging-optimized PID control of a two-wheeled machine with a two-directional handling mechanism,” Robotics and Biomimetics, vol. 4, no. 1, p. 5, 2017.
[46] X. Yu, Y. Fan, S. Xu, and L. Ou, “A self-adaptive SAC-PID control approach based on reinforcement learning for mobile robots,” Int. J. Robust Nonlinear Control, vol. 31, no. 21, pp. 8389–8408, 2021.
[47] S. Jin and Y. Ou, “A wheeled inverted pendulum learning stable and accurate control from demonstrations,” Appl. Sci., vol. 9, no. 24, p. 5279, 2019.
[48] S. Roy, S. B. Roy, and I. N. Kar, “Adaptive-robust control of Euler-Lagrange systems with linearly parametrizable uncertainty bound,” IEEE Trans. Control Syst. Technol., vol. 26, no. 5, pp. 1842–1850, 2018.
[49] K. Ogata, System Dynamics, 4th ed. Upper Saddle River, NJ, USA: Prentice Hall, 2003, ch. 11.
[50] PythonRobotics, “Inverted Pendulum Control,” GitHub repository. [Online]. Available: https://github.com/AtsushiSakai/PythonRobotics
[51] zjor, “Inverted Pendulum on a Cart,” Arduino Project Hub. [Online]. Available:

https://projecthub.arduino.cc/zjor/inverted-pendulum-on-a-cart-d4fdfc
[52] MRCE, “Circuit Analysis & Design Introduction.” [Online]. Available: https://mrce.in/ebooks/Circuit%20Analysis%20&%20Design%20Introduction.pdf
[53] Creality, “Ender-3 V2 3D Printer User Manual.” [Online]. Available: https://m.media-amazon.com/images/I/B1f9eP6H3OS.pdf
[54] Z. C. M. Davidson, S. Dang, and X. Vasilakos, “Blended laboratory design using Raspberry Pi Pico for digital circuits and systems,” IEEE Trans. Learn. Technol., vol. 17, 2024.
[55] S. R. Doty, “Python Basics,” Comput. Sci., pp. 1–20, 2008.
[56] Y. Li, K. H. Ang, and G. C. Y. Chong, “PID control system analysis and design,” IEEE Control Syst. Mag., vol. 26, no. 1, pp. 32–41, Feb. 2006.
[57] H. H. Asada, “Manufacturing robotics: Basic issues and challenges,” 1996. [Online]. Available: https://www.sciencedirect.com/science/article/pii/S147466701757682X
[58] A. Prati, G. Peruzzini, M. Pellicciari, and M. Raffaeli, “How to include user experience in the design of human-robot interaction,” 2021. [Online]. Available: https://www.sciencedirect.com/science/article/pii/S0736584520302805
[59] G. Hoffman and W. Ju, “Designing robots with movement in mind,” 2014. [Online]. Available: https://dl.acm.org/doi/10.5898/JHRI.3.1.Hoffman
[60] Mamatnabiyev, “Design and implementation of an open-source educational robot for hands-on learning experiences in IoT,” 2023. [Online]. Available: https://ieeexplore.ieee.org/document/10146599
[61] S. Dai, H. Li, Y. Peng, Z. Zhu, J. Jiang, and Y. Gao, “Design and control of a multi-DOF two-wheeled inverted pendulum robot,” 2014. [Online]. Available: https://ieeexplore.ieee.org/document/7052763
[62] Y. Li, Y. Gao, J. Huang, H. Du, and J. Duan, “Mechanical design and dynamic modeling of a two-wheeled inverted pendulum mobile robot,” 2007. [Online]. Available: https://ieeexplore.ieee.org/document/4338830
[63] Siddhartha, Ghosh, and D. M., “Design and implementation of self-balancing interactive robot,” 2023. [Online]. Available: https://ieeexplore.ieee.org/document/10584954
[64] Formlabs, “3D printing threads and adding threaded inserts to 3D printed parts.” [Online]. Available: https://formlabs.com/blog/adding-screw-threads-3d-printed-parts/
[65] JuggerBot 3D, “Polylactic acid (PLA) filament review.” [Online]. Available: https://juggerbot3d.com/pla-filament-review/
[66] WikiFactory, “Ultimate guide: How to design for 3D printing,” 2020. [Online]. Available: https://wikifactory.com/+wikifactory/stories/ultimate-guide-how-to-design-for-3d-printing
[67] 井手隆統, 本田功輝, 金田礼人, 中島康貴, and 山本元司, “Comparison of CoP estimation and center-of-gravity sway measurement in human standing posture using inertial sensors,” M.S. thesis, Grad. Sch. Eng., Kyushu Univ., Fukuoka, Japan.
[68] S. Sasagawa, J. Ushiyama, M. Kouzaki, and H. Kanehisa, “Effect of the hip motion on the body kinematics in the sagittal plane during human quiet standing,” Neurosci. Lett., vol. 450, no. 1, pp. 27–31, Jan. 2009, doi: 10.1016/j.neulet.2008.11.027.
[69] J. L. Cabrera and J. G. Milton, “Human stick balancing: Tuning Lèvy flights to improve balance control,” Chaos, vol. 14, no. 3, pp. 691–698, Sep. 2004, doi: 10.1063/1.1785453.
[70] B. Sprenger, L. Kucera, and S. Mourad, “Balancing of an inverted pendulum with a SCARA robot,” IEEE/ASME Trans. Mechatronics, vol. 3, no. 2, pp. 91–97, Jun. 1998, doi: 10.1109/3516.686676.
[71] J. Winkler and J. Suchý, “Erecting and balancing of the inverted pendulum by an industrial robot,” IFAC Proc. Volumes, vol. 42, no. 16, pp. 323–328, 2009, doi: 10.3182/20090909-4-JP-2010.00056.
[72] Y. Y. Lim, C. L. Hoo, and Y. M. F. Wong, “Stabilizing an inverted pendulum with PID controller,” MATEC Web Conf., vol. 152, p. 02009, 2018, doi: 10.1051/matecconf/201815202009.

[73] D. Zhang, J. Wang, H. Zhang, and L. Yu, “Research on inverted pendulum control system based on vision sensor,” in Proc. 2nd Int. Conf. Mach. Learn. Comput. Appl. (ICMLCA), Shenyang, China, 2021, pp. 1–5.
[74] A. Kastner, J. Inga, T. Blauth, F. Kopf, M. Flad, and S. Hohmann, “Model-based control of a large-scale ball-on-plate system with experimental validation,” Karlsruhe Inst. Technol., Karlsruhe, Germany, Mar. 2019, doi: 10.1109/ICMECH.2019.8722850.
[75] S. E. Mathe, H. K. Kondaveeti, S. Vappangi, S. D. Vanambathina, and N. K. Kumaravelu, “A comprehensive review on applications of Raspberry Pi,” Comput. Sci. Rev., vol. 52, p. 100636, May 2024, doi: 10.1016/j.cosrev.2024.100636.
[76] A. S. Silva, R. M. Cotta, and L. A. Ismail, “Uncertainty analysis of infrared thermography in convective heat transfer,” 2014. [Online]. Available: https://www.researchgate.net/publication/265540159

15 APPENDICES

15.1 Appendix A: Bill of materials (BOM) of Robot #1 and #2 for the RTV Capstone throughout the 2026 spring semester; listing the products used to manufacture the final product with the name of parts, vendor, costs, quantity, link of purchases, and dimensions of the products.

BILL OF MATERIALS - Robotics Traveling Van (RTV) Capstone Project

Project: Robotics Traveling Van (RTV) | Two Robot Assembly | Spring 2026

Drawn By: Freddy R. · Florence Fasugbe · Colin Parsinia · Andres Gonzales | April 2026

HOW TO READ THIS BOM: Column A = Item # cross-referencing balloon numbers in the Pendulum Robot CAD drawing (RTV_Robot_1_Final_CAD_Assembly). Column B = Item # cross-referencing balloon numbers in the Ball-on-Beam Robot CAD drawing (RTV_Robot_2_Final_CAD_Assembly). A dash (—) means the part is not used in that robot. Parts with quantities in both columns are shared components. ***Section 1 shows estimated print material costs for reference — these are NOT included in the grand total.***

Pendulum Robot Item #	Ball-on-Beam Robot Item #	Part Name (Material)	Make / Buy	Vendor & Purchase Link	Pendulum Robot QTY	Ball-on-Beam QTY	Pack Unit / Est. Weight	Pack Cost / Mat. Cost*	Cost / Piece or / Gram*	Total Cost Pendulum Robot	Total Cost Ball-on-Beam
SECTION 1 — Custom 3D Printed & Fabricated Parts (Make) | * Columns I–L show estimated print material cost (grams × $/g) for reference only — NOT included in grand total											
↳ *RTV Pendulum Robot — 3D Printed Parts | Ref: RTV_Robot_1_Final_CAD_Assembly*											
1	—	Frame Base (PLA)	Make	*3D Printed In-House*	1	—	~200g (PLA @ $17.99/kg)	*$3.60*	*$3.598*	*$3.60*	*$0.00*
2	—	Frame Top (PLA)	Make	*3D Printed In-House*	1	—	~160g (PLA @ $17.99/kg)	*$2.88*	*$2.878*	*$2.88*	*$0.00*
3	—	Magnetic Potentiometer Mount (PLA)	Make	*3D Printed In-House*	1	—	~30g (PLA @ $17.99/kg)	*$0.54*	*$0.540*	*$0.54*	*$0.00*
4	—	Yahboom Motor Bracket (PLA)	Make	*3D Printed In-House*	4	—	~15g ea (PLA @ $17.99/kg)	*$0.27*	*$0.270*	*$1.08*	*$0.00*
16	—	Pendulum Shell (TPU)	Make	3D Printed In-House	1	—	~100g (TPU @ $22.99/kg — est.)	*$2.30*	*$2.299*	*$2.30*	*$0.00*
↳ *Pendulum Arm Sub-Assembly — R1 Item #7 | Ref: RTV_Pendulum_Arm_Final_Sub_Assembly*											
7·1	—	Pendulum Interior Bracket (PLA)	Make	*3D Printed In-House*	1	—	~50g (PLA @ $17.99/kg)	*$0.90*	*$0.900*	*$0.90*	*$0.00*
7·4	—	Pendulum Shoulder Bracket / Elbow (PLA)	Make	*3D Printed In-House*	2	—	~50g ea (PLA @ $17.99/kg)	*$0.90*	*$0.900*	*$1.80*	*$0.00*
7·5	—	Pendulum Arm Side Beam (Aluminum 6061, Ø6×82.5mm)	Make	*Cut from Aluminum Rod Stock (see Section 2)*	2	—	82.5mm × Ø6mm cut	*$0.00*	*$0.000*	*$0.00*	*$0.00*
7·3	—	Pendulum Long Interior Segment (Aluminum 6061, Ø4.67×53.3mm)	Make	*Cut from Aluminum Rod Stock (see Section 2)*	1	—	53.3mm × Ø4.67mm cut	*$0.00*	*$0.000*	*$0.00*	*$0.00*
7·2	—	Pendulum Small Inner Segment (Aluminum 6061, Ø4.67×37mm)	Make	*Cut from Aluminum Rod Stock*	1	—	37mm × Ø4.67mm cut	*$0.00*	*$0.000*	*$0.00*	*$0.00*

				(see Section 2)							
19	—	Acrylic Window (Acrylic, 153.4×122×3.13mm)	Make	*Cut from Acrylic Sheet (see Section 2)*	1	—	153.4×122mm cut	*$0.00*	*$0.000*	*$0.00*	*$0.00*
↳ *RTV Ball-on-Beam Robot — 3D Printed Parts | Ref: RTV_Robot_2_Final_CAD_Assembly*											
—	1	Center Hub (PLA)	Make	*3D Printed In-House*	—	1	~175g (PLA @ $17.99/kg)	*$3.15*	*$3.148*	*$0.00*	*$3.15*
—	2	Motor Holder (PLA)	Make	*3D Printed In-House*	—	1	~140g (PLA @ $17.99/kg)	*$2.52*	*$2.519*	*$0.00*	*$2.52*
—	3	Beam (PLA, 304.8mm)	Make	*3D Printed In-House*	—	1	~110g (PLA @ $17.99/kg)	*$1.98*	*$1.979*	*$0.00*	*$1.98*
—	7	Shelf / Protoboard Shelf (PLA)	Make	*3D Printed In-House*	—	1	~55g (PLA @ $17.99/kg)	*$0.99*	*$0.989*	*$0.00*	*$0.99*
—	8	Shaft Plug Key (PLA)	Make	*3D Printed In-House*	—	1	~15g (PLA @ $17.99/kg)	*$0.27*	*$0.270*	*$0.00*	*$0.27*
—	19	Railroad / Bracket (PLA, 194.15mm)	Make	*3D Printed In-House*	—	2	~27.5g ea (PLA @ $17.99/kg)	*$0.49*	*$0.495*	*$0.00*	*$0.99*
—	21	Center Hub Acrylic (Acrylic, 60.96×72.2×4.12mm)	Make	*Cut from Acrylic Sheet (see Section 2)*	—	2	60.96×72.2mm cut	*$0.00*	*$0.000*	*$0.00*	*$0.00*
—	22	Motor Hub Acrylic (Acrylic, 88.9×99.06×3.4mm)	Make	*Cut from Acrylic Sheet (see Section 2)*	—	2	88.9×99.06mm cut	*$0.00*	*$0.000*	*$0.00*	*$0.00*
SECTION 1 — Estimated Print Material Cost (Reference Only — NOT included in grand total below)										$13.09	$9.89

SECTION 2 — Mechanical & Structural Components (Buy)											
5, 8	—	520 DC Motors w/ Wheels & Brackets (GM3865-520)	Buy	Amazon — Yahboom	4	—	4-pack	$31.56	$7.890	$31.56	$0.00
—	4	Nema 17 Stepper Motor	Buy	Amazon	—	1	1 (each)	$14.99	$14.990	$0.00	$14.99
10	—	606-2RS Deep Groove Bearings (6mm bore)	Buy	Amazon — uxcell	2	—	1 (each)	$0.85	$0.850	$1.70	$0.00
—	5	686-2RS Ball Bearings	Buy	Amazon — uxcell	—	1	10-pack	$8.59	$0.859	$0.00	$0.86
—	—	Acrylic Sheets 4"×6" (raw stock for Cut parts in Section 1)	Buy	Amazon — KAITELA	1	1	~10-sheet pack	$16.99	$1.699	$1.70	$1.70
7·5–7·2	—	Aluminum 6061 Round Rod (1/4"×13", raw stock for Pendulum Arm sub-parts)	Buy	Amazon	3	—	10-pack	$11.99	$1.199	$3.60	$0.00
6	6	LiFePO4 Batteries (3.2V 32700)	Buy	Amazon — CITYORK	4	4	4-pack	$38.97	$9.743	$38.97	$38.97
SECTION 3 — Fasteners & Hardware (Buy)											
9	—	Longer M3 Threaded Inserts (M3×5.7) — R1: 19 pcs | R2: 12 pcs	Buy	Amazon — Ruthex	19	12	50-pack	$9.99	$0.200	$3.80	$2.40

12	—	Shorter M3 Threaded Inserts (M3×4.0) — R1: 12 pcs | R2: 2 pcs	Buy	Amazon — Ruthex	12	2	50-pack	$9.99	$0.200	$2.40	$0.40
—	—	M2 Threaded Inserts — R2: 4 pcs	Buy	Amazon — Ruthex	—	4	50-pack	$9.99	$0.200	$0.00	$0.80
15	10	M3 × 8mm Socket Head Cap Screws — R1: 47 pcs | R2 item #10: 6 pcs	Buy	Digital Machinery Inc.	47	6	100-pack	$8.95	$0.090	$4.21	$0.54
—	20	M3 × 12mm Socket Head Cap Screws — R2 item #20: 8 pcs	Buy	Digital Machinery Inc.	—	8	100-pack	$8.95	$0.090	$0.00	$0.72
—	18	M2 Screw Assortment — R2 item #18: 4×M2×8mm pcs	Buy	Amazon	—	4	200-pc asst.	$14.99	$0.075	$0.00	$0.30
—	12	M3 Zinc Hex Nuts — R2 item #12: 2 pcs	Buy	Home Depot — Everbilt	—	2	5-pack	$3.75	$0.750	$0.00	$1.50
SECTION 4 — Electrical & Electronics (Buy)											
—	16	Stepper Motor Driver (TMC2208)	Buy	Amazon — TMC2208	—	1	1 (each)	$17.99	$17.990	$0.00	$17.99
19	—	Motor Driver (DRV8871) — Pendulum Robot only	Buy	Amazon / DigiKey	2	—	1 (each)	$4.33	$4.330	$8.66	$0.00
11	—	AS5600 Magnetic Encoder — Pendulum Robot only	Buy	Amazon — UMLIFE	1	—	1 (each)	$2.60	$2.600	$2.60	$0.00
—	11	ToF Distance Sensor (VL53L0X) — Ball-on-Beam only	Buy	Amazon — Qoroos	—	1	1 (each)	$12.99	$12.990	$0.00	$12.99
—	—	*Voltage Step-Down / Buck Converter*	Buy	Amazon — Euogeudel	1	1	1 (each)	$8.69	$8.690	$8.69	$8.69
17	13	BMS Board (4S 30A, 14.8V)	Buy	Amazon	1	1	1 (each)	$8.99	$8.990	$8.99	$8.99
18	15	*Microcontroller (RP2040 / Pi Pico)*	Buy	Amazon / Adafruit	1	1	1 (each)	$12.99	$12.990	$12.99	$12.99
—	—	LiFePO4 Battery Charger (14.6V)	Buy	Amazon	1	1	1 (each)	$14.59	$14.590	$14.59	$14.59
—	14	Protoboard / Solderable Breadboard	Buy	Amazon — EPLZON	1	1	1 (each)	$14.59	$14.590	$14.59	$14.59
14	9	*Rocker Switch (On/Off)*	Buy	Amazon — DaierTek KCD1	1	1	1 (each)	$7.99	$7.990	$7.99	$7.99
—	—	Dupont Jumper Wire Set (120-piece)	Buy	Amazon — Elegoo	1	1	120-pc set	$6.98	$6.980	$6.98	$6.98
—	—	Header Pins (40-pin strip)	Buy	Amazon — Honbay	1	1	40-pc strip	$7.39	$7.390	$7.39	$7.39
—	—	DIP Socket Kit — Pendulum Robot only	Buy	Amazon — CHIPNEW	1	—	1 (kit)	$9.99	$9.990	$9.99	$0.00
—	—	22 AWG Hookup Wire — Ball-on-Beam only	Buy	Amazon — TUOFENG	—	1	1 roll	$15.29	$15.290	$0.00	$15.29
SECTION 5 — UI Components (Buy)											
13	17	LCD Capacitive Touchscreen (4-inch, 320×480)	Buy	Amazon — Hosyond	1	1	1 (each)	$20.99	$20.990	$20.99	$20.99

SECTION 6 — Bulk Materials (Reference Only — Do Not Include in Per-Unit Cost Total) | PLA: $17.99/kg · TPU: $22.99/kg (est. — verify on Elegoo store)											
—	—	PLA Filament (R1: ~600g used | R2: ~550g used | 1 roll covers each robot with surplus)	Buy	R1: Amazon — Overture | R2: Creality Hyper PLA	1	1	1 kg roll (1,000g)	$17.99	$17.990	$10.79	$9.00
—	—	TPU Filament (R1: ~100g used — Pendulum Shell only | est. price — verify on Elegoo store)	Buy	Elegoo — Rapid TPU Filament 1.75mm	1	—	1 kg roll (1,000g)	$22.99	$22.990	$2.30	$0.00

GRAND TOTAL — PURCHASED COST PER UNIT (Sections 2–5 only | Section 1 print material costs shown separately above)	$246.46	$242.62

LEGEND & NOTES

Make (Section 1): Parts designed and produced in-house by the team. Columns I–L show estimated filament material cost calculated as: grams used × (filament price ÷ 1,000g). This cost is NOT included in the grand total — it is shown for transparency. Aluminum and acrylic cut parts show $0.00 here because their raw material cost is already captured in Section 2.

Buy (Sections 2–5): Parts purchased from an external vendor. Cost Per Piece = Pack Cost ÷ Pack Size. Total = Cost Per Piece × Quantity per robot.

Section 6 — Bulk Materials: PLA and TPU filament are listed for procurement reference only. R1 uses ~600g PLA + ~100g TPU. R2 uses ~550g PLA. One 1kg roll covers each robot with surplus. TPU pack cost is an estimate — verify current price at the Elegoo store link.

** Column headers 'Pack Cost / Mat. Cost' and 'Cost/Piece or /Gram' serve dual purpose: for Buy rows they show purchasing data; for Make rows (Section 1) they show print material cost data.*